

AATP PROJECT 06-01

**A LABORATORY AND FIELD INVESTIGATION TO DEVELOP TEST PROCEDURES FOR
PREDICTING NON-LOAD ASSOCIATED CRACKING OF AIRFIELD HMA PAVEMENTS**

FINAL REPORT

Submitted to:

AIRFIELD ASPHALT PAVEMENT
TECHNOLOGY PROGRAM
(AATP)

Phil Blankenship
Asphalt Institute, Inc.

R. Michael Anderson
Asphalt Institute, Inc.

Gayle N. King
GHK, Inc

Douglas I. Hanson
AMEC Earth and Environmental, Inc.

Submitted by:

AMEC Earth and Environmental, Inc.
Tempe, Arizona

DECEMBER 2010

AMEC Project No. 09-119-00948

ACKNOWLEDGEMENT OF SPONSORSHIP

This report has been prepared under the Airport Asphalt Pavement Technology Program (AAPTP). Funding is provided by the Federal Aviation Administration (FAA) under Cooperative Agreement No. 04-G-038. Dr. Satish Agrawal is the Manager of the Pavement Test Facility at the William J. Hughes Technical Center. Dr. David Brill is the Contracting Officer's Technical Representative and a Program Manager in the FAA Technology Research and Development Branch at the William J. Hughes Technical Center. Mr. Monte Symons served as the Project Director for this project.

The AAPTP and the FAA thank the Project Technical Panel members who willingly gave of their expertise and time for the development of this report. They were responsible for the oversight and the technical direction. The names of the individuals on the panel are as follows:

1. Monte Symons
2. Gregory Cline
3. Jeffrey L. Rapol
4. John D'Angelo
5. Mike DeVoy

DISCLAIMER

The contents of this report reflect the views of the authors, who are responsible for the facts and the accuracy of the data presented within. The contents do not necessarily reflect the official views and policies of the FAA. The report does not constitute a standard, specification or regulation. Neither the authors nor the United States government endorse products or manufacturers. The names of companies or equipment manufacturers are included herein only because they are considered essential to the purpose of this report.

EXECUTIVE SUMMARY

Hot Mix Asphalt (HMA) pavements represent a considerable investment in the infrastructure of airfields. It is estimated that 80 to 85 percent of the airfield pavements are surfaced with HMA. The majority of these pavements are on smaller, lightly trafficked airfields that have limited funding for repairs and pavement maintenance activities. These airfields are subjected to a wide range of climatic conditions that often result in thermal cracking, large block cracking and surface deterioration that are not load related. The Airfield Asphalt Pavement Technology Program identified a need to provide guidance to airfield engineers and managers on the steps that could be taken to cost effectively prevent and/or mitigation strategies this damage thereby extending pavement the life of HMA pavements. Therefore they funded a two phase project to provide comprehensive technical guidance on the causes and measures required to correct and/or prevent non-load related distress on HMA airfield pavements

The first phase of the project was directed at the following:

1. Identifying the elements that contribute to non-load related distress with emphases on HMA mixture design and the construction of HMA pavements.
2. Identifying and qualifying the extent of non-load related distresses on HMA airfield pavements.
3. Identifying products and procedures currently that could be used correct and/or prevent non-load related distresses in airfield pavements.
4. Identifying the most promising laboratory test methods and procedures that could be used by a pavement manager to determine when preventative maintenance is needed to prevent the development of cracking (specifically block cracking). During the first phase very limited testing was accomplished. The chapter from the first phase report with regard to laboratory testing is included as Appendix B in this report.

This project is the second phase of this study. There were two main objectives for this phase of the project:

1. Develop a practical guide identifying means to prevent and mitigate cracking caused by environmental effects.
2. Develop one or more test procedures that could be used by a pavement manager to determine when preventative maintenance is needed to prevent the development of cracking (specifically block cracking).

The results of the first objective are reported in the AAPTTP Report *Guide for Prevention and Mitigation of Non-Load Associated Distress*. This report is focused on the laboratory and field studies performed to accomplish the second objective.

General Concept

As asphalt mixtures age in service, they are exposed to a variety of environmental conditions leading to oxidation and the ultimate loss of flexibility at intermediate and low temperatures. Block-cracking results when environmental (non-load) conditions create thermal stresses that

cause strain in the asphalt mixture that exceeds the asphalt's failure strain. The key to preventing or mitigating block cracking would be to identify a property of the asphalt binder or mixture that sufficiently correlates with its flexibility and provides a means to monitor when that flexibility reaches a state where corrective action is needed.

Laboratory Studies

To attempt to identify the property related to flexibility, the research team conducted laboratory testing on asphalt binders and mixtures that had been aged to varying degrees. For the testing, three asphalt binders were selected representing different expected aging characteristics. This ranking was not based upon physical changes that occur during laboratory accelerated aging. Instead, binders were selected based upon the relative relationships between low temperature stiffness and relaxation (m-value) properties as measured by the Bending Beam Rheometer (BBR) using a relationship referred to as m-control. These asphalt binders were identified as West Texas Sour, Gulf Southeast, and Western Canadian. The asphalt binder produced from the West Texas Sour crude was expected to have the worst aging properties (i.e., the greatest embrittlement with concurrent loss of flexibility). The asphalt binder produced from the Western Canadian crude was expected to have the best aging properties (i.e., the least loss of flexibility).

Testing was conducted on asphalt binders in their unaged condition, as well as on asphalt binders that had undergone long-term aging in the Pressure Aging Vessel (PAV) at 100°C and 2.1 MPa pressure for 20, 40, and 80 hours. For reference, AASHTO M320, the specification for performance-graded (PG) asphalt binders, uses 20 hours of PAV aging as the standard long-term aging procedure intended to represent approximately 5-10 years in service. The purpose of the longer PAV aging times was not to correlate with any expected service life, but simply to create a more highly-aged sample.

Mixture testing was conducted on asphalt mixture specimens in their unaged condition, as well as on mixtures that had undergone loose-mix aging in a forced draft oven at 135°C for 4 (standard practice), 24, and 48 hours.

Findings from Laboratory Studies

Past research indicated some relationship between ductility (conducted at an intermediate temperature) and the durability of an asphalt pavement. Using ductility as the hypothesized property related to flexibility, two parameters were identified that related well to ductility and the expected loss of flexibility with aging. The first is a parameter suggested by other researchers – $G'/(η'/G')$ – as determined using the Dynamic Shear Rheometer (DSR). The second is a parameter that quantifies the difference in continuous grade temperature for stiffness and relaxation properties – referred to in the report as $ΔT_c$. In both cases, the parameters quantify the loss of relaxation properties as an asphalt binder ages.

Mixture testing was conducted using two relatively new procedures – the Disk-Shaped Compact Tension [DC(t)] fracture energy test (ASTM D7313) and the Mixture BBR test. The DC(t) test

provides a measure of fracture energy of a mixture specimen when tested at cold temperatures. The Mixture BBR test provides a measure of the creep stiffness and relaxation properties of a mixture specimen when tested at cold temperatures. Both tests are believed to be related to cracking in asphalt mixtures. Both tests showed a loss of relaxation properties – either through lower fracture energy or lower m-value – as aging increased and temperature decreased. This matches expectations.

Field Studies

Limited field testing was conducted due to project constraints. However, four airfield pavements were cored and tested from three general aviation (GA) airports in New Mexico and Montana. Two of the pavements were considered older and two were considered newer. The older pavements exhibited more cracking than the newer pavements, but not excessively so.

Cored specimens were tested using the DC(t). After testing, the specimens were subjected to solvent extraction and recovery procedures to recover the aged asphalt binder from the mixture. The recovered asphalt binder was then tested using DSR and BBR procedures to determine $G'/(η'/G')$ and $ΔT_c$ for each of the airfield pavements. Findings from this testing generally matched the lab studies, with the newer pavements having values of $G'/(η'/G')$, $ΔT_c$ and fracture energy that indicated less aging and more flexibility than the older pavements. Results from the Mixture BBR test also generally matched the findings of the lab studies.

Study Conclusions

The studies indicate that testing could be conducted on an airfield pavement that would indicate when the asphalt is reaching a critical state of loss of flexibility that would lead to an increased risk of block cracking. Mixture testing is an option, but requires non-standard test equipment and/or intensive specimen preparation techniques. However, mix testing has the advantage of testing the properties of the asphalt mixture as it exists in-situ. Binder testing has the advantage of being conducted using standard asphalt binder testing equipment and familiar test procedures. However, it must be first recovered from the asphalt mixture using a solvent extraction and recovery procedure that could, theoretically, affect its physical properties.

Recommended Use

Based on the findings from this study, the research team recommends that the airfield pavement manager coordinate the extraction and recovery of asphalt binder from the mixture and determine the value of $G'/(η'/G')$ and/or $ΔT_c$ at the time of pavement construction to establish baseline values. Periodically during the life of the pavement, the manager should coordinate the removal of one or more cores and have a testing lab perform a solvent extraction and recovery to obtain aged asphalt binder, which can then be tested to determine values of $G'/(η'/G')$ and/or $ΔT_c$ at an aged state. As the values approach a critical state – defined in this research as either $G'/(η'/G') = ±9.00E-04$ MPa/s or $ΔT_c = 2.5°C$ – the airport manager should consider that the risk of cracking is increased and preventative action should be taken.

The Bending Beam Rheometer mixture test also showed promise as a predictor of block cracking in the very limited field study. Although needing further validation, limited test results suggest that block cracking may be imminent as the mixture m-value at the lowest pavement temperature approaches 0.12.

If DC(t) testing is desired, either cores or lab-compacted specimens can be tested at a temperature that is 10°C warmer than the design low pavement temperature (e.g. test at -12°C in a climate where the design low pavement temperature is -22°C). Based on limited test results in this and other studies, minimum fracture energy of 300 J/m² is suggested to indicate the onset of cracking. As with the rest of the data generated in this research, additional testing and validation is needed.

Study Limitations and Future Research Needs

This study has several limitations that could affect its general use. First, only three asphalt binders were evaluated in the laboratory studies and they may or may not represent the range of expected aging performance of asphalt binders in the United States. Second, no modified asphalt binders were evaluated. The relationships found between physical properties and aging of unmodified asphalt binders may not be valid for modified asphalt binders (modified asphalt binders may not be routinely used in GA airport asphalt pavements, rendering this last limitation somewhat irrelevant). Third, only four airport asphalt pavements were studied in the field validation portion of the study from three airports in two sets of environmental conditions. Unfortunately, none of the four pavements exhibited high levels of cracking needed to validate the proposed parameters. Further field validation is needed. Lastly, the recommended use presumes that an airport manager will have the desire, time, and resources to conduct testing and analysis throughout the pavement's life. It would be advantageous if prequalification testing of the asphalt materials could be used to identify the risk for early cracking and provide a general time frame when preventative maintenance should occur (e.g., "Early cracking expected; suggested preventative action in 3-5 years" or "Early cracking possible, but not expected; suggested preventative action in 6-8 years"). To accomplish this goal will require significantly more study and performance modeling.

Additional work is needed to fully validate the assumptions and hypotheses used in the report. We do know that the parameters discussed in the report seem to be related to aging based on the laboratory studies and that there is enough promising data to suggest an approach for additional validation work.

Airfield Asphalt Pavement Technology Program
A Laboratory And Field Investigation To Develop
Test Procedures For Predicting Non-Load Associated
Cracking Of Airfield HMA Pavements
AMEC Project # 09-119-00948
December 21, 2010

THIS PAGE INTENTIONALLY LEFT BLANK

TABLE OF CONTENTS

CHAPTER 1.0	INTRODUCTION.....	1
1.1	PROBLEM STATEMENT	1
1.2	OBJECTIVES	1
CHAPTER 2.0	BACKGROUND	3
2.1	LITERATURE REVIEW	3
2.1.1	Binder and Mixture Aging Protocols	3
2.1.2	Test Procedures Related to Aging	5
2.2	MATERIALS AND PROJECT SELECTION.....	5
2.2.1	Test Matrix and Materials Preparation	6
CHAPTER 3.0	LABORATORY STUDY	9
3.1	INTRODUCTION	9
3.2	ASPHALT BINDER.....	9
3.2.1	MATERIALS	10
3.2.2	BINDER AGING PROTOCOL	10
3.2.3	Test Results	12
3.3	ASPHALT MIXTURE	40
3.3.1	Sample Preparation and Laboratory Aging to Simulate Field Conditions.....	40
3.3.2	Maximum Theoretical Specific Gravities (G_{mm})	41
3.3.3	Bending Beam Rheometer (BBR) on Mixtures.....	43
3.3.4	Disk-Shaped Compact Tension [DC(t)] Test	59
CHAPTER 4.0	FIELD STUDY	73
4.1	INTRODUCTION	73
4.2	PAVEMENT CONDITION AT TIME OF CORING	74
4.2.1	Roundup Airport, MT (RPX)-Top Lift (Newer pavement) and Bottom Lift (older pavement).....	75
4.2.2	Clayton Airport, NM (KCAO)-Newer Pavement.....	76
4.2.3	Conchas Lake, NM (E89)-Older Pavement.....	77
4.3	LABORATORY TESTING OF AIRFIELD PAVEMENT CORES.....	79
4.3.1	Asphalt Binder	79
4.3.2	Asphalt Mixture Testing.....	83
CHAPTER 5.0	LABORATORY TOOLS FOR PREDICTING TRANSVERSE AND BLOCK CRACKING	99
5.1	EXISTING PAVEMENT	99
5.1.1	Binder Tools to Rank Propensity for Cracking	99
5.1.2	Mixture Tools to Predict Cracking	100
5.2	TESTS FOR DESIGN AND SPECIFICATION - ACCELERATED LABORATORY AGING PROCEDURES	101
5.2.1	Binder.....	101
5.2.2	Mixture.....	102
CHAPTER 6.0	CONCLUSIONS AND RECOMMENDATIONS	103
6.1	STUDY LIMITATIONS AND FUTURE RESEARCH NEEDS	105
CHAPTER 7.0	PRIMARY REFERENCES	107

LIST OF FIGURES

Figure 2.1 Illustration of Severe Aging Gradients in Asphalt Pavements	4
Figure 3.1 G' and G'' Isotherms for Gulf-Southeast PAV20 Sample 2	12
Figure 3.2 Complex Modulus and Phase Angle Mastercurves for	13
Gulf-Southeast PAV20 Sample 2.....	13
Figure 3.3 Relationship between Ductility and DSR Parameter (Glover et.al. 2005).....	14
Figure 3.4 Effect of PAV Aging Time on G'/(η' /G')	16
Figure 3.5 Effect of PAV Aging Time on G'/(η' /G') Measured at 44.7°C, 10 rad/s	18
Figure 3.6 Effect of PAV Aging Time on G'/(η' /G') Measured at 44.7°C, 10 rad/s	18
Figure 3.7 Monotonic Shear Test Results – PAV20	20
Figure 3.8 Comparison of Measured and Predicted Ductility.....	22
Figure 3.9 Relationship between Ductility and G'/(η' /G') Using the Mastercurve Procedure	22
Figure 3.10 Relationship between Ductility and G'/(η' /G') Using the Standard DSR Procedure.....	23
Figure 3.11 Force Ductility Stress-Strain Curves – Gulf-Southeast.....	24
Figure 3.12 Effect of PAV Aging Time on Peak Stress in Force Ductility	24
Figure 3.13 Effect of PAV Aging Time on Strain at Peak Stress in Force Ductility	25
Figure 3.14 Effect of PAV Aging Time on Tc – West TX Sour	28
Figure 3.15 Effect of PAV Aging Time on Tc – Gulf-Southeast	28
Figure 3.16 Effect of PAV Aging Time on Tc – Western Canadian	29
Figure 3.17 Effect of PAV Aging Time on the Difference between Tc,m(60) and Tc,S(60)	29
Figure 3.18 Relationship between ΔT_c and Ductility.....	30
Figure 3.19 Thermal Stress Curves for West TX Sour Asphalt Binder	31
Figure 3.20 Thermal Stress Curves for Gulf-Southeast Asphalt Binder	32
Figure 3.21 Thermal Stress Curves for Western Canadian Asphalt Binder.....	32
Figure 3.22 Effect of PAV Aging Time on CCT (assuming $\sigma_f = 3.5$ MPa).....	33
Figure 3.23 Relationship Between G'/(η' /G') and ΔT_c	34
Figure 3.24 Relationship between Log G'/(η' /G') and ΔT_c	35
Figure 3.25 Black Space Diagram for Western Canadian Asphalt Binder	36
Figure 3.26 Mastercurve Characteristic Parameters	38
Figure 3.27 Relationship Between G'/(η' /G') and R (15°C, $\delta = 45^\circ$)	39
Figure 3.28 Relationship Between G'/(η' /G') and R (15°C, 0.005 rad/s).....	40
Figure 3.29 Mixture Gravity and Aging Time of the Loose Asphalt Mixture	42
Figure 3.30 Impact of Aging on BBR Mixture Properties (Bending Mode).....	45
Figure 3.31 BBR Loading curves for mixes below Tcritical (S vs. log time).....	47
Figure 3.32 BBR Loading Curves for Mixes Below Tcritical (m-value vs. log time).....	48
Figure 3.33 BBR Mixture Bending Test	50
Figure 3.34 BBR Mixture Bending Test	51
Figure 3.35 BBR Mixture Bending Test	53
Figure 3.36 Unaged WTS CCT: Shenoy (SAP) vs. “Limiting Stiffness” of 6 MPa.....	54
Figure 3.37 48 hr aged WTS CCT: Shenoy (SAP) vs. “Limiting Stiffness” of 6 MPa	55
Figure 3.38 Sample Preparation (Cutting) BBR Mixture Beams	56
Figure 3.39 Loading BBR Mixture Beams.....	56
Figure 3.40 BBR Fracture Stress for Three Asphalts After Loose-Mix Aging	58

Figure 3.41 Laboratory Samples Prepared for DC(t) Testing from the Three Binder Sources. ...60
Figure 3.42 Cox and Sons DC(t) Testing Device without sample (left) and with sample loaded (right) and instrumented.....61
Figure 3.43 DC(t) Loading Showing Peak Load and Fracture Energy for CMOD and Delta 25 Gages.61
Figure 3.44 DC(t) Sample after Testing Showing Crack Progression.....62
Figure 3.45 DC(t) Testing on Laboratory Prepared Samples from the Three Binder Sources at Three Testing Temperatures with CMOD Gage65
Figure 3.46 DC(t) Testing on Laboratory Prepared Samples from the Three Binder Sources at “Climatic Temp - 6°C” with CMOD Gage65
Figure 3.47 DC(t) Testing on Laboratory Prepared Samples from the Three Binder Sources at “Climatic Temp -12°C” with CMOD Gage66
Figure 3.48 DC(t) Testing on Laboratory Prepared Samples from the Three Binder Sources Normalized for the PG Low Binder Grade with CMOD Gage66
Figure 3.49 DC(t) Testing on Laboratory Prepared Samples from the Three Binder Sources at Three Testing Temperatures with Delta 25 Gages68
Figure 3.50 DC(t) Testing on Laboratory Prepared Samples from the Three Binder Sources at “Climatic Temp -12°C” with Delta 25 Gages68
Figure 3.51 DC(t) Testing on Laboratory Prepared Samples from the Three Binder Sources Normalized for the PG Low Binder Grade with Delta 25 Gages69
Figure 3.52 Peak Load using DC(t) Testing on Laboratory Prepared Samples from the Three Binder Sources71
Figure 3.53 Peak Load using DC(t) Testing on Laboratory Prepared Samples from the Three Binder Sources at -12°C71
Figure 3.54 Peak Load using DC(t) Testing on Laboratory Prepared Samples from the Three Binder Sources at Climatic Temperature72
Figure 3.55 Peak Load using DC(t) Testing on Laboratory Prepared Samples from the Three Binder Sources at “Climatic Temp -6°C”72
Figure 4.1 Planned Coring Sites for Cracked and Non-Cracked Surfaces.74
(Hazard was not cored.).....74
Figure 4.2 Samples Cores from Roundup, MT (RPX) and Conchas Lake, NM (E89)74
Figure 4.3 Roundup Pavement surface (top layer) Condition at Time of Coring76
Figure 4.4 Clayton Airport Condition at Time of Coring77
Figure 4.5 Conchas Lake Airport Condition at Time of Coring78
Figure 4.7 Recovered Asphalt Binders – Black Space80
Figure 4.8 Relationship Between $G'/(η'/G')$ and $ΔT_c$ – with Recovered Asphalt Binders.....82
Figure 4.9 Relationship Between $G'/(η'/G')$ and $ΔT_c$ – with Recovered Asphalt Binders (Magnified).....82
Figure 4.10 Replicate Results for S and m-value for All Field Specimens Tested @-12°C.....84
Figure 4.11 Average BBR Mixture loading Curves for All Field Mixes at Three Temperatures ..85
Figure 4.12 BBR Stiffness for Field Cores – 4 Locations.....86
Figure 4.13 BBR m-value for Field Cores – 4 Locations.....86
Figure 4.14 Comparison of Binder vs. Mixture Stiffness for 4 Field Sites89
Figure 4.15 Comparison of Minder vs. Mixture m-value for 4 Field Sites89

Figure 4.16 Binder and Mixture Physical Properties for BBR Bending Tests – Clayton90
Figure 4.17 Binder and Mixture Physical Properties for BBR Bending Tests – 4 Field Sites..... 90
Figure 4.18 BBR Fracture Test: Force vs. Deflection for Clayton (3 temps, 3 reps).....92
Figure 4.19 BBR Fracture Test: Stress vs. Time for Clayton (3 temps, 3 reps).....92
Figure 4.20 BBR Fracture Test: Strain vs. Time for Clayton (3 temps, 3 reps).....93
Figure 4.21 BBR Fracture Test: Stress vs. Strain for Clayton (3 temps, 3 reps)93
Figure 4.22 CMOD Fracture Energies for Pavement Cores with Suggested Cracking Limit, New Mexico Sites97
Figure 4.23 CMOD Fracture Energies for Pavement Cores with Suggested Cracking Limit, Montana Site.....97

LIST OF TABLES

Table 2.1 Selected Asphalt Binders for Laboratory Testing.....6
Table 2.2 Aggregate Stockpile Percentages and JMF.....7
Table 2.3 Lab Standard Gradation.....7
Table 2.4 Coring Plan8
Table 3.1 Experimental Matrix9
Table 3.2 Asphalt Binder Testing Matrix11
Table 3.3 West Texas Sour (WTX) – $G'/(η'/G')$ at 15°C, 0.005 rad/s (MPa/s)15
Table 3.4 Gulf-Southeast (GSE) – $G'/(η'/G')$ at 15°C, 0.005 rad/s (MPa/s)15
Table 3.5 Western Canadian (WC) – $G'/(η'/G')$ at 15°C, 0.005 rad/s (MPa/s)15
Table 3.6 West Texas Sour – $G'/(η'/G')$ at 44.7°C, 10 rad/s (MPa/s).....17
Table 3.7 Gulf-Southeast – $G'/(η'/G')$ at 44.7°C, 10 rad/s (MPa/s)17
Table 3.8 Western Canadian – $G'/(η'/G')$ at 44.7°C, 10 rad/s (MPa/s).....17
Table 3.9 Ductility Results at 15°C, 1cm/min. (cm).....21
Table 3.10 Comparison of Predicted and Measured Ductility21
Table 3.11 BBR Data for West TX Sour Asphalt Binder26
Table 3.12 BBR Data for Gulf-Southeast Asphalt Binder26
Table 3.13 BBR Data for Western Canadian Asphalt Binder.....27
Table 3.14 CCT Results.....33
Table 3.15 Phase Angle as a Function of Aging – Western Canadian Asphalt Binder.....37
Table 3.16 Determination of R (15°C, $δ = 45°$)39
Table 3.17 Determination of R (15°C, 0.005 rad/s).....39
Table 3.18 Aging Effect on Mixture Gravity (G_{mm})42
Table 3.19 BBR Mixture Bending Test: Evolution of Stiffness and m-Value with Aging44
Table 3.20 BBR Mixture Bending Test.....51
Table 3.21 BBR Mixture Bending Test.....52
Table 3.22 Results from BBR Fracture Tests on Aged Mixtures56
Table 3.23 Statistical Variability for BBR Fracture Tests on Aged Mixtures57
Table 3.24 Fracture Energy from DC(t) Tests on Lab Mixtures using Crack Mouth Opening Displacement (CMOD) Gage64
Table 3.25 Fracture Energy from DC(t) Tests on Lab Mixtures using Delta 25 Gages.....67
Table 3.26 Peak Load from DC(t) Tests on Lab Mixtures.....70
Table 4.1 Pavement Layer Thicknesses for Roundup Airport75

Airfield Asphalt Pavement Technology Program
A Laboratory And Field Investigation To Develop
Test Procedures For Predicting Non-Load Associated
Cracking Of Airfield HMA Pavements
AMEC Project # 09-119-00948
December 21, 2010

Table 4.2 Pavement Layer Thicknesses for Clayton Airport.....	77
Table 4.3 Pavement Layer Thicknesses for Conchas Lake Airport	78
Table 4.4 BBR Data for Recovered Asphalt Binder	81
Table 4.5 Comparison of Durability Parameters for Recovered Asphalt Binder Data.....	81
Table 4.6 Low PG Climate Temperatures for the Airport Field Sites (98% reliability).....	87
Table 4.7 Low Temperature Cracking Predictions from Shenoy Method.....	88
Table 4.8 Using ΔT_c , °C as a Cracking Predictor	91
Table 4.9 BBR Failure Stresses (MPa) for Clayton Airport Cores	94

APPENDIX

APPENDIX A – A Universal Hypothesis for Non-Load Induced Cracking

APPENDIX B – Laboratory Test Methods and Procedures used to Simulate and Evaluate
Non-Load Associated Distress in HMA Pavements

Airfield Asphalt Pavement Technology Program
A Laboratory And Field Investigation To Develop
Test Procedures For Predicting Non-Load Associated
Cracking Of Airfield HMA Pavements
AMEC Project # 09-119-00948
December 21, 2010

THIS PAGE INTENTIONALLY LEFT BLANK

CHAPTER 1.0 INTRODUCTION

1.1 PROBLEM STATEMENT

Hot-mix asphalt (HMA) pavements in the United States represent a considerable investment in the infrastructure of airfields. Many of those pavements are found at small, lightly trafficked airfields that have limited funds for the repair and pavement maintenance to protect their investment. These airfields exhibit a wide variety of distresses, most of which are unrelated to traffic loading. Rather, these distresses are caused by age-related hardening of the asphalt binder, which results in block cracking or raveling of the surface, or by extreme fluctuations in the temperature of the HMA surface, which results in thermal cracking.

Many products and procedures exist to deter, reduce, repair or prevent these types of distresses and to extend the usable life of an HMA pavement. Unfortunately there has been no quantitative test procedure that that could be used by airfield managers and engineers to predict when action would need to be taken. The study discussed in this report provides tools that could be used to make this prediction, although these tools need further refinement and development.

1.2 OBJECTIVES

AAPTP Project No. 06-01 represents the second phase of AAPTP Project No. 05-07, *Techniques for Prevention and Remediation of Non-Load Associated Distresses on HMA Airport Pavements*, which was a study into common non-load-associated problems affecting HMA airfield pavements and the products and procedures that could be used to combat those problems and a study to identify promising test procedures that could be used to predict when action needs to be taken to prevent non-load associated distress. Appendix B contains the chapter from the 05-07 report that discusses the promising test procedures. This project (AAPTP 06-01) was directed at applying the information from the 05-07 report to develop a test procedure that can be used to predict when action needs to be taken to prevent the initiation of Non-Load Associated Distress (specifically block cracking).

This report, *A Laboratory and Field Investigation to Develop Testing Procedures for Predicting Non-Load Associated Cracking of HMA Pavements* presents the results of a study that shows techniques that can be used to predict when action needs to be taken to prevent Non-Load Associated Distress. These techniques could be used as a diagnostic technique to predict when maintenance or rehabilitation is needed. The information and recommendations in this report are based on an extensive laboratory study and limited field validation data which support similar conclusions.

Airfield Asphalt Pavement Technology Program
A Laboratory And Field Investigation To Develop
Test Procedures For Predicting Non-Load Associated
Cracking Of Airfield HMA Pavements
AMEC Project # 09-119-00948
December 21, 2010

THIS PAGE INTENTIONALLY LEFT BLANK.

CHAPTER 2.0 BACKGROUND

2.1 LITERATURE REVIEW

Appendix A presents a hypothesis for non-load associated cracking on Hot Mix Asphalt pavements.

There have been a number of procedures developed to simulate the long term aging of asphalt binders and HMA mixtures. The primary goal of those procedures has been to simulate the effect of oxidation on asphalt binders.

In a comprehensive Strategic Highway Research Program SHRP review of laboratory aging protocols for asphalt binders and mixes, Bell (1) described a broad range of simulation tests that have been proposed throughout the years. Chemical and rheological changes occurring during HMA construction at elevated temperatures have been relatively easy to replicate for conventional asphalt binders, using tests such as the Thin-Film Oven Test (TFOT), the Rolling Thin-Film Oven Test (RTFO), the Stirred Air-Flow Test (SAFT), and the German Rolling-Flask Test (GRF), to name a few. It has proven difficult to develop tests which accurately replicate the rheological changes that occur in an asphalt binder in the pavement over time. Attempts to accelerate the process for laboratory convenience by increasing temperatures, and/or exposing the binder to elevated pressure in air or pure oxygen have been problematic.

2.1.1 Binder and Mixture Aging Protocols

Laboratory Binder Aging

There have been a number of test procedures developed that have been or are being used to evaluate the aging characteristics of asphalt binders. The most common today are Rolling Thin-Film Oven (RTFO), AASHTO T240, and Pressure Aging Vessel (PAV), AASHTO R28, to simulate short and long-term aging of the binder (2). Testing of binder properties is performed to try to correlate these binder aging procedures to the actual aging that occurs in asphalt binders utilized in asphalt mixtures, or hot-mix asphalt (HMA), when in service. Developing correlations between lab binder aging procedures and actual field aging has been limited for the following reasons:

First, the binder must be extracted from aged pavement cores. The extraction procedure may alter binder properties.

Second, the binder ages differently at different depths in the asphalt pavement cross section. Most aging will occur in the top of the pavement where the materials are most exposed to climatic changes and the sun. As an example, typical results from the Witczak and Mirza global aging prediction model, that was calibrated using field data, are shown in Figure 2.1

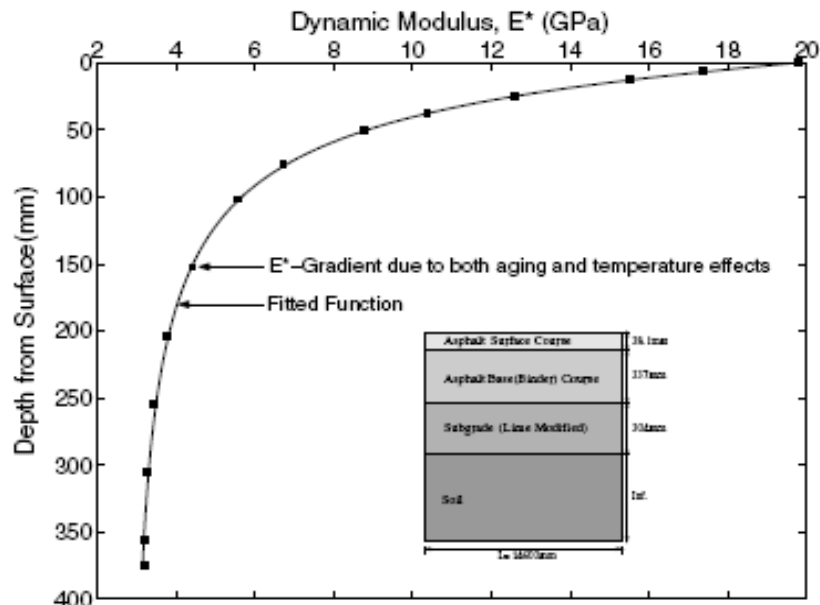


Figure 2.1 Illustration of Severe Aging Gradients in Asphalt Pavements

The aging gradient presents a dilemma with respect to both the development and calibration of mechanical laboratory tests to simulate field aging, which involve the testing of discrete thickness specimens. Usually, a minimum thickness of 50 mm or possibly 25 mm for mixtures with finer aggregates is required depending on the test method. Removing the top portion of the mixture can make the specimen more uniform for testing. However, by removing the top portion of the mixture the ability to properly measure the mixture's surface brittleness where environmental aging occurs has been reduced.

Third, binder aging is dependent on mix properties. In particular, density or compaction level, which is not consistent across or within an asphalt pavement system, affects binder aging.

Fourth, binder film thickness (asphalt coating on an aggregate particle) in a mixture is variable within a given mix and has not been simulated through a lab binder aging procedure. There are other reasons as well.

Laboratory Mixture Aging

As with the aging of asphalt binders, there are a number of test procedures developed that have been or are being used to evaluate the aging characteristics of an HMA mixture. The most commonly used are the AASHTO R30 Short-Term Oven Aging (Conditioning) of Loose Mixture and Long-Term Oven Aging (Conditioning) of Prepared Specimens. The test results from these procedures have been correlated to the field aging of HMA pavements. The problem associated with these procedures is their limited ability to predict the aging characteristics within an HMA pavement due to variable climatic conditions and HMA density levels. Another problem with these test procedures as was also mentioned with the binder aging protocols is that they

are typically associated with the thicker pavement structure versus the top layer or surface where most of the environmental aging occurs.

2.1.2 Test Procedures Related to Aging

It was concluded from the APTP 05-07 abbreviated lab study (Phase 1) that current binder and mixture aging procedures and tests were lacking in the ability to predict non-load associated cracking; specifically block cracking on an aged pavement. (3)

The limited Phase I study showed that the Disk-Shaped Compact Tension (DC(t)) fracture energy test could differentiate the effect of aging on various asphalt surfaces. It was recommended in that report that measurements on field cores from a sampling of pavements were needed. It further recommended a comparison be made of cores from non-cracked pavements to cracked pavements, assuming the surfaces are made of similar materials per location; that cores should be taken from new construction as a baseline for a new pavement that should exhibit no cracking; and that cores need to be sampled from varying locations of non-load distresses in wet-freeze, dry-freeze, wet no freeze, and dry-no freeze climatic zones.

Another strong potential mixture test identified was the Bending Beam Rheometer (BBR) mixture test by Dr. Marasteanu. This test has shown much initial promise using a small sample. In this test, mixtures can be compacted and cut into small beams similar in size to asphalt binder BBR beams. The beams are then tested in a BBR that has been retrofitted to handle the stiffer mixture sample. The small sample size lends itself to high variability.

The Phase I report also recommended the evaluation of binder tests that could be used to further evaluate the aging of the mixture. These tests included classification using the dynamic shear rheometer (DSR) and bending beam rheometer (BBR), capillary tube viscosity, and the newer Multiple Stress Creep Recovery (MSCR) test. The binder tests are useful when sample size is limited, but require chemical extraction of the asphalt binder.

Since the most severe environmental aging occurs near the surface, it seems logical that any chosen test must be able to evaluate this material. Any test that is chosen should meet constraints of being able to take measurements from relatively thin (~25mm) pavement surfaces obtained from coring with as little trimming as possible.

2.2 MATERIALS AND PROJECT SELECTION

One of the goals of this report was to identify mixture and binder test(s) that measure non-load or environmental aging effects on asphalt surface mixtures taken from airfield pavements. Since surface layers are usually placed in 25mm lifts up to a typical maximum of 50 mm in thickness, many current mixture tests are eliminated. Current asphalt mixture tests are designed to measure materials properties on laboratory compacted samples where the thickness can be specified. These tests usually require 50mm thick beams or 50mm tall or taller cores.

This laboratory study focuses on newer tests that show promise in measuring the potential non-load associated cracking of asphalt pavements.

2.2.1 Test Matrix and Materials Preparation

Laboratory Study

Asphalt and aggregates were selected in anticipation of producing “extremes” in reference to non-load associated aging. Three asphalt and one aggregate sources were selected.

Materials Selection

Asphalt Binder - The three asphalts are from different types of crudes: Western Canadian, West Texas sour, and Gulf-southeast blended crude (Table 2.1). The latter two were used in the AAPTP 95-07 project. The three asphalt binders were selected to have essentially the same high temperature grade, and similar low temperature binder stiffness as measured by the BBR. However, these three asphalts have very different low temperature relaxation properties as defined by the BBR m-value while having different low temperature properties. The asphalt grades for the binders were PG 64-25, PG 64-22, and PG 64-16.

Table 2.1 Selected Asphalt Binders for Laboratory Testing

	Limiting Low-Temperature binder Property	Expected Result in Performance
Western Canadian PG 64-28	Stiffness (S) by about 3°C	Should produce the least amount of cracking
Gulf-southeast PG 64-22	Similar Stiffness and m-value limiting temperatures	Average performer
West Texas sour PG 64-16	m-value by about 3°C	May exhibit early cracking. Early aging binder from Strategic Highway Research Program asphalt evaluations

NOTE: The comments in the Table above are expected results based upon the low Performance Grade (PG) temperatures. This is not a reflection on the supplier performance.

Aggregate - A standard Kentucky job mix formula (JMF) that has been used in Frankfort, KY at the general aviation airport was chosen. This is a low-absorption, limestone aggregate blend. The blend composition of the aggregates and job mix formula are shown in Tables 2.2 and 2.3.

Mixture - This mixture meets the FAA P-401 specification and is a 75-blow Marshall design at 5.4 percent optimum asphalt binder. The Marshall design parameters are: 3.7 percent air voids, 15.2 percent VMA with a 2450lbf stability and 0.10in flow.

The mixture was also verified in a SuperPave Gyratory Compactor (SGC) with the newer 1.16° internal angle requirement. Using 75 gyrations, the average air voids of three samples was 3.5 percent which is similar on this particular mixture to the Marshall design voids of 3.7 percent reported above. The 3.5 percent air voids can also be report as 96.5 percent of maximum theoretical mixture gravity ($G_{mm} = 2.497$ after 2 hours standard aging).

Table 2.2 Aggregate Stockpile Percentages and JMF

Aggregate Type	G _{sb}	Percent of Total
Harrod Stone-Limestone #68's	2.710	21
Harrod Stone-Limestone Sand (unwashed)	2.680	30
Harrod Stone-Limestone Sand (washed)	2.690	39
Nugent-Natural Sand	2.610	10

Table 2.3 Lab Standard Gradation

Sieve Size	Sieve Size (mm)	Lab Standard Mixture, % passing	Lower Limit, % passing	Upper Limit, % passing
¾ in.	19.0	100	100	100
½ in.	12.5	93	90	100
3/8 in	9.5	88		90
# 4	4.75	68		
# 8	2.36	43	28	58
# 16	1.18	27		
# 30	0.60	17		
# 50	0.30	9		
# 100	0.15	6		
# 200	0.075	5.0	2	10

Field Study

Site Selection

Three projects were planned for coring to represent three different climate and asphalt crude sources. Coring locations on General Aviation (GA) pavements were Montana, New Mexico, and a location originally planned in Kentucky. All project cores except for the Kentucky site were obtained. Due to logistical problems it was not possible to obtain cores from the Kentucky site.

The projects were evaluated with the goal of obtaining cores from both cracked and non-cracked sections. The areas without cracking could be old or relatively new (at least 3 winters) pavements. The cracked areas were identified as non-load associated cracking. These cores should represent two cracking extremes as referenced in the test plan. This range in cracking performance should provide two different sets of lab test data to help predict a test limit where a crack may form in that climate. About 15 cores will be gathered from each section for a total of 30 cores per project.

The locations selected were matched to the binder source wherever possible. For example, it is believed that the Montana airport cores would reflect an asphalt source similar to the Western Canadian crude, whereas the New Mexico sites would more likely resemble asphalt as refined from the West Texas Sour crude. Table 2.4 illustrates the coring plan.

Table 2.4 Coring Plan

Location & Airport Name	Corresponding Asphalt Binder Source	Climatic Zone	Elevation	Cores to Obtain
Roundup Airport, MT (FAA ID: RPX)	Canadian	Severe freeze, wet region	1064m (3491ft)	15 from cracked section in previous surface that is now overlaid 15 from non-cracked surface
Conchas Lake, NM (FAA ID: E89)	West Texas sour	No to moderate freeze, dry region	1289m (4230ft)	15 from cracked surface
Clayton, NM (FAA ID: CAO)			1513m (4965ft)	15 from non-cracked surface

Requirements for the pavement cores were:

- 14 cores for testing plus 1 for inspection for a total of 15 from each section or 30 per project.
- Cores from the same general aviation (GA) airport location, but from different locations in the pavement (taxiway vs. runway)
- Cores should have surface layers as thick as possible. A surface thickness of 2" is desirable. A minimum 1.5" is required because the sample must be trimmed for testing.
- Pavement should have at least two winters to have some aging and an opportunity to crack. The optimum would be to find two pavements that are 10 years old, where one is cracked and the other is not cracked.
- Test cores from cracked areas should be taken from sections where the crack does NOT go through the core. To aid visual inspection of crack severity, take at least one core with a crack.
- The cores should be flat on the surface (not sloped) and not damaged (i.e. no screwdriver marks). If necessary, core through the pavement. The final sample can be trimmed in the laboratory.

CHAPTER 3.0 LABORATORY STUDY

3.1 INTRODUCTION

The experimental matrix in Table 3.1 was developed according to the proposed test plan from the AAPT 05-07, Phase I research. The binder aging intervals are based upon current aging times plus extended times in search of more severe aging techniques. The asphalt binders were tested in their original, unaged state and after aging in the Rolling Thin Film Oven (RTFO) and Pressure Aging Vessel (PAV). All PAV aging was conducted using standard conditions of 100°C and 2.1 MPa air pressure. Aging times included the standard practice (AASHTO R28) aging of 20 hours, as well as two extended times – 40 and 80 hours.

In Phase I, it was determined that the standard AASHTO aging on compacted samples did not produce sufficient conditioning to represent a pavement that may be 10 years old and cracked. For this work, all aging was performed on loose mixture before compaction to speed the aging process. The aging times of the loose mixture were determined from recent work at the University of Illinois-Champaign (4) and experimental testing in Phase 1 of this project. The DC(t) and various asphalt binder tests were performed on all cells in the Table. A total of 36 specimens, three replicates for each cell, per asphalt & aggregate combination have been made at 7±0.5 percent air voids (93±0.5 percent of G_{mm}). Of the 36 samples, 27 were used for DC(t) testing. The remaining samples were used for BBR mixture testing.

Table 3.1 Experimental Matrix

Conditioning: Aging Time of Binder	No Aging (0 hours)	RTFO	RTFO + PAV @ 20 hours	RTFO + PAV @ 40 hours	RTFO + PAV @ 80 hours
West Canadian PG 64-28	X	X	X	X	X
Gulf-Southeast PG 64-22	X	X	X	X	X
West-Texas Sour PG 64-16	X	X	X	X	X

Conditioning: Aging Time of Loose Mixture	No aging (0 hours)	4 hours	24 hours	48 hours
West Canadian PG 64-28	X	X	X	X
Gulf-Southeast PG 64-22	X	X	X	X
West-Texas Sour PG 64-16	X	X	X	X

3.2 ASPHALT BINDER

The asphalt binder testing and data analysis focuses on establishing correlations between the fracture and rheological properties as asphalt binders age in a mix or in the Pressure Aging Vessel (PAV). It was hypothesized that aging causes a significant loss in relaxation properties of

the asphalt binder at lower temperatures, and this rheological change results in deteriorating fracture properties as measured by either failure strain or failure energy.

Tests were performed on binders sampled from three suppliers.

3.2.1 MATERIALS

Three asphalt binders selected have essentially the same high temperature grade, while having different low temperature properties primarily because of differences in relaxation properties as measured by “m-value”. The asphalt binders are identified as West Texas Sour (PG 64-16), Gulf-Southeast (PG 64-22), and Western Canadian (PG 64-28).

3.2.2 BINDER AGING PROTOCOL

The asphalt binders were tested in their original, unaged state and after aging in the Rolling Thin Film Oven (RTFO) and Pressure Aging Vessel (PAV). All PAV aging was conducted using standard conditions of 100°C and 2.1 MPa air pressure. Aging times included the standard practice (AASHTO R28) aging of 20 hours, as well as two extended times – 40 and 80 hours.

Testing

Testing on the unaged and aged asphalt binder samples included:

- Texas A&M Standard DSR Test method - From the research conducted at Texas A&M, a DSR parameter was proposed which the researchers believed would relate to ductility at 15°C. The test was performed using the DSR at 44.7°C and 10 rad/s. Parallel plate geometry (25 mm) with a 1-mm gap was used at a test strain of 10% to determine G' and η' . The Texas A&M DSR parameter ($G'/\eta'/G'$) can be calculated from this data.
- DSR Mastercurve - DSR frequency sweeps were conducted at three temperatures (5, 15, 25°C) using the 8-mm parallel plate geometry with a 2-mm gap. At each temperature the specimen was tested from 0.1 to 100 rad/s using a 1% strain. The frequency sweep data was then combined into a unified mastercurve at 15°C using the RHEA™ software. Different parameters, including the aforementioned Texas A&M DSR parameter (calculated at 15°C and 0.005 rad/s) were determined using the mastercurve.
- The DSR Monotonic Shear Procedure (Wisconsin) - This test had been researched by the University of Wisconsin (Dr. Hussain Bahia) as a potential replacement fatigue parameter in the asphalt binder specification. It is a monotonic DSR test that can be used to evaluate loss of strength with applied strain.
- Ductility @ 15°C and 1 cm/min - Previous research by Kandhal cited loss of ductility upon asphalt aging as a primary contributor to raveling and block cracking. Glover's recent work at Texas A&M with rheological methods target Kandhal's findings as a means to estimate when binders are reaching critical fracture limits.

- Force Ductility @ 4°C and 1 cm/min. - This test is used to capture failure strain and energy. It is thought that block cracking probably initiates at temperatures below 25°C, but it clearly can occur above the lowest critical cracking temperature where thermal cracking occurs. If rapid temperature changes are in fact responsible for the environmental stresses that induce cracking, then the fastest rates of thermal expansion and contraction would not occur at the lowest temperature, but on the way down or up. Force ductility offers a fast and inexpensive means to estimate tensile properties and failure energy at intermediate temperatures comparable to those where research has shown correlations with failure.
- Bending Beam Rheometer (BBR) – The BBR is used to determine the low temperature rheological properties of an asphalt binder. To provide for an evaluation of critical cracking temperature and determine the continuous low temperature grade to the nearest 0.1°C for both Stiffness and m-value, testing was conducted at 2-3 test temperatures. Plots of the critical temperatures for Stiffness vs. m-value will be plotted to determine the relative rate of change in both hardness and relaxation properties as asphalts age.

Although originally planned, direct tension (DTT) tests were not conducted.

The testing matrix (Table 3.2) is shown below for each asphalt binder:

Table 3.2 Asphalt Binder Testing Matrix

	Unaged	PAV20	PAV40	PAV80
DSR Mastercurve	x	x	x	x
DSR Function (Texas A&M)	x	x	x	x
DSR Monotonic (Wisconsin)	n/a	x	n/a	n/a
Ductility, 15°C	x	x	x	x
Force Ductility	x	x	x	x
BBR	x	x	x	x
DTT	n/a	n/a	n/a	n/a

Where possible, replicate (2-3) tests were performed for each cell. An “x” indicates that testing was conducted. An “n/a” indicates that testing was not conducted.

3.2.3 Test Results

DSR Mastercurve -

Frequency sweep testing was conducted at 5, 15, and 25°C from 0.1 to 100 rad/s for each of the asphalt binder samples. From the frequency sweep data, a mastercurve was generated using the RHEA software (Abatech) at a reference temperature of 15°C. This temperature was selected as it corresponded with ductility testing. An example of the isotherms and mastercurve construction is shown in Figures 3.1 and 3.2 below.

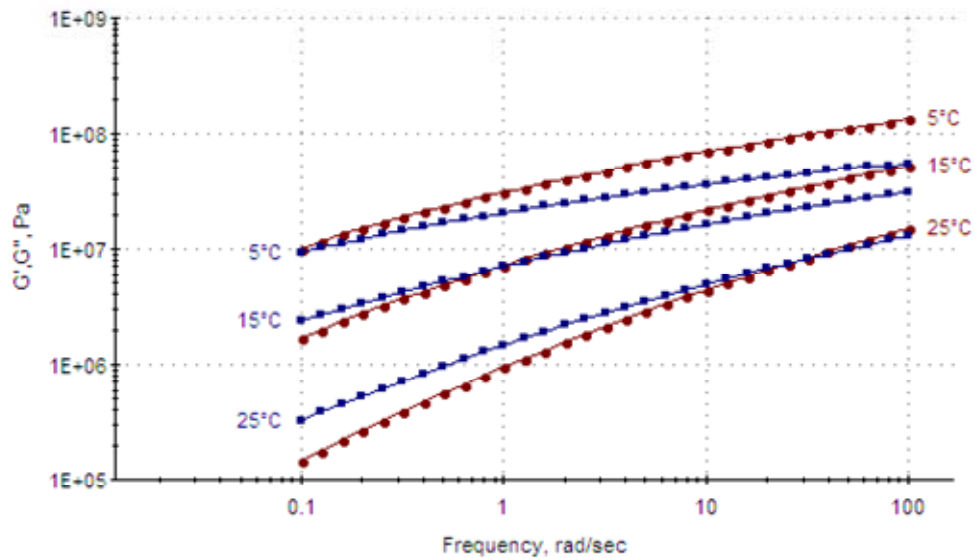


Figure 3.1 G' and G'' Isotherms for Gulf-Southeast PAV20 Sample 2

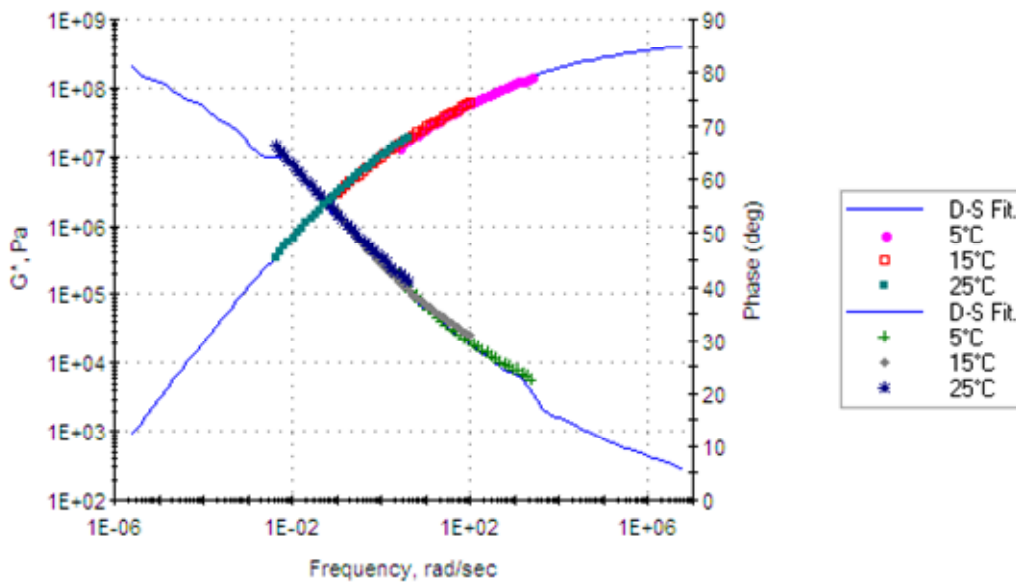


Figure 3.2 Complex Modulus and Phase Angle Mastercurves for Gulf-Southeast PAV20 Sample 2

Research by Glover et.al. at Texas A&M found that the ductility at 15°C and 1 cm/min correlated with DSR results at 15°C and 0.005 rad/s. Specifically, a DSR parameter, calculated as $G' / (\eta' / G')$, was found to be correlated with ductility at 15°C and 1 cm/min, Figure 3.3. Higher values of the DSR function have been related to lower ductility values.

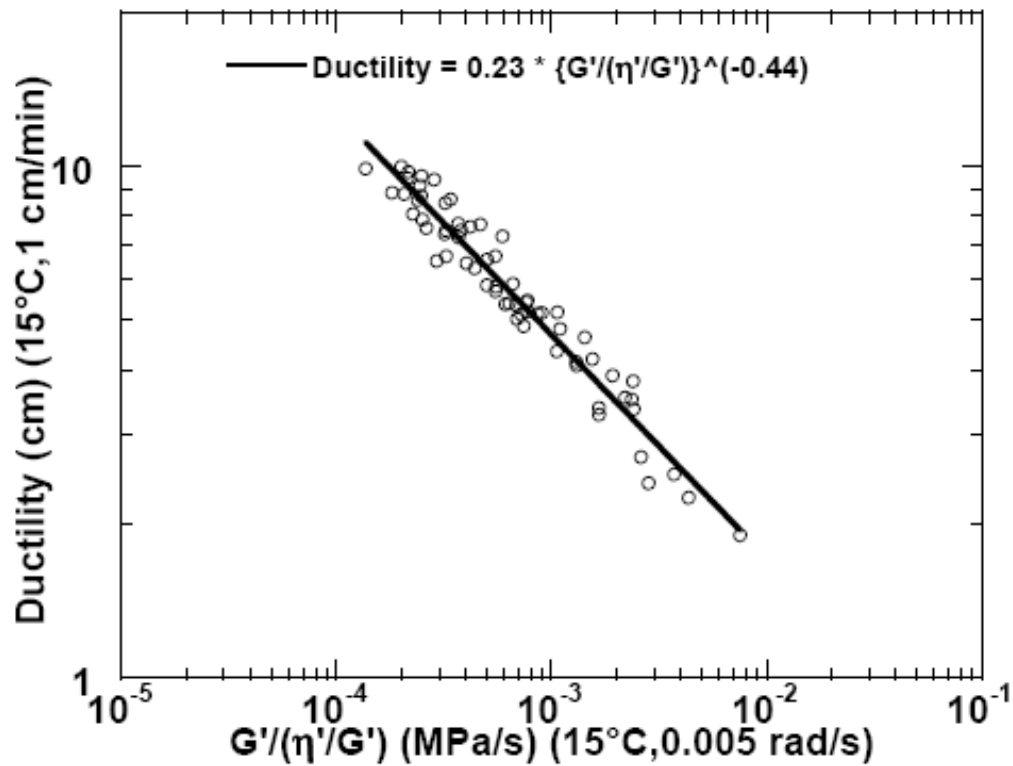


Figure 3.3 Relationship between Ductility and DSR Parameter (Glover et.al. 2005)

Although the parameter $G'/(η'/G')$ is determined at 15°C and 0.005 rad/s, - it was determined that this slow loading rate would make testing very difficult (requiring almost 20 minutes to complete one oscillatory cycle). As a result, it was decided to use time-temperature superposition principles to conduct testing at a standard frequency (10 rad/s). From their data, the researchers suggested that the same values for $G'/(η'/G')$ determined at 15°C and 0.005 rad/s could be obtained by testing at 44.7°C and 10 rad/s. This is the frequency used in AASHTO T315 and is most familiar to asphalt technologists performing DSR testing.

After the mastercurve was generated, the $G'/(η'/G')$ value was determined at 15°C and 0.005 rad/s. Data is shown in Tables 3.3 to 3.5 and graphically in Figure 3.4.

Table 3.3 West Texas Sour (WTX) – $G'/(η'G')$ at 15°C, 0.005 rad/s (MPa/s)

	Aging Time, hrs.			
	PAV0	PAV20	PAV40	PAV80
Replicate 1	1.32E-05	1.93E-03	1.56E-03	2.25E-02
Replicate 2	2.33E-05	1.92E-03	2.50E-03	2.01E-02
Replicate 3	2.47E-05	1.83E-03	n/a ¹	2.02E-02
Average	2.04E-05	1.89E-03	2.03E-03	2.09E-02
Standard Deviation (1s)	6.27E-06	5.51E-05	6.65E-04	1.36E-03
Coefficient of Variation (1s%)	30.7%	2.9%	32.7%	6.5%

¹ Data not available. Two re-tests were conducted with neither producing a valid mastercurve.

Table 3.4 Gulf-Southeast (GSE) – $G'/(η'G')$ at 15°C, 0.005 rad/s (MPa/s)

	Aging Time, hrs.			
	PAV0	PAV20	PAV40	PAV80
Replicate 1	3.12E-06	4.44E-04	1.36E-03	6.19E-03
Replicate 2	3.71E-06	3.87E-04	1.42E-03	6.09E-03
Replicate 3	2.03E-05	4.02E-04	1.48E-03	6.40E-03
Average	9.03E-06	4.11E-04	1.42E-03	6.23E-03
Standard Deviation (1s)	9.73E-06	2.95E-05	6.00E-05	1.58E-04
Coefficient of Variation (1s%)	107.7%	7.2%	4.2%	2.5%

Table 3.5 Western Canadian (WC) – $G'/(η'G')$ at 15°C, 0.005 rad/s (MPa/s)

	Aging Time, hrs.			
	PAV0	PAV20	PAV40	PAV80
Replicate 1	3.53E-07	1.98E-04	6.36E-04	5.72E-03
Replicate 2	2.66E-07	2.04E-04	6.13E-04	6.25E-03
Replicate 3	3.77E-07	1.98E-04	7.56E-04	2.92E-03
Average	3.32E-07	2.00E-04	6.68E-04	4.96E-03
Standard Deviation (1s)	5.48E-08	3.46E-06	7.67E-05	1.79E-03
Coefficient of Variation (1s%)	17.6%	1.7%	11.6%	36.1%

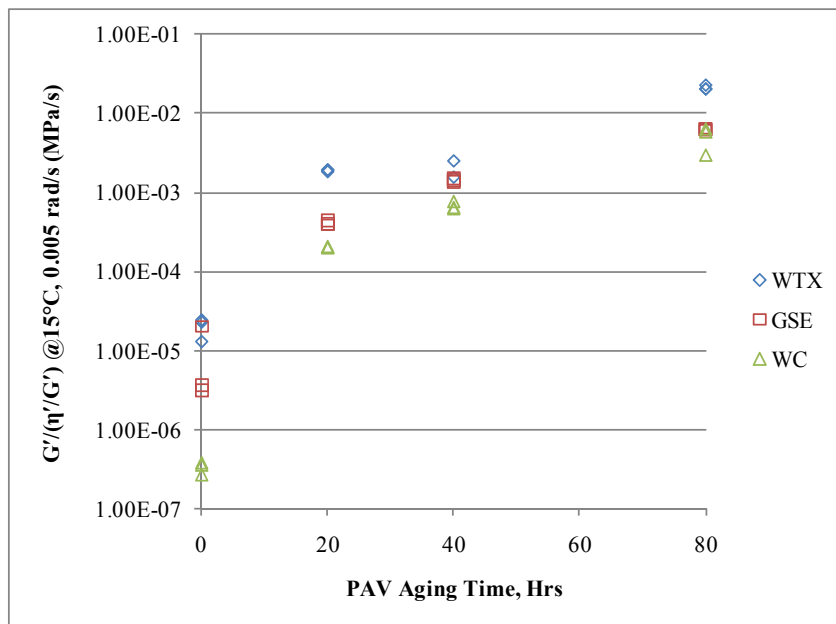


Figure 3.4 Effect of PAV Aging Time on $G'/(η'/G')$

As seen in Tables 3.3, 3.4, and 3.5 and Figure 3.4, $G'/(η'/G')$ values increase as aging increases for all three asphalt binders. Using the relationship in Figure 3.3, this increase in $G'/(η'/G')$ should indicate a decrease in ductility and, taking it a step further, to a related decrease in expected durability

Texas A&M Standard DSR Test

As noted earlier, it is procedurally difficult to determine $G'/(η'/G')$ directly at 15°C and 0.005 rad/s. However, Texas A&M researchers reported that by using time-temperature superposition principles the same data can be generated at a single higher test temperature (44.7°C) and faster loading frequency (10 rad/s).

The standard DSR test was conducted on the asphalt binder samples using 25-mm parallel plates with a gap of 1-mm. The AASHTO T315 procedure was followed for all samples, using a target strain amplitude of 10%. In retrospect, the strain should have been lowered for the tests on the more highly-aged asphalt binder samples, as some non-linearity was noted during the test.

After the test, the $G'/(η'/G')$ value was calculated using G^* and $δ$ (phase angle). To convert to a value at 15°C and 0.005 rad/s, the calculated value is divided by 2000 (ratio of 10 rad/s to 0.005 rad/s). Data is shown in Tables 3.6 to 3.8 and graphically in Figure 3.5.

Table 3.6 West Texas Sour – $G'/(η'G')$ at 44.7°C, 10 rad/s (MPa/s)

	Aging Time, hrs.			
	PAV0	PAV20	PAV40	PAV80
Replicate 1	1.14E-06	2.10E-04	2.60E-04	3.39E-03
Replicate 2	1.23E-06	2.18E-04	2.53E-04	3.25E-03
Replicate 3	1.64E-06	2.25E-04	2.52E-04	3.51E-03
Average	1.34E-06	2.18E-04	2.55E-04	3.38E-03
Standard Deviation (1s)	2.67E-07	7.42E-06	4.39E-06	1.32E-04
Coefficient of Variation (1s%)	19.9%	3.4%	1.7%	3.9%

Table 3.7 Gulf-Southeast – $G'/(η'G')$ at 44.7°C, 10 rad/s (MPa/s)

	Aging Time, hrs.			
	PAV0	PAV20	PAV40	PAV80
Replicate 1	1.32E-06	1.20E-04	3.38E-04	1.11E-03
Replicate 2	1.90E-06	1.19E-04	3.36E-04	1.12E-03
Replicate 3	2.07E-06	1.21E-04	3.45E-04	1.32E-03
Average	1.76E-06	1.20E-04	3.40E-04	1.18E-03
Standard Deviation (1s)	3.94E-07	1.21E-06	4.52E-06	1.17E-04
Coefficient of Variation (1s%)	22.4%	1.0%	1.3%	9.9%

Table 3.8 Western Canadian – $G'/(η'G')$ at 44.7°C, 10 rad/s (MPa/s)

	Aging Time, hrs.			
	PAV0	PAV20	PAV40	PAV80
Replicate 1	1.96E-06	1.48E-04	3.84E-04	1.51E-03
Replicate 2	2.88E-06	1.47E-04	3.79E-04	1.80E-03
Replicate 3	2,91E-06	1.41E-04	4.08E-04	1.88E-03
Average	2.58E-06	1.45E-04	3.90E-04	1.73E-03
Standard Deviation (1s)	5.42E-07	3.71E-06	1.55E-05	1.97E-04
Coefficient of Variation (1s%)	21.0%	2.6%	4.0%	11.4%

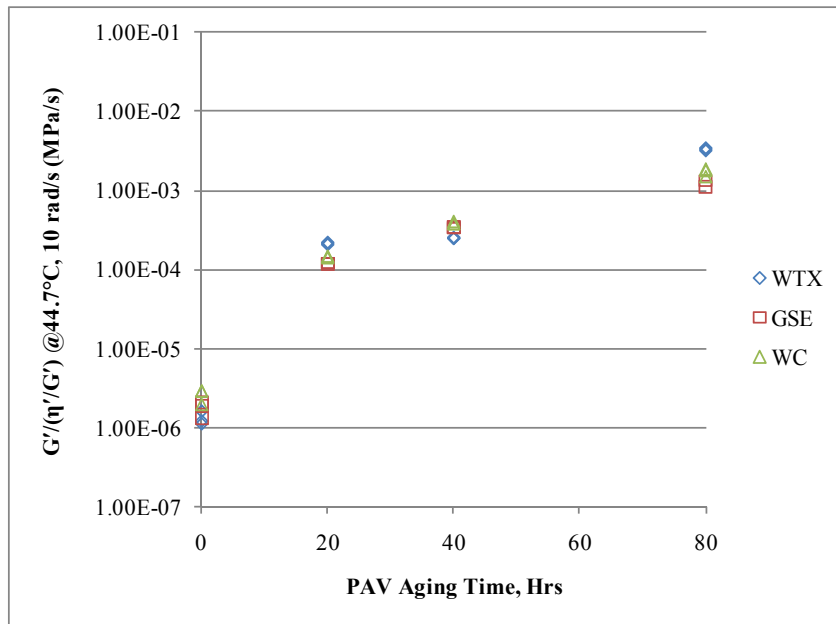


Figure 3.5 Effect of PAV Aging Time on $G'/(η'/G')$ Measured at 44.7°C, 10 rad/s

As seen in Tables 3.6 to 3.8 and Figure 3.5, $G'/(η'/G')$ values increase as aging increases for all three asphalt binders. However, unlike the data in Figure 3.4, there doesn't appear to be much discrimination among the different asphalt binders. Additionally, the West TX Sour asphalt – which would be expected to have the highest $G'/(η'/G')$ value – actually has the lowest value at two of the four PAV aging times (Figure 3.6).

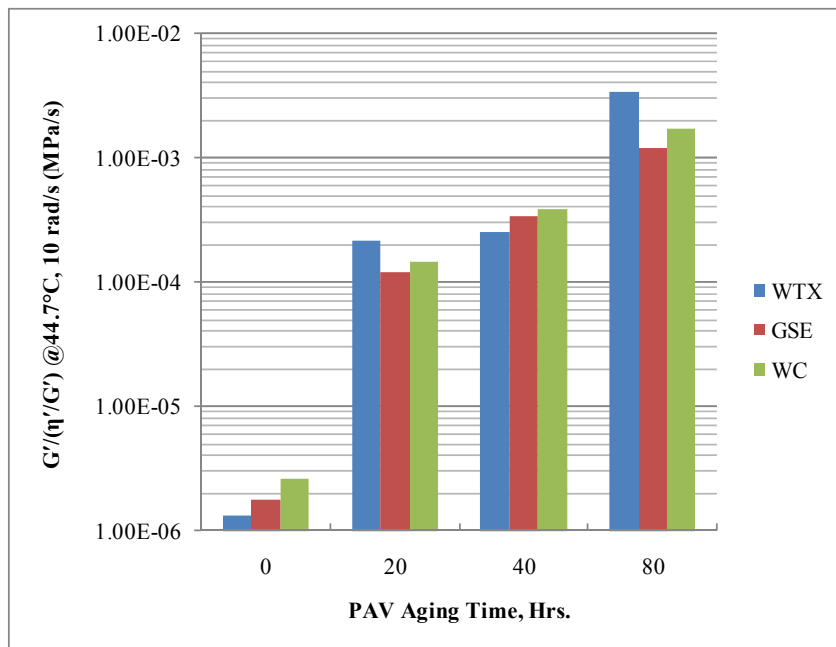


Figure 3.6 Effect of PAV Aging Time on $G'/(η'/G')$ Measured at 44.7°C, 10 rad/s

Comparison of $G'/(η'G')$ Determinations: Mastercurve and Standard DSR

The $G'/(η'G')$ values determined from the mastercurve procedure (15°C and 0.005 rad/s) and the Standard DSR procedure (44.7°C and 10 rad/s) were compared to determine if they were similar. From the data in Tables 3.3 to 3.8, it appears that the mastercurve procedure gives generally higher values of $G'/(η'G')$ than the Standard DSR procedure. This could be an indication that the temperature in the standard DSR procedure is too high to correlate with the data generated in the mastercurve procedure. This will need to be further investigated.

One of the concerns with the mastercurve procedure was that the temperature-frequency sweep and corresponding development of a mastercurve could result in significant variability in $G'/(η'G')$ values. An examination of the coefficient of variation for the mastercurve procedure (Tables 3.3 to 3.5) indicates that it is as good as, if not slightly better, than the coefficient of variation for the Standard DSR procedure (Tables 3.6 to 3.8). Both procedures exhibit acceptable levels of repeatability. The published single-operator coefficient of variability for DSR testing of PAV residue is 4.9%. The majority of coefficients of variation in Tables 3.3 to 3.8 for PAV-aged binders are less than this value.

With the understanding that the data in Figure 3.3 was generated with $G'/(η'G')$ values determined using the mastercurve procedure, it appears that this is the best approach at this time to determine the value of $G'/(η'G')$. The speed and ease of the Standard DSR procedure compared to the mastercurve procedure are certainly factors that need to be considered for users wishing to determine the value of $G'/(η'G')$ for a given asphalt binder, but this research did not support the use of the shortened procedure run at 10 rad/sec.

DSR Monotonic Shear Procedure

The DSR Monotonic Shear Procedure (also called the Binder Yield Energy Test) is a procedure that was explored by the Asphalt Research Consortium at the University of Wisconsin – Madison under the direction of Dr. Hussain Bahia. The test is conducted using a standard DSR with 8-mm parallel plates and a 2-mm gap. A constant shear rate is applied to the sample until a peak shear stress is recorded. The area under the stress-strain curve is then determined as the Binder Yield Energy (BYE). The researchers hypothesized that this BYE is related to the ability of an asphalt binder to withstand cracking, with higher energy values indicating better cracking resistance.

In this research, all testing was to be conducted at 15°C to coincide with other test measurements. An initial shear rate of 0.005 s⁻¹ was used. Data from the test is shown in Figure 3.7.

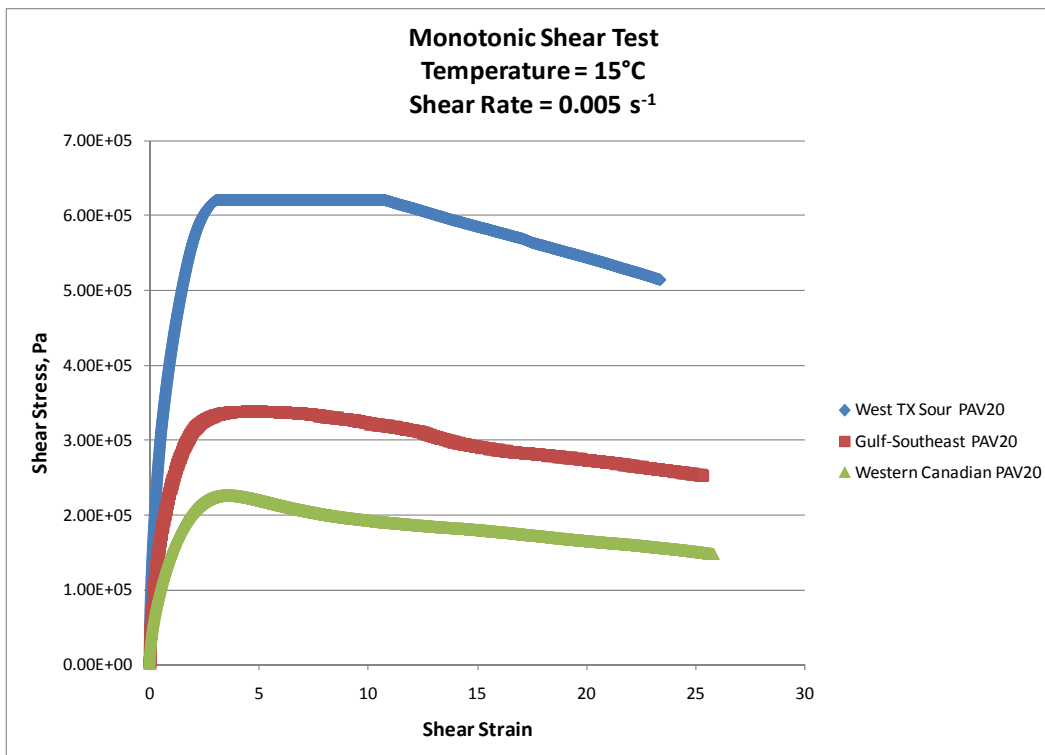


Figure 3.7 Monotonic Shear Test Results – PAV20

As can be seen in Figure 3.7, the area under the stress-strain curve – the Binder Yield Energy – is highest for the West TX Sour asphalt binder and lowest for the Western Canadian asphalt binder. This is exactly opposite of the expectations for cracking resistance. Because these binders were selected to have approximately equal high temperature grades but different low temperature grades, it seems logical that the Western Canadian crude with the best temperature grade range would be softer than the other asphalts at intermediate temperatures. It is believed that this data reflects that fact. It might further be assumed that the softer binder should have better resistance to cracking. Note also the plateau for the West TX Sour asphalt binder. After discussions with the researchers and DSR manufacturer, we believe this is due to delamination that is occurring at the binder-plate interface.

After this initial testing was reviewed, new information was presented at an Asphalt Binder Expert Task Group Meeting that indicated that the Monotonic Shear test procedure did not appear to be related to cracking resistance. As a result, further testing for this research was stopped.

Ductility

One of the starting assumptions in the Texas A&M research was that durability was a function of the ductility of the asphalt binder, specifically at 15°C and a loading rate of 1 cm/minute. Ductility data for the asphalt binders in this research are shown in Table 3.9.

Table 3.9 Ductility Results at 15°C, 1cm/min. (cm)

	Aging Time, hrs.			
	PAV0	PAV20	PAV40	PAV80
West TX Sour	150+	1 ^A	4	0.5
Gulf-Southeast	150+	6	4.25	1
Western Canadian	150+	10	5	1

^A Retest validated this result. Did not retest PAV40 sample to validate.

As expected, the ductility values were very low for the PAV-aged asphalt binders and generally decreased as aging time increased. The relationship between ductility and $G'/(η'/G')$ from Figure 3.8 is:

$$\text{Ductility (15°C, 1cm/min.)} = 0.23*[G'/(η'/G')]^{-0.44}$$

Using this relationship and the measured values of $G'/(η'/G')$, the measured ductility and predicted ductility can be compared. This comparison is shown in Table 3.10 and Figure 3.8.

Table 3.10 Comparison of Predicted and Measured Ductility

Measured Ductility (cm)	Texas A&M Standard DSR		Mastercurve	
	Meas. $G'/(η'/G')$ MPa/s	Pred. Ductility (cm)	Meas. $G'/(η'/G')$ MPa/s	Pred. Ductility (cm)
0.5	3.38E-03	2.8	2.09E-02	1.3
1	1.18E-03	4.5	6.23E-03	2.1
1	1.73E-03	3.8	4.96E-03	2.4
1	2.18E-04	9.4	1.89E-03	3.6
4	2.55E-04	8.8	2.03E-03	3.5
4.25	3.40E-04	7.7	1.42E-03	4.1
5	3.90E-04	7.3	6.68E-04	5.7
6	1.20E-04	12.2	4.11E-04	7.1
10	1.45E-04	11.2	2.00E-04	9.8

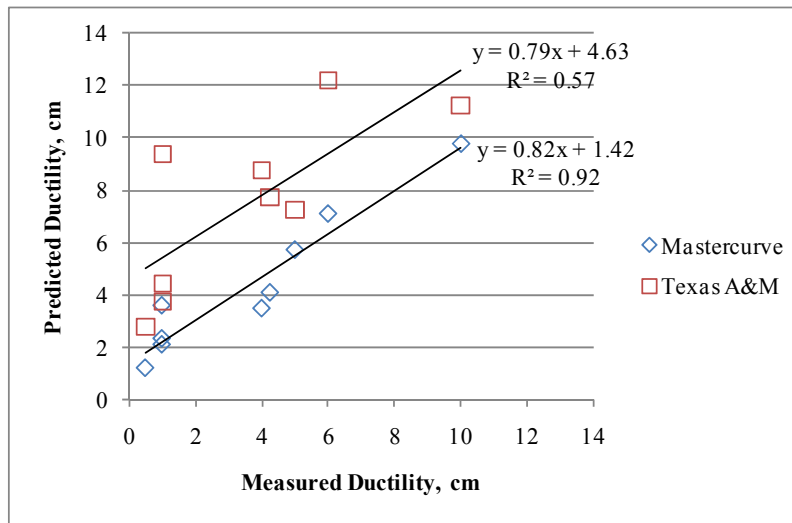


Figure 3.8 Comparison of Measured and Predicted Ductility

The $G'/(η'/G')$ value is used with the relationship in Figure 3.3 to predict the ductility. As seen in Figure 3.8, the predicted ductility using $G'/(η'/G')$ determined from the Mastercurve procedure is much closer to the measured ductility than predicted ductility using $G'/(η'/G')$ determined from the Standard DSR procedure. Additionally, the correlation is much better for the Mastercurve procedure – validating the relationship between ductility and $G'/(η'/G')$ as shown in Figure 3.3. The relationship between ductility and $G'/(η'/G')$ determined using the Mastercurve and Standard DSR procedures are shown in Figures 3.9 and 3.10.

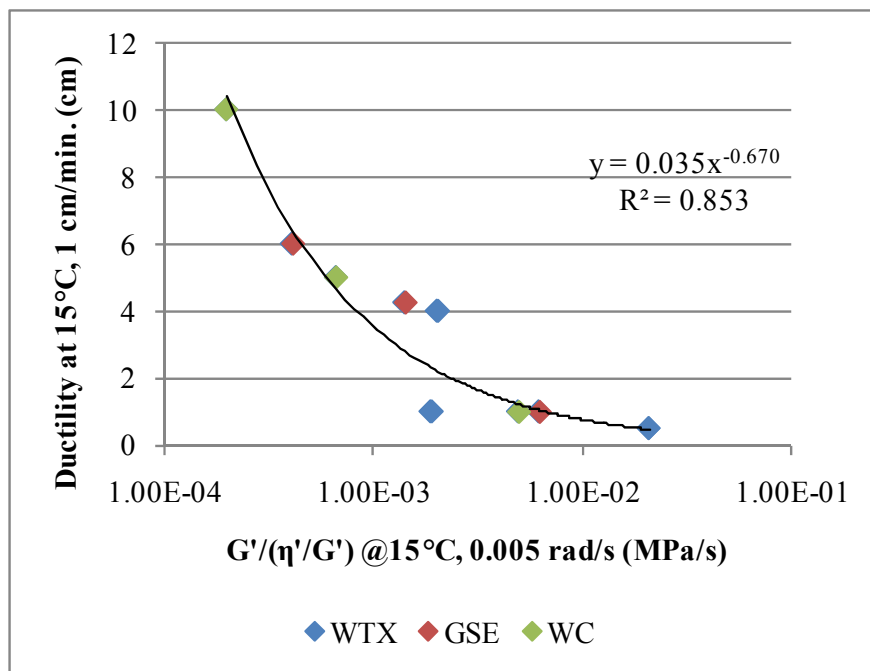


Figure 3.9 Relationship between Ductility and $G'/(η'/G')$ Using the Mastercurve Procedure

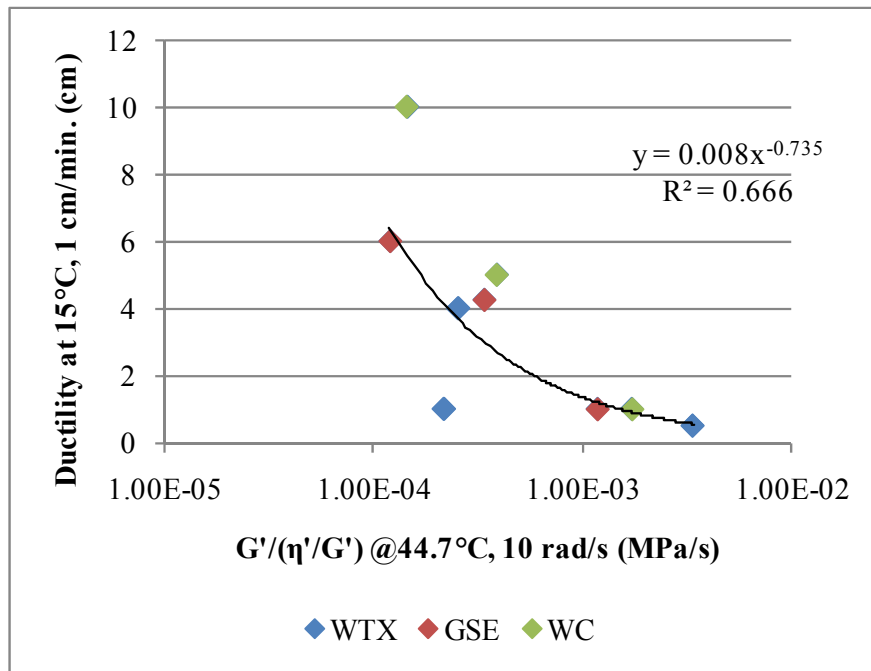


Figure 3.10 Relationship between Ductility and $G'/(η'/G')$ Using the Standard DSR Procedure

Force Ductility

Force Ductility testing was conducted in accordance with AASHTO T300 except that the test temperature was 15°C and the loading rate was 1 cm/minute. Figure 3.11 shows the stress-strain curves for the Gulf-Southeast asphalt binder. Figures 3.12 and 3.13 illustrate the effect of PAV aging time on peak stress and strain at peak stress from the Force Ductility test.

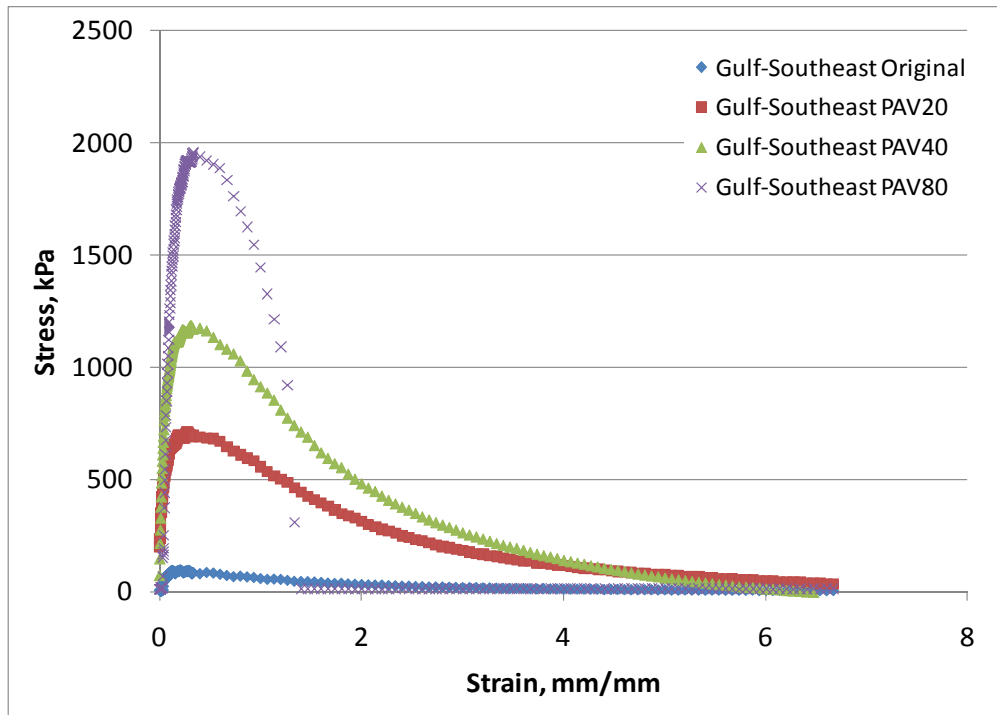


Figure 3.11 Force Ductility Stress-Strain Curves – Gulf-Southeast

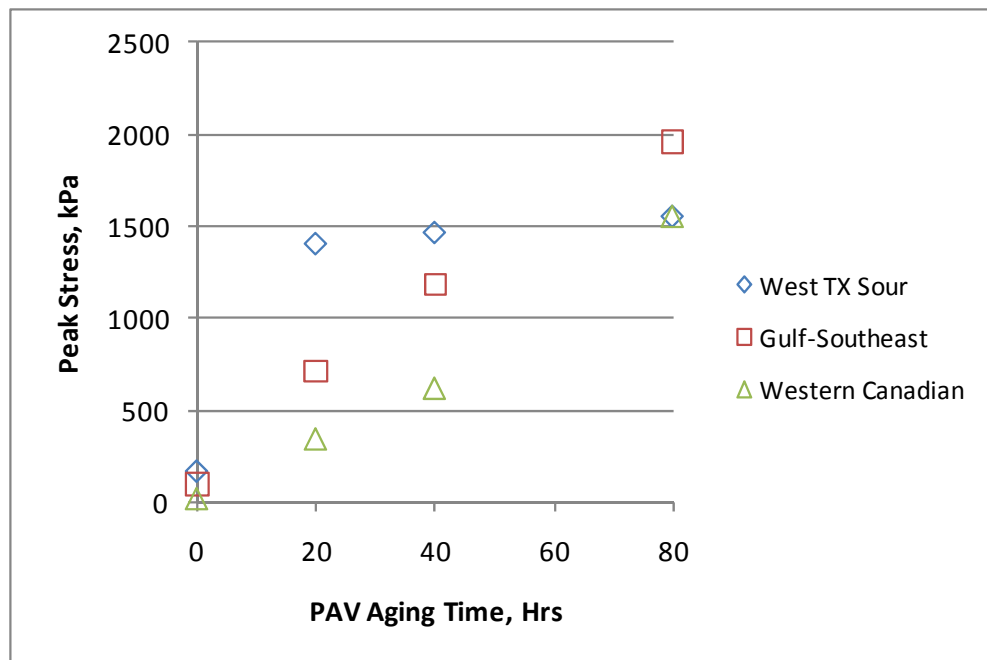


Figure 3.12 Effect of PAV Aging Time on Peak Stress in Force Ductility

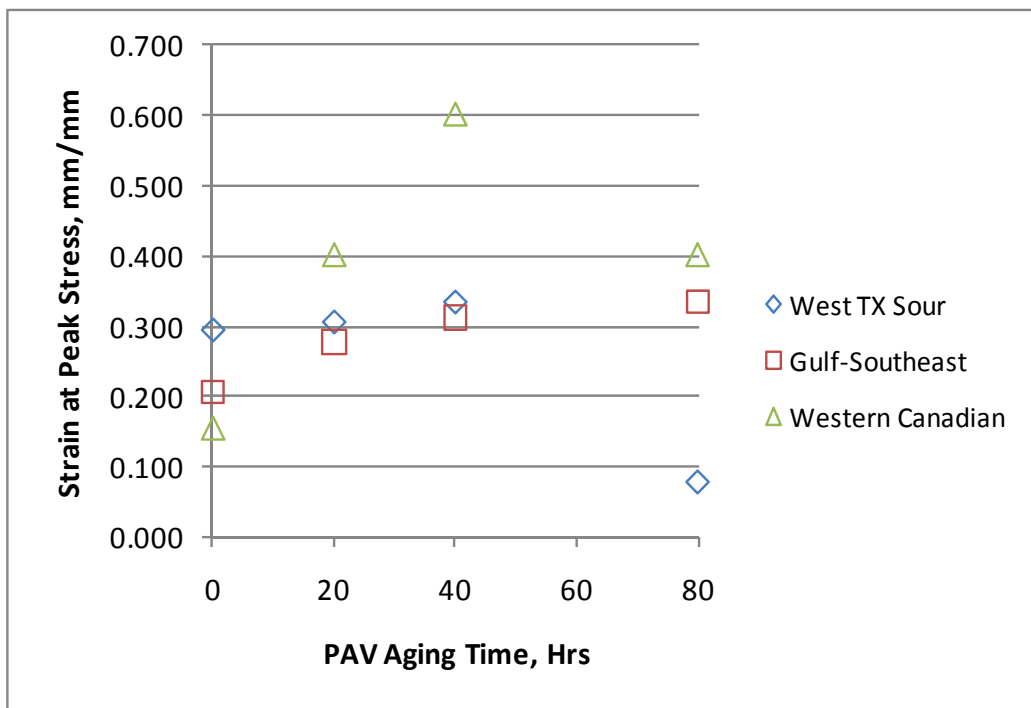


Figure 3.13 Effect of PAV Aging Time on Strain at Peak Stress in Force Ductility

Figure 3.12 indicates that the peak stress increases consistently with PAV aging time while the strain at peak stress, Figure 3.13, increases to a maximum and then decreases for two of the three asphalt binders. The area under the stress-strain curve appears very similar to the monotonic shear test. The large drop in peak strain for West Texas Sour after 80 hours aging suggests this sample has gone from ductile to brittle behavior under these test conditions. The Western Canadian crude appears to be transitioning from ductile to brittle, but is still slightly more ductile than the Gulf-Southeast bitumen after 80 hours in the PAV. Although these findings are consistent with other indicators of potential cracking, it isn't immediately apparent what Force Ductility parameter might predict performance. Based upon previous DTT research indicating that tensile failure strain is a performance parameter for cracking, there may be merit in further pursuing this test, perhaps by determining how much aging time was needed for the Strain-at-Peak-Load to fall below 0.10.

Bending Beam Rheometer

Low temperature testing was conducted following the procedures in AASHTO T313, *Determining the Flexural Creep Stiffness of Asphalt Binder Using the Bending Beam Rheometer (BBR)*. Data are shown in Tables 3.11 to 13.

Table 3.11 BBR Data for West TX Sour Asphalt Binder

		PAV0	PAV20	PAV40	PAV80
S(60), MPa	0°C		67	77	115
	-6°C	72	140	141	206
	-12°C	198	306	336	363
	T_{c,s} °C	-24.4	-21.9	-21.2	-20.0
m(60)	0°C		0.405	0.388	0.304
	-6°C	0.479	0.335	0.298	0.252
	-12°C	0.371	0.258	0.261	0.217
	T_{c,m} °C	-26.0	-18.7	-15.9	-10.4
	T_{c,m} - T_{c,s} °C	-1.5	3.1	5.4	9.6

Table 3.12 BBR Data for Gulf-Southeast Asphalt Binder

		PAV0	PAV20	PAV40	PAV80
S(60), MPa	-6°C	41	100	116	151
	-12°C	140	229	249	264
	-18°C	355	451	464	505
	T_{c,s} °C	-26.9	-24.4	-23.8	-23.2
m(60)	-6°C	0.553	0.381	0.338	0.300
	-12°C	0.421	0.312	0.282	0.253
	-18°C	0.314	0.246	0.236	0.207
	T_{c,m} °C	-28.8	-23.1	-20.0	-15.9
	T_{c,m} - T_{c,s} °C	-1.9	1.3	3.8	7.3

Table 3.13 BBR Data for Western Canadian Asphalt Binder

		PAV0	PAV20	PAV40	PAV80
S(60), MPa	-6°C		47	58	94
	-12°C	42	118	147	183
	-18°C	147	260	298	347
	T_{c,s} °C	-31.4	-29.1	-28.1	-26.7
m(60)	-6°C		0.453	0.397	0.319
	-12°C	0.552	0.377	0.335	0.283
	-18°C	0.439	0.317	0.286	0.253
	T_{c,m} °C	-35.4	-29.7	-26.2	-19.1
	T_{c,m} - T_{c,s} °C	-4.0	-0.6	1.8	7.5

For each combination of asphalt binder and PAV aging time, the critical temperature was calculated for Stiffness, S(60), and m-value, m(60). The critical temperature, T_c, is the temperature at which the specification limit is exactly met. For BBR Stiffness, T_{c,S(60)} is the temperature where the BBR Stiffness at 60 seconds loading, S(60), is exactly 300 MPa. For m-value, T_{c,m(60)} is the temperature where the BBR m-value at 60 seconds loading, m(60), is exactly 0.300. Formulas for determining T_c for S(60) and m(60) are shown below:

$$T_c = T_1 + \left[\frac{\text{Log}(300) - \text{Log}(S_1)}{\text{Log}(S_1) - \text{Log}(S_2)} \times (T_1 - T_2) \right] - 10$$

$$T_c = T_1 + \left[\frac{0.300 - m_1}{m_1 - m_2} \times (T_1 - T_2) \right] - 10$$

Where T₁ = Temperature #1, °C

T₂ = Temperature #2, °C

S₁ = Stiffness at 60 seconds loading at Temperature #1, MPa

S₂ = Stiffness at 60 seconds loading at Temperature #2, MPa

m₁ = m-value at 60 seconds loading at Temperature #1

m₂ = m-value at 60 seconds loading at Temperature #2

The critical temperatures for S(60) and m(60) are shown as a function of PAV aging time for the three asphalt binders in Figures 3.14 to 3.16.

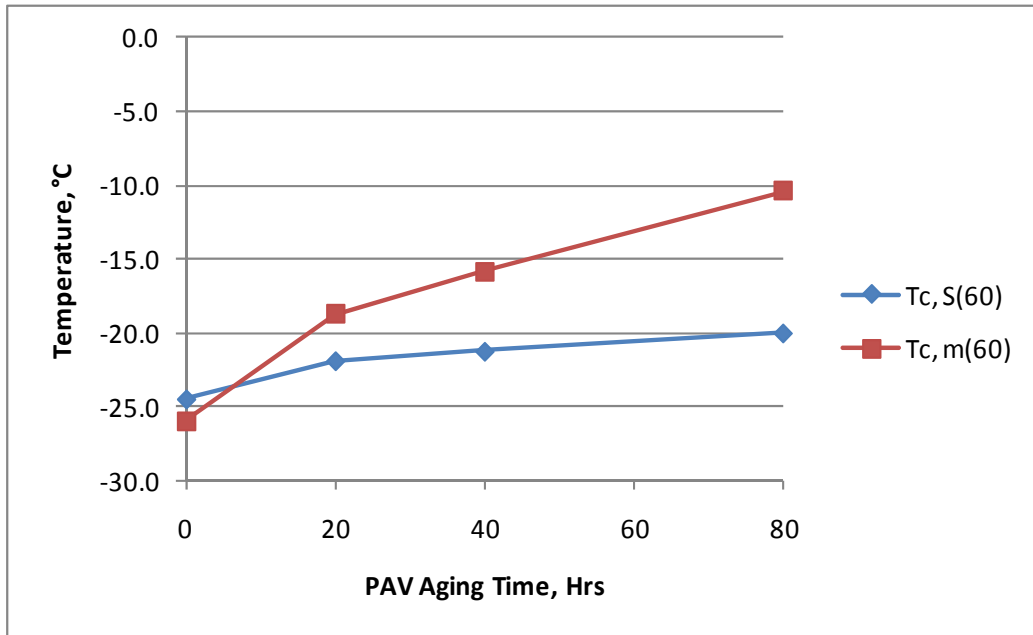


Figure 3.14 Effect of PAV Aging Time on Tc – West TX Sour

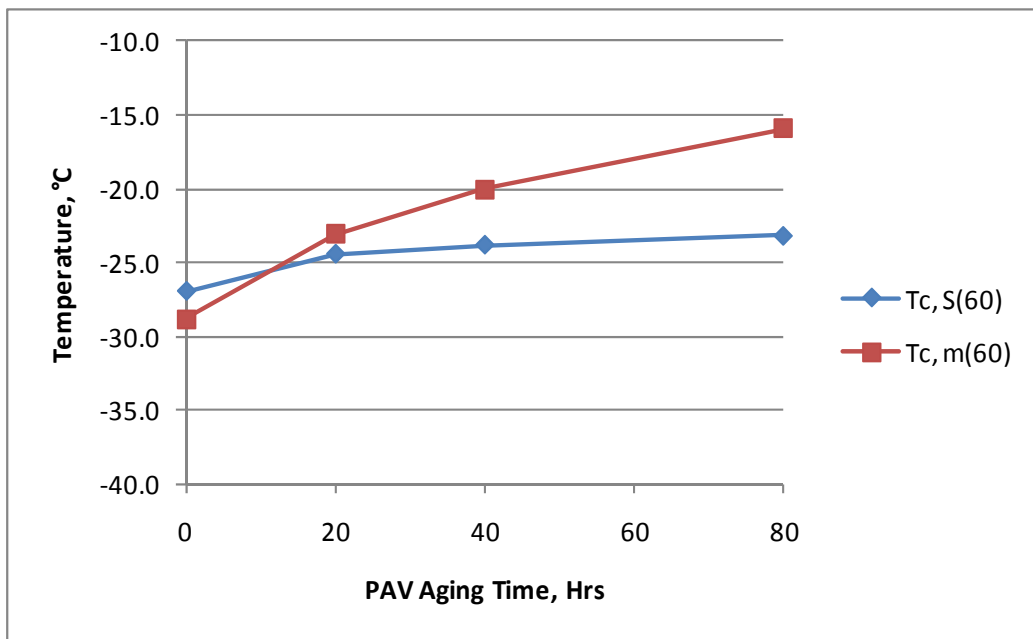


Figure 3.15 Effect of PAV Aging Time on Tc – Gulf-Southeast

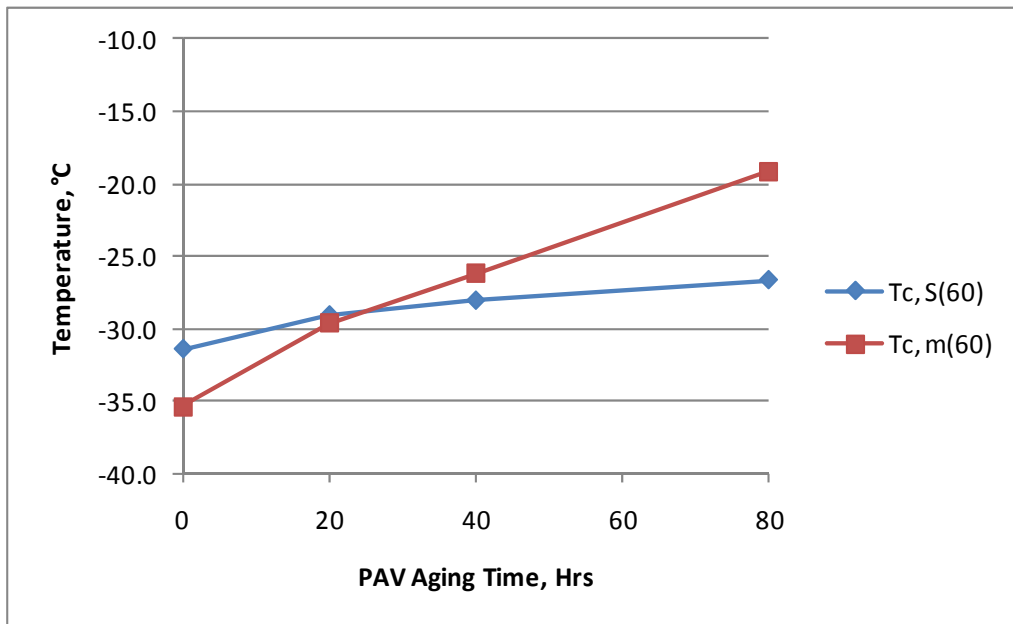


Figure 3.16 Effect of PAV Aging Time on Tc – Western Canadian

As shown in Figures 3.14 to 3.16, as PAV aging time increases the critical temperature for S(60) and m(60) both increase. However, the critical temperature for m(60) increases at a much more rapid rate indicating a loss of relaxation properties in the asphalt binder as aging increases. To quantify this change, the difference between Tc,m(60) and Tc,S(60) was determined. This difference is shown as a function of PAV aging time in Figure 3.17.

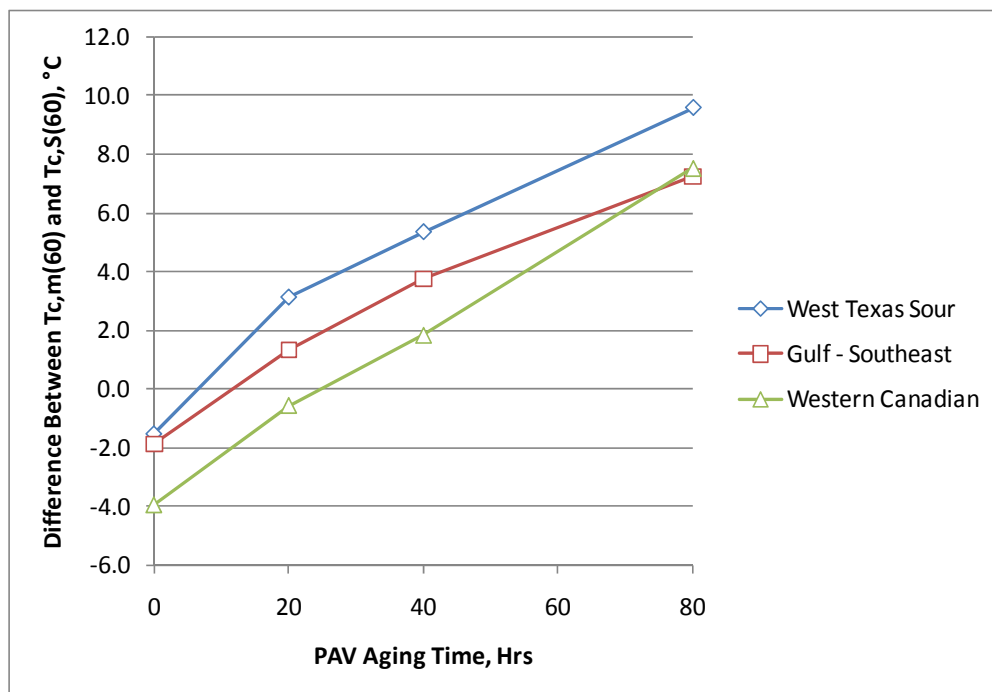


Figure 3.17 Effect of PAV Aging Time on the Difference between Tc,m(60) and Tc,S(60)

In Figure 3.17, the difference between $T_{c,m}(60)$ and $T_{c,S}(60)$ increases as aging time increases. This indicates a loss of relaxation properties relative to stiffness as the asphalt binder ages.

It is hypothesized that an increase in the difference between $T_{c,m}(60)$ and $T_{c,S}(60)$ indicates a loss of relaxation properties. As such, there should be a relationship between this parameter and ductility. This relationship is explored in Figure 3.18.

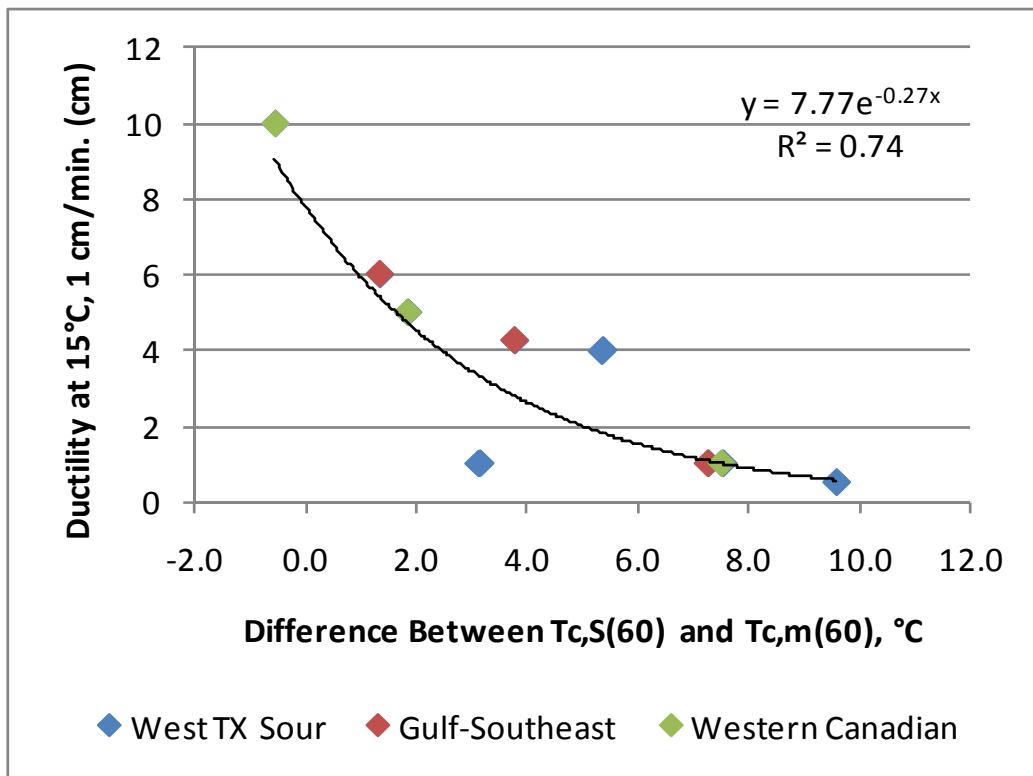


Figure 3.18 Relationship between ΔT_c and Ductility

As shown in Figure 3.18, there appears to be a fairly good relationship between ductility and the difference between $T_{c,m}(60)$ and $T_{c,S}(60)$ – termed ΔT_c . As ΔT_c increases (i.e., the asphalt binder becomes more m-controlled), the ductility decreases.

Critical Cracking Temperature Determination

The determination of an asphalt binder's critical cracking temperature (CCT) requires BBR testing at two or more temperatures and direct tension testing at two or more temperatures. BBR data is used to generate a mastercurve and, from that and other materials assumptions, to generate a thermal stress curve. Following the procedures in AASHTO PP42, the CCT is determined where the direct tension failure stress curve intersects the thermal stress curve.

Thermal stress curves are shown in Figures 3.19 to 21 for the three asphalt binders. The thermal stress curves and estimated critical cracking temperature were produced using the TSAR™ software developed by Abatech.

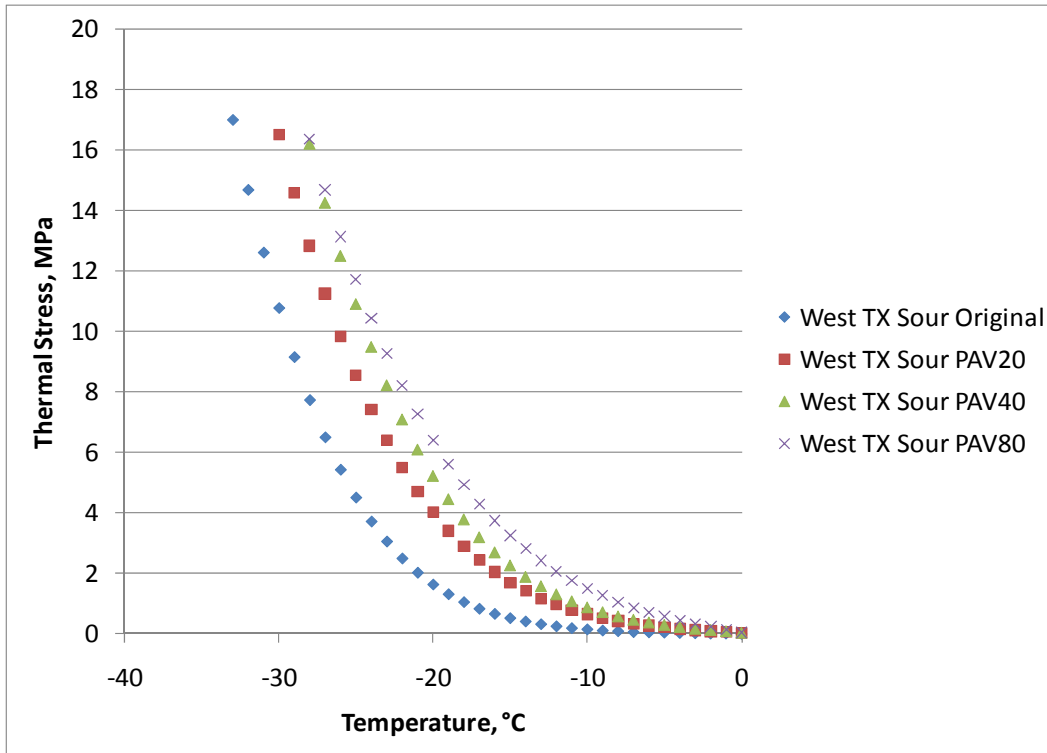


Figure 3.19 Thermal Stress Curves for West TX Sour Asphalt Binder

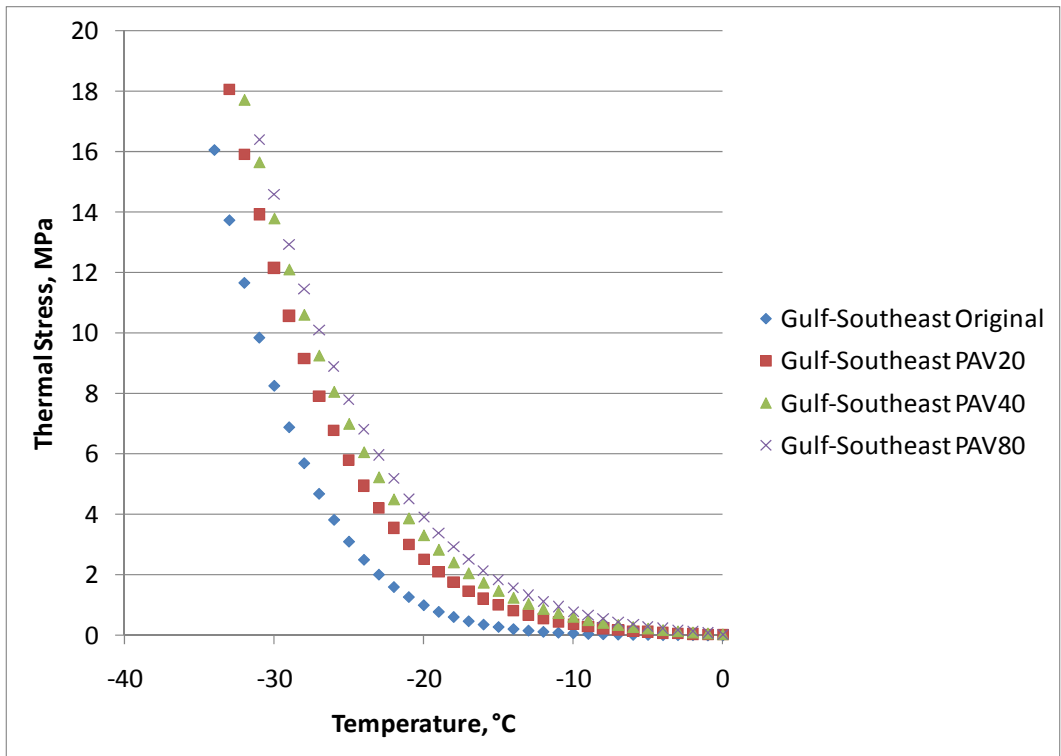


Figure 3.20 Thermal Stress Curves for Gulf-Southeast Asphalt Binder

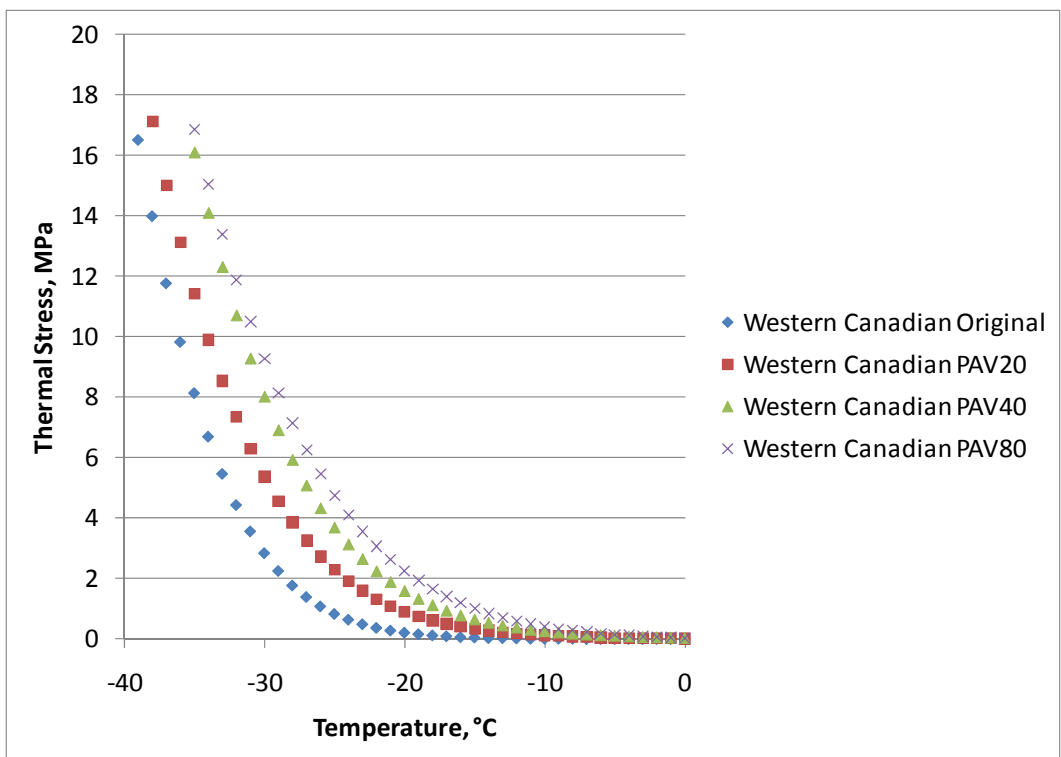


Figure 3.21 Thermal Stress Curves for Western Canadian Asphalt Binder

Direct tension tests were not conducted due to time and testing constraints. However, unmodified asphalt binders generally have very similar failure stresses. Based on published data, it seemed reasonable to assume that the failure stress of the asphalt binder was 3.5 MPa. By assuming a failure stress value, the CCT could be determined. This data is shown in Table 3.14 and Figure 3.22.

Table 3.14 CCT Results

	CCT, °C ^A			
	PAV0	PAV20	PAV40	PAV80
West TX Sour	-23.7	-19.2	-17.5	-15.5
Gulf-Southeast	-25.5	-21.9	-20.4	-19.2
Western Canadian	-30.9	-27.4	-24.7	-22.9

^A Assumes failure stress is 3.5 MPa for all asphalt binders and aging conditions.

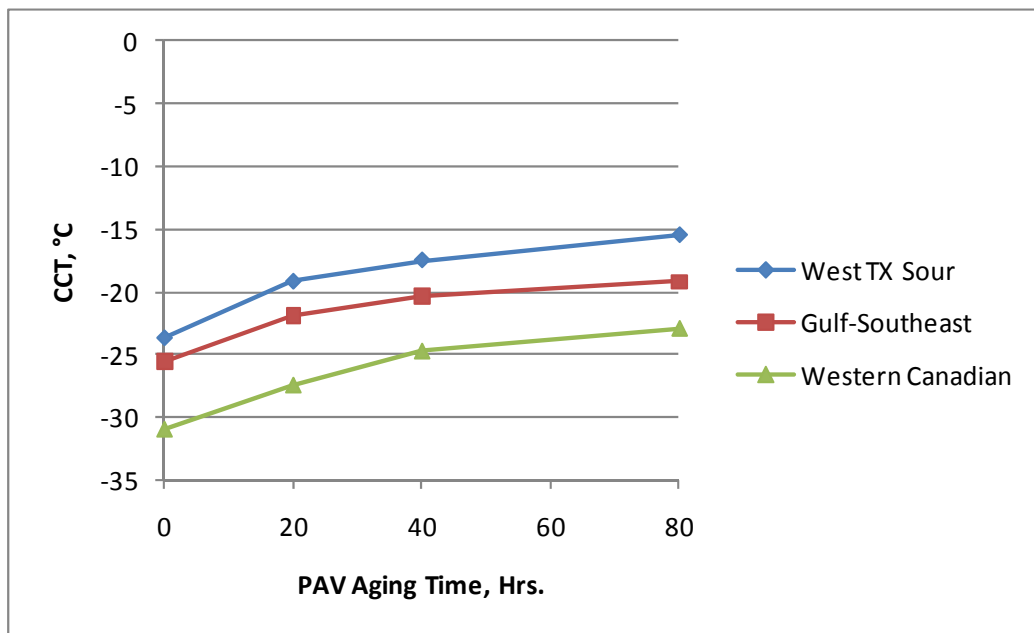


Figure 3.22 Effect of PAV Aging Time on CCT (assuming $\sigma_f = 3.5$ MPa)

As seen in Table 3.14 and Figure 3.22, the CCT of an asphalt binder increases as aging time increases. The change in CCT appears to be comparable to the change in the ΔT_c value determined from the BBR. This is to be expected as the thermal stress curves use both time and temperature-dependency of the binder stiffness to create the shape of the curve.

Discussion of Results

If we assume that ductility is related to durability, as suggested by the Texas A&M (and other) research, then the two best parameters identified during this experiment are the $G''/(\eta'/G')$ value determined from the Mastercurve procedure (15°C, 0.005 rad/s) and ΔT_c , the difference

between $T_{c,m}(60)$ and $T_{c,S}(60)$. Both parameters appeared correlated with measured ductility as shown in Figures 3.9 and 3.18.

The Texas A&M research identified two cracking values for $G'/(η'/G')$ corresponding to 5 cm and 3 cm ductility. The research suggests that asphalt binders having a ductility of 5 cm are approaching the point where cracking will occur. The research also suggests that asphalt binders having a ductility of 3 cm will exhibit cracking. The $G'/(η'/G')$ values corresponding to this cracking warning and cracking limit are $9.00E-04$ and $1.00E-03$ MPa/s when determined at $15^{\circ}C$ and 0.005 rad/s. The data in Figure 3.9 generally agrees with these values.

If $G'/(η'/G')$ is plotted as a function of ΔT_c , there appears to be, as expected, a good relationship. This is illustrated in Figure 3.23 with the cracking warning and cracking limit values shown for illustrative purposes. Upon reflection, the very high correlation ($r^2 > 0.98$) between these two parameters seems extraordinary when one considers that $G'/(η'/G')$ is reported to be a fatigue parameter as measured at $15^{\circ}C$, whereas ΔT_c is being proposed for prediction of block cracking that is thought to occur at much lower pavement temperatures.

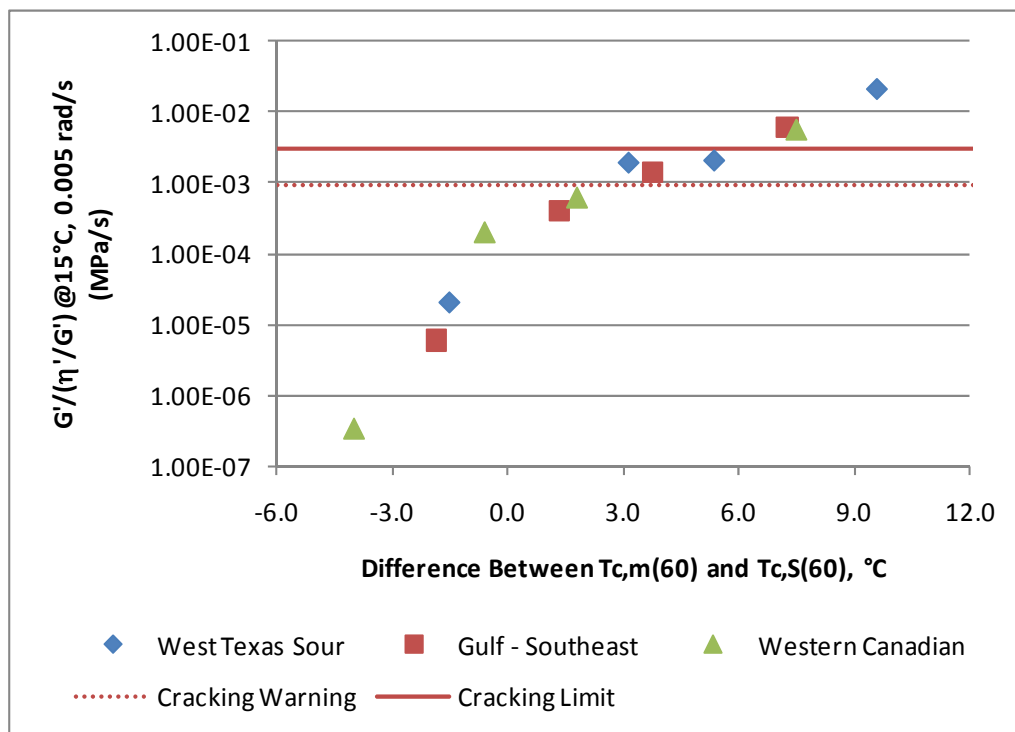


Figure 3.23 Relationship Between $G'/(η'/G')$ and ΔT_c

If the log of $G'/(η'/G')$ is plotted as a function of ΔT_c , the same curve shape is shown, but it becomes easier to fit a trend line to the data. This is shown in Figure 3.24.

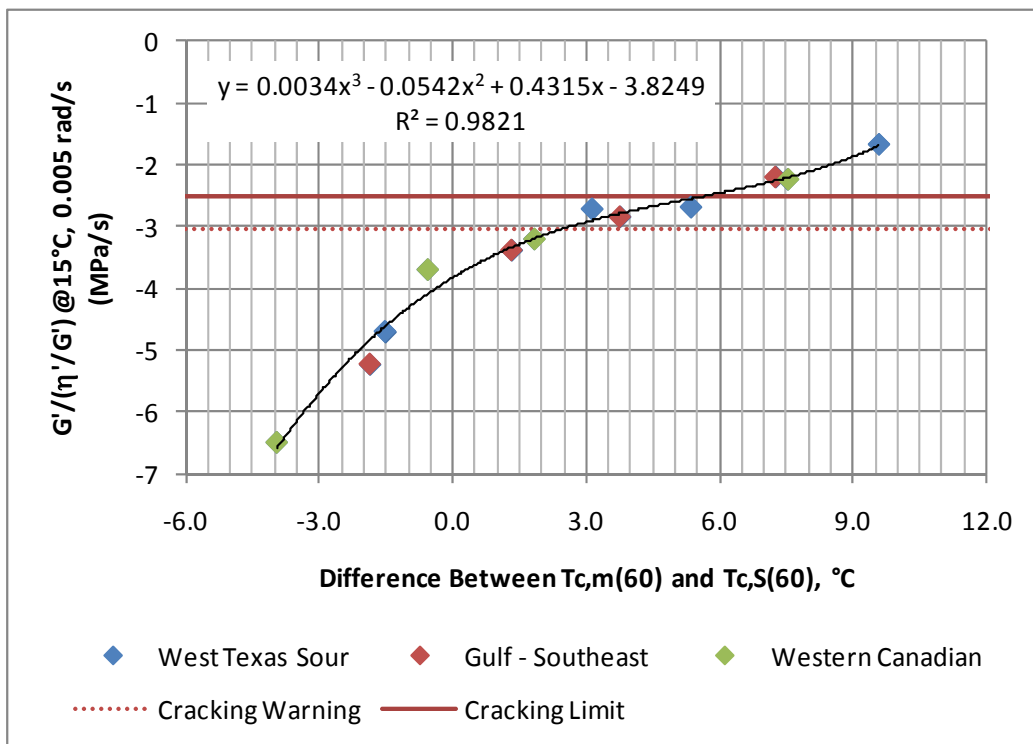


Figure 3.24 Relationship between Log $G'/(η'/G')$ and $ΔTc$

In Figure 3.24, the trend line is a 3rd-order polynomial, which may not be representative of the actual relationship, but does show how the data can be modeled (a 2nd-order polynomial has an R^2 value of 0.96). More importantly, it allows for a visual interpretation of the $ΔTc$ values at the cracking warning and cracking limit. Using the curve in Figure 3.24, the $ΔTc$ values at the cracking warning and cracking limit are 2.5°C and 5.0°C, respectively. These provide some target values to validate in further experiments.

Both binder parameters appear to have potential to relate to durability. The $G'/(η'/G')$ parameter has the advantage of being determined using a DSR, so a small sample size (less than 10 grams) is all that is needed. However, the best procedure at this time seems to be the mastercurve procedure in which a temperature-frequency sweep is conducted and data is used to produce a mastercurve from which the $G'/(η'/G')$ parameter can be calculated. This is non-standard testing and analysis for agencies, but it can be done with standard DSR's and applicable software.

The $ΔTc$ parameter uses the BBR (standard testing procedures) and is temperature-independent. Regardless of the binder grade or climate, when $ΔTc$ reaches 5.0°C, the ductility will have dropped to a level indicating a loss of durability. The negative to this procedure is that multiple temperatures (probably 3) are needed to accurately determine $Tc,S(60)$ and $Tc,m(60)$ using interpolation rather than extrapolation. When extracting asphalt from thin slabs of field cores, the Texas A&M Standard DSR method may be preferred because it can be run on much smaller sample sizes.

The temperature at which the $G''/(\eta'/G')$ value is determined needs to be reviewed. Kandhal's original work using 15°C ductility was validated using test sections in Ohio and Pennsylvania. Ductility is very sensitive to temperature, so warmer or colder climates would logically require the ductility limits be met at other temperatures. Some tie to pavement temperatures through LTPPBind should be made for each of these proposed cracking parameters, and further validation will be required. The ΔT_c parameter is already tied to climate because the BBR is run at the recommended low pavement temperature for that locale.

Effect of Aging on Shear Modulus and Phase Angle

The DSR parameter, $G''/(\eta'/G')$, and the difference between $T_{c,m}(60)$ and $T_{c,S}(60)$ – termed ΔT_c – both appear to relate to ductility, as shown in Figures 3.10 and 3.18, respectively. Both parameters provide an indication of a loss of relaxation properties as the asphalt binder ages.

A convenient way to look at this behavior is through the use of Black Space diagrams. In Black Space, the complex shear modulus (G^*) is plotted as a function of the phase angle (δ). An example of this data is shown in Figure 3.25 for the Western Canadian asphalt binder.

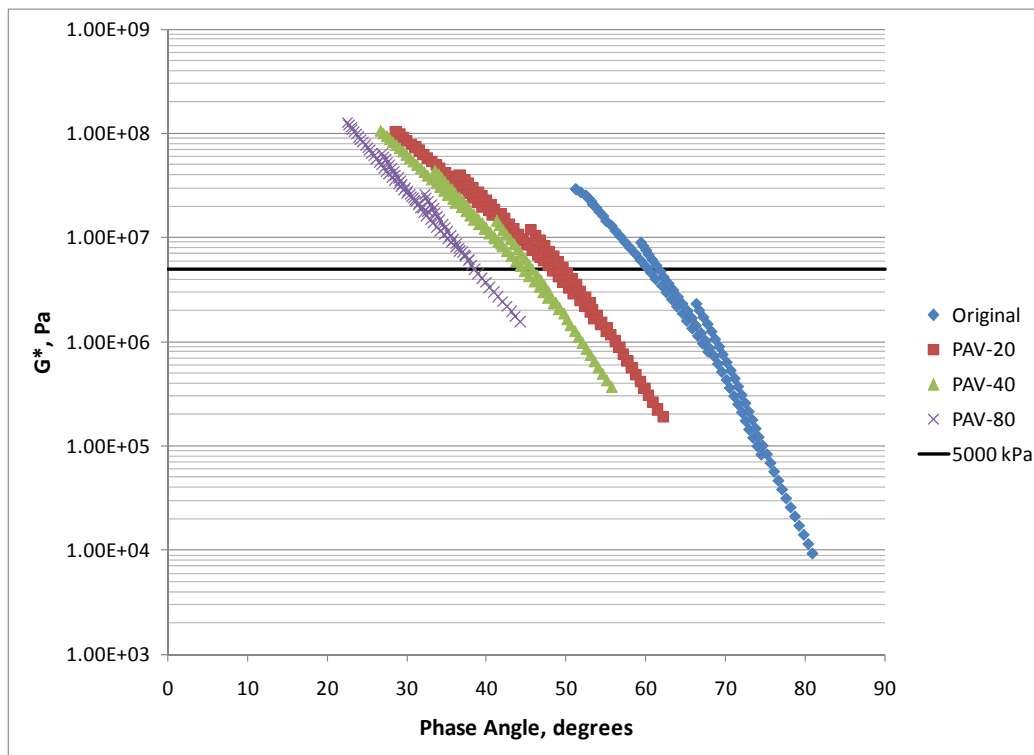


Figure 3.25 Black Space Diagram for Western Canadian Asphalt Binder

As the asphalt binder ages, the Black Space curves move to the right on the x-axis indicating a decrease in phase angle at a given stiffness. To illustrate this response, a horizontal line is

drawn at a G^* value of $5E+06$ Pa (5000 kPa). Approximate phase angles are shown in Table 3.154 as a function of aging, assuming a constant complex shear modulus value.

Table 3.15 Phase Angle as a Function of Aging – Western Canadian Asphalt Binder

Condition	Approximate Phase Angle, degrees (at $G^* = 5E+06$ Pa)
Original	61
PAV-20	49
PAV-40	45
PAV-80	38

The data in Table 3.14 and Figure 3.25 indicate that the asphalt binder exhibits more elastic (solid) behavior as it ages. This response is rational considering the DSR parameter, ΔT_c , and ductility.

The DSR parameter can be re-written as

$$\frac{G'}{\eta'} = \frac{\omega G^* \cos \delta}{\tan \delta}$$

As shown in the rewritten equation, the DSR parameter captures both G^* and phase angle. As the phase angle (δ) decreases towards 0 degrees, the denominator decreases rapidly and the value of the equation increases rapidly. As the phase angle increases towards 90 degrees, the denominator increases rapidly and the value of the equation decreases rapidly. In other words, at a given G^* , the greater the phase angle the lower the DSR parameter and the higher the ductility.

As the DSR parameter was determined from a mastercurve at 15°C, it seemed appropriate to examine the characteristic parameters of the mastercurves – particularly R, the Rheological Index - to see how it was affected by aging.

As discussed in SHRP and other reports, the Rheological Index, R, is the difference between the glassy modulus and the complex shear modulus at the crossover frequency (where $\tan \delta = 1$). According to SHRP Report A-369, "...[R] is directly proportional to the width of the relaxation spectrum and indicates rheologic type. R is not a measure of temperature, but reflects the change in modulus with frequency or loading time and therefore is a measure of the shear rate dependency of asphalt cement. R is asphalt specific." This is illustrated in Figure 3.26.

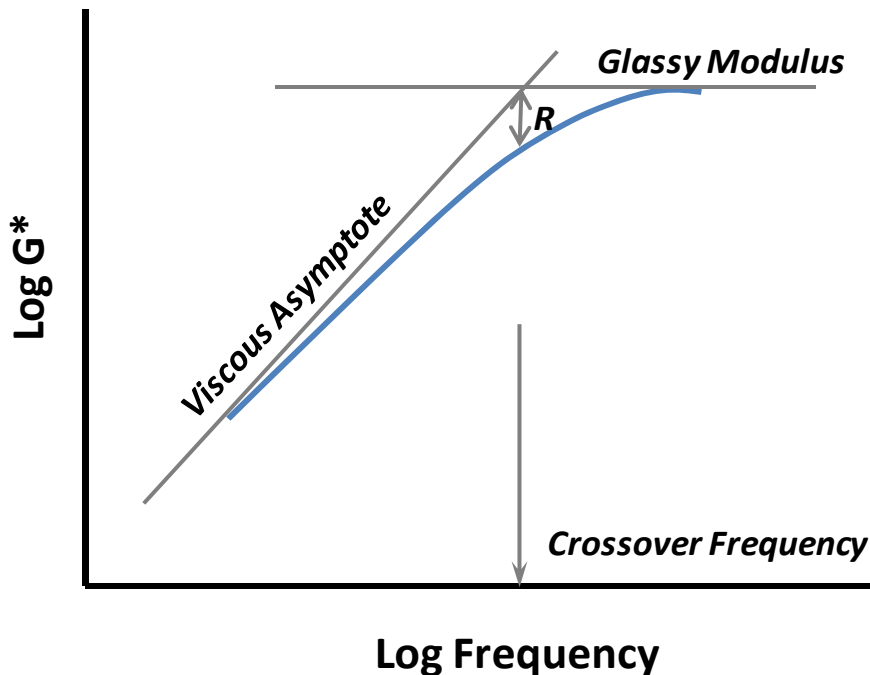


Figure 3.26 Mastercurve Characteristic Parameters

Since R is a measure of shear rate dependency, it was hypothesized that it should relate to the DSR parameter at the same temperature. Using equations developed during SHRP, R was calculated for each of the mastercurves as follows:

$$R = \frac{(\log 2) * \log \frac{G^*(\omega)}{G_g}}{\log \left(1 - \frac{\delta(\omega)}{90} \right)}$$

where: $G^*(\omega)$ = complex shear modulus at frequency ω (rad/s), Pa
 G_g = glassy modulus, Pa (assumed to be 1E+09 Pa)
 $\delta(\omega)$ = phase angle at frequency ω (rad/s), degrees (valid between 10 and 70°)

By observation, one can see that R becomes larger as the phase angle decreases at a given value of G^* . By converse, R becomes smaller at a given phase angle as G^* increases. This response is similar to the type of response seen with the Glover DSR parameter.

Note that R can be determined using the preceding equation at any phase angle. As a result, R was calculated at two conditions: (1) at the crossover frequency at 15°C where $\delta = 45$ degrees; and (2) at the same frequency at 15°C as the DSR parameter (0.005 rad/s). Tables 3.16 and 3.17 indicate the average R values for the three asphalt binders and four aging conditions.

Figures 3.27 and 3.28 illustrate the relationship between $G'/(η'/G')$ and R for the PAV-aged samples.

Table 3.16 Determination of R (15°C, δ = 45°)

	West Texas Sour	Gulf Southeast	Western Canadian
Original	1.70	1.70	2.06
PAV-20	2.14	2.03	2.10
PAV-40	2.22	2.22	2.35
PAV-80	2.88	2.62	2.95

Table 3.17 Determination of R (15°C, 0.005 rad/s)

	West Texas Sour	Gulf Southeast	Western Canadian
Original	1.38	1.43	1.37
PAV-20	1.95	1.89	2.16
PAV-40	1.95	2.12	2.43
PAV-80	2.67	2.51	2.92

The data in Tables 3.16 and 3.17 indicate that R increases as the aging increases. The only contradictory data points are for the unaged West Texas Sour asphalt binder. However, these data are very suspect due to the poor mastercurve fit from the temperature-frequency sweep data.

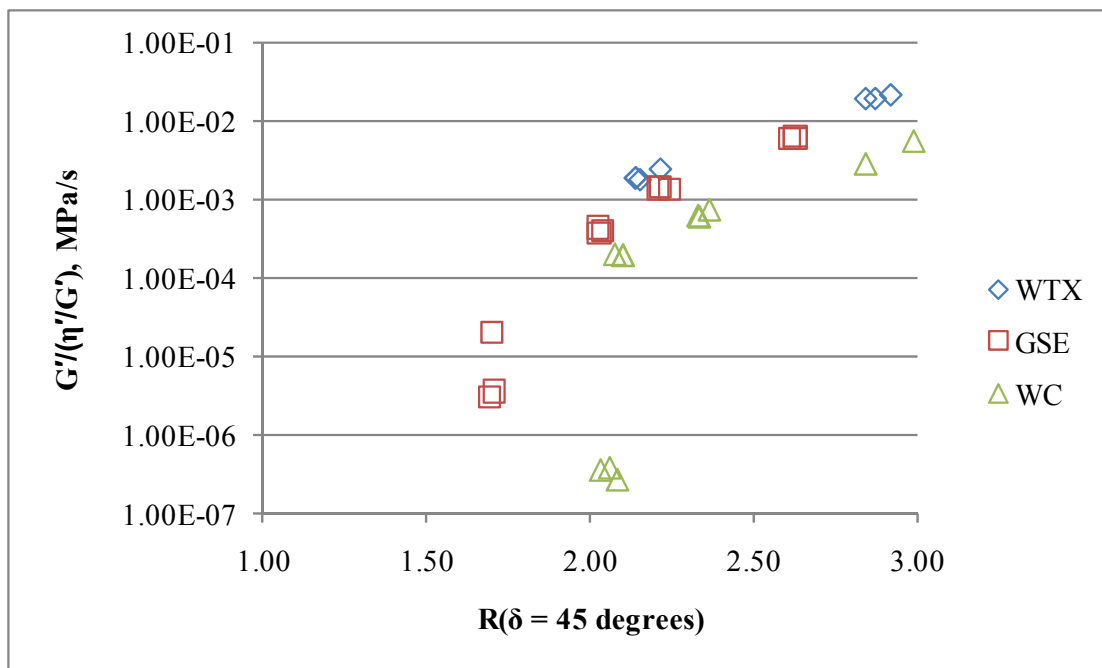


Figure 3.27 Relationship Between $G'/(η'/G')$ and R (15°C, δ = 45°)

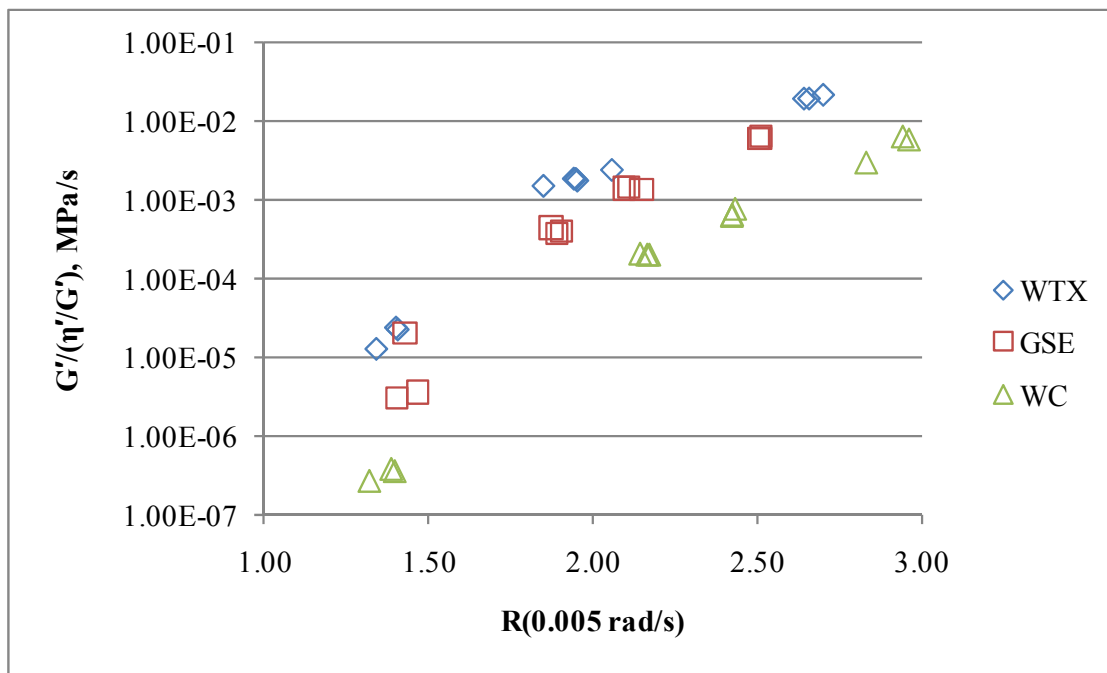


Figure 3.28 Relationship Between $G'/(η'G')$ and R (15°C, 0.005 rad/s)

As can be seen in Figures 3.27 and 3.28, there is a clear relationship between $G'/(η'G')$ and R , with increasing R related to increasing values of $G'/(η'G')$. Unlike the data in Figure 3.23, however, it appears that there is a unique relationship between $G'/(η'G')$ and R for each asphalt binder. In other words, a single value of R cannot be related to a single value of $G'/(η'G')$, because the two parameters are very different functions of the same two variables, G^* and phase angle. Thus, if ductility, ΔT_c , and the DSR parameter are found to predict any specific cracking mechanism, the rheological index (R) cannot predict that same cracking mode. At this time, the research team does not believe that R can be an effective predictor of non-load associated cracking, so no further analysis was included in mix and field validation experiments.

3.3 ASPHALT MIXTURE

3.3.1 Sample Preparation and Laboratory Aging to Simulate Field Conditions

Laboratory mixtures were made using standard testing procedures except for the loose-mix laboratory aging/conditioning. As mentioned earlier, the compacted sample aging procedure in AASHTO R30 was determined to not be severe enough for non-load associated surface cracking. All samples used the same batch of aggregates described in Chapter 2.

Samples were mixed for Maximum Theoretical Specific Gravities, Disk-Shaped Compact Tension [DC(t)] testing, and Bending Beam Rheometer (BBR) testing at each loose mix aging time aging time of 0, 4, 24, and 48 hours. The G_{mm} was also determined at 2 hours of aging.

Aggregates were heated and mixed at 149°C (300°F) with the asphalt binder representing each crude source. All mixtures were aged at 135°C (275°F). To lessen the variable of various aging temperatures, one mixing and compacting temperature was used.

During aging, the mixtures were placed in a forced-draft oven. Due to the impracticality of stirring every hour, the mixtures were not disturbed until time to compact. Once the mixtures were aged, the mixtures were removed from the oven and mixed with a metal scraper/spatula. The 24 and 48-hour samples had some pieces that had to be broken up more than the lesser aged mixtures.

G_{mm} samples were removed from the oven and spread on a Table to cool before testing. Samples to be used for DC(t) and BBR mixture testing were removed from the oven and compacted to a constant height in order to obtain 7.0 ± 0.5 percent air voids using a Superpave Gyrotory Compactor (SGC) to target air voids that are representative of in-place airfield pavements.

3.3.2 Maximum Theoretical Specific Gravities (G_{mm})

Maximum Theoretical Specific Gravities of the mixture (G_{mm}) were determined for each aging time and incorporated into the fabrication of the test samples. The value of G_{mm} varied with the asphalt type and continued to increase as the mixtures aged (Table 3.18 and Figure 3.29). The aging mixtures absorbed asphalt at different rates depending on the absorption of the aggregate, aging temperature, and viscosity and stiffness of the binder. As the mixtures absorbed asphalt, they became heavier, approaching the gravity of the aggregate.

While all G_{mm} values started at about 2.500 at time 0 hours and approached 2.520 after 48 hours, they varied while aging. The PG 64-22 and PG 64-25 reached 2.522 and 2.521 after 24 hours, while the PG 64-16 was only 2.511. This was expected since the PG 64-16 should absorb into the aggregate more slowly if it is “stiffer” (-16 low temperature grade). Figure 3.29 indicates the PG 64-16’s flatter absorption slope.

The allowed error for the G_{mm} test is 0.010 with the same operator. Although measured changes are not large with respect to allowed test variability, there does seem to be a trend in the data as the values increased from 2.50 to about 2.52. In Figure 3.29, the 0 hour aging was treated as 0.1 hour in order to utilize a logarithmic trend line.

Table 3.18 Aging Effect on Mixture Gravity (G_{mm})

Aging Time, hr	Average G_{mm}		
	Gulf-Southeast PG 64-22	West Texas Sour PG 64-16	Canadian PG 64-28
0	2.501	2.504	2.494
2	2.503	2.501	2.511
4	2.503	2.508	2.505
24	2.522	2.511	2.521
48	2.521	2.518	2.519

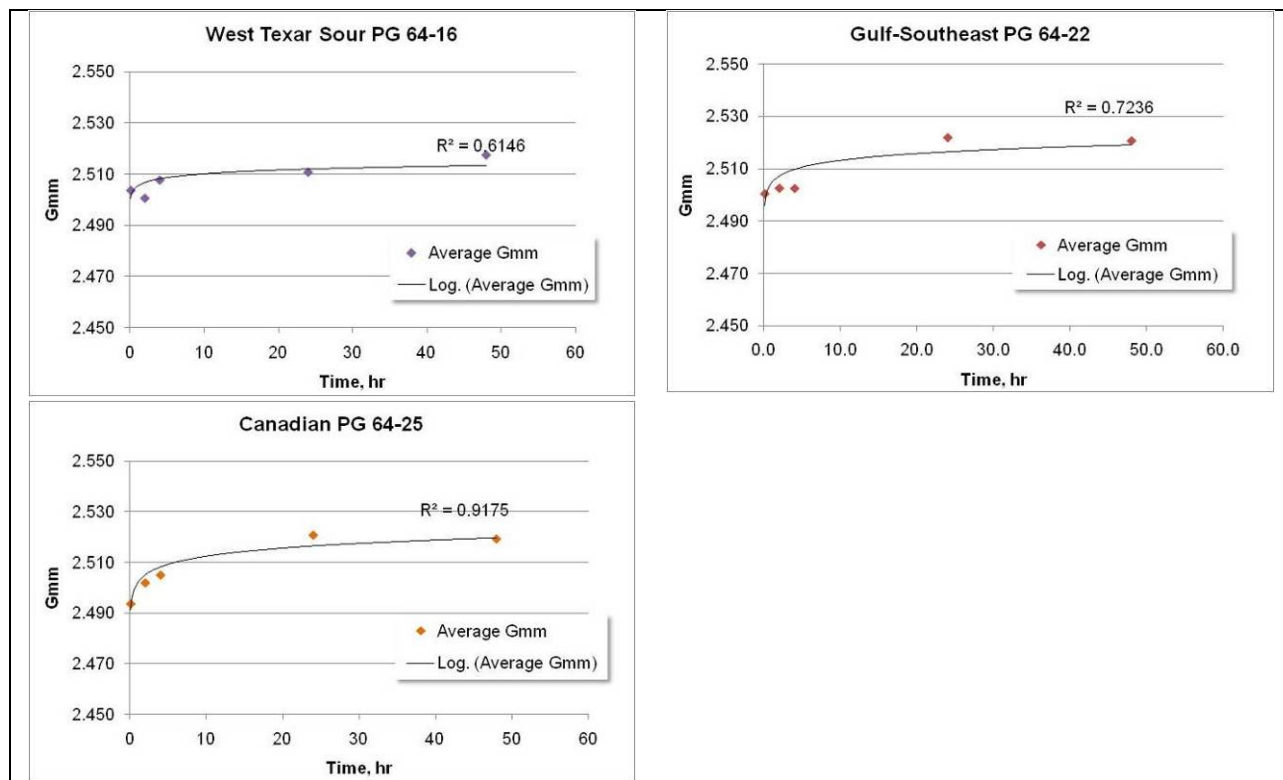


Figure 3.29 Mixture Gravity and Aging Time of the Loose Asphalt Mixture

3.3.3 Bending Beam Rheometer (BBR) on Mixtures

Mixture Bending Beam Rheometer (BBR) Testing

The rate of asphalt oxidation varies significantly with depth, creating the most pronounced rheological changes near the pavement surface. Therefore, any field mixture test used to predict the onset of surface cracking must be able to test thin specimens of ½” or less at relatively low temperatures where damage is thought to initiate. In a study evaluating the performance of RAP in asphalt mixtures, Marasteanu (5) found that the Bending Beam Rheometer (BBR) can test asphalt mixtures in thin beams to derive creep compliance curves. He then applied the Hirsch model to back-calculate the binder stiffness and obtain critical cracking temperatures. The BBR Mixture Bending Test was included in the laboratory mixture aging phase of this study.

Testing Protocol

Mixture Aging - Loose, uncovered mixtures were aged in a force-draft oven for 4hr, 24hr, and 48hr at 135°C. After aging, mixtures were compacted in a Superpave Gyratory Compactor (SGC) to target air voids that are representative of in-place airfield pavements. This method is also currently being explored by the University of Illinois at Champaign-Urbana.

Note: During phase 1 of this study, compacted specimens were aged using typical Superpave mixture aging protocols. This initial test series raised concerns that aging of compacted specimens does not result in uniform oxidation throughout, particularly at longer aging times where more oxygen is consumed. All BBR mixtures were tested within 2 months of laboratory preparation.

Sample Prep – Following compaction, eight BBR-sized beams and 1” thick DCT slabs were cut from each specimen. Remaining mix from each specimen was then extracted for later binder testing.

BBR Testing – The aged mixture beams were tested in the BBR using Marasteanu’s method which applies a 500-gram load. Four beams were tested at each of two temperatures selected from the standard PG grading temperatures immediately above and below the continuous low temperature PG grade of the binder itself. For West Texas Sour, the BBR test temperatures were -6°C and -12°C. For Gulf-Southeast and Western Canadian, the BBR test temperatures were -12°C and -18°C.

Analysis of Rheological Properties Stiffness (S) and m-value:

The working hypothesis for this study assumes that low temperature relaxation properties (m-value) deteriorate more quickly than stiffness as asphalt oxidizes. As m-value falls, the binder can no longer flow fast enough to heal any damage that might accumulate in the mix. The binder testing phase of this study validated the hypothesis by demonstrating that the BBR critical temperature for m-value deteriorates much faster than the critical temperature for stiffness

during PAV aging. The parameter ΔT_c , defined as the difference in these two critical cracking temperatures, was identified as a possible predictive parameter for the onset of block and fatigue cracking.

The problem now is to determine whether these same trends exist in mixes. Using Marasteanu's method, BBR results for S and m-value were collected for aged mixtures as reported in Table 3.19 and as shown graphically in Figure 3.30.

Table 3.19 BBR Mixture Bending Test: Evolution of Stiffness and m-Value with Aging

BBR Temp			-6°C				-12°C				-18°C			
Aging Time, hours			0	4	24	48	0	4	24	48	0	4	24	48
West Texas Sour	S (Mpa)	Ave.	8828	10298	13295	15893	12053	17245	19765	16960				
		SD	528	304	963	1595	2359	2435	3223	2154				
		CV	5.98%	2.96%	7.24%	10.04%	19.57%	14.12%	16.31%	12.70%				
	m- value	Ave.	0.228	0.184	0.146	0.120	0.149	0.144	0.132	0.147				
		SD	0.009	0.011	0.007	0.014	0.017	0.009	0.013	0.025				
		CV	3.75%	5.77%	4.53%	11.88%	11.20%	6.47%	9.94%	16.92%				
Gulf- Southeast	S (Mpa)	Ave.					11705	13035	15450	14580	19340	19513	21055	18400
		SD					1560	2358	2021	2629	1138	2114	2064	4265
		CV					13.33%	18.09%	13.08%	18.03%	5.89%	10.84%	9.80%	23.18%
	m- value	Ave.					0.159	0.158	0.127	0.114	0.125	0.131	0.116	0.133
		SD					0.020	0.008	0.002	0.002	0.008	0.007	0.008	0.005
		CV					12.90%	4.99%	1.44%	1.31%	6.31%	5.01%	7.17%	4.00%
Western Canadian	S (Mpa)	Ave.					7715	8228	12263	13460	13245	14865	20048	16270
		SD					995	470	900	887	1577	2203	1024	2325
		CV					12.90%	5.72%	7.34%	6.59%	11.91%	14.82%	5.11%	14.29%
	m- value	Ave.					0.264	0.224	0.158	0.130	0.186	0.171	0.134	0.132
		SD					0.016	0.012	0.006	0.005	0.011	0.013	0.005	0.009
		CV					6.21%	5.31%	3.48%	3.57%	5.75%	7.70%	4.01%	7.02%

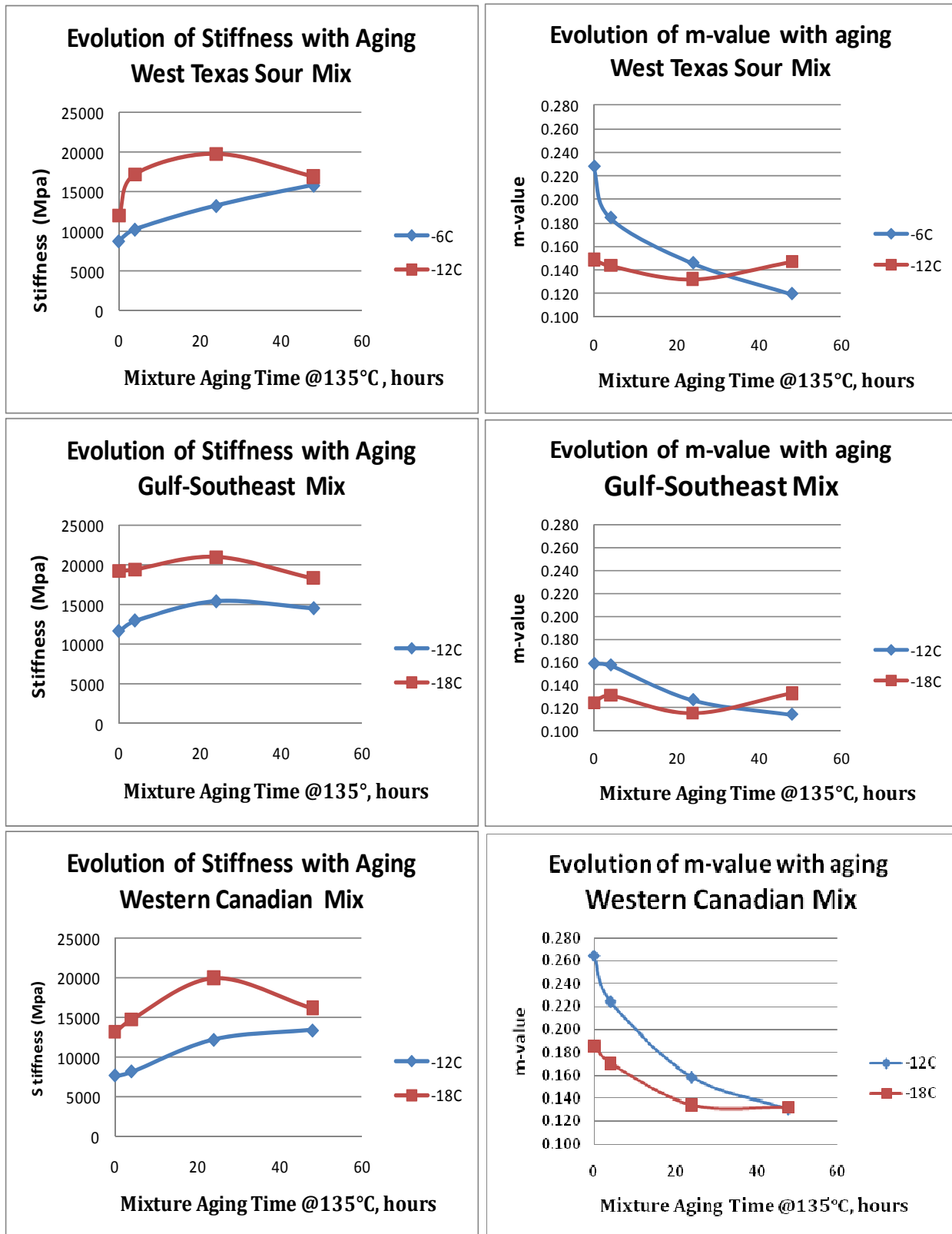


Figure 3.30 Impact of Aging on BBR Mixture Properties (Bending Mode)

At first glance, the graphs in Figure 3.30 appear to contradict findings from the binder study that BBR Stiffness continues to increase and phase angle continues to decrease with additional aging. For all three mixes tested at the temperature immediately above its low temperature PG grade, the mixture stiffens and the phase angle continues to drop with longer aging times. However, at test temperatures below the recommended PG binder grade, the Stiffness reaches a maximum and the m-value exhibits a minimum value after approximately 24 hours of aging, and then both S and m-value reverse direction in a manner that is inconsistent with the comparable binder rheology from PAV experiments. It is particularly interesting to note that for all three asphalts, the maximum stiffness is consistently near 20,000 MPa as the minimum m-value approaches 0.13 ± 0.01 . Since the stiffness of the binder as monitored by PAV continues to increase with aging time, the only plausible explanation is that damage (micro cracking) has occurred at some point in the highly aged mixture specimen, either as it was cooled below its critical cracking temperature or during the first sixty seconds of loading in the BBR. Although one expects thermal stresses to build upon cooling, there are several curious circumstances here that deserve further analysis:

- The BBR Specimen is unconfined. If one were to place this highly aged mix in the Thermal Stress – Restrained Cooling Test chamber and cool it rapidly, the building thermal stresses should result in a single-event cracking failure well before reaching this low temperature. But here, the very small BBR specimen is unconfined on any side, and yet is still damaged.
- The BBR specimen has not cracked even though it is clearly damaged. Loading does not further damage the specimen. The BBR applies a 500-gram load for 240 seconds to bend the specimen. If the beam has been damaged during cooling, then an applied load would be expected to further damage the specimen, probably even to the point of breaking the beam. Figure 3.31 shows that this is not the case for any of the three asphalts as tested in the damaged condition. The BBR loading curves (S vs. log loading time) are all straight and parallel, regardless of aging time. For the West Texas Sour mix, the 48 hr aged specimen with damage so closely overlays the 4 hr aged (undamaged) results that they look like replicates of the same material. It is also useful to review the BBR relaxation properties on Figure 3.32 (m-value vs. log loading time). Again, none of the 48 hr aged specimens indicate any break in continuity with BBR loading even though the phase angle is now higher than the 24 hr aged specimen. For the West Texas example, there is a slight difference in slope between the 4 hr and 48 hour aged beams, but the relative magnitude of the phase angles is still nearly the same at all loading times. Most importantly, these moderately damaged specimens never broke, even though restrained cooling tests should have failed the highly aged mix well before these cold temperatures were met. It seems clear from this data that damage can occur from thermal stresses even when the mix is unconfined, but failure temperatures are lower. Curiously, the additional stress applied by the BBR is not significantly propagating micro cracks during the loading sequence. Hence, the damage seems to stabilize with constant temperature, at least over relatively short relaxation times.

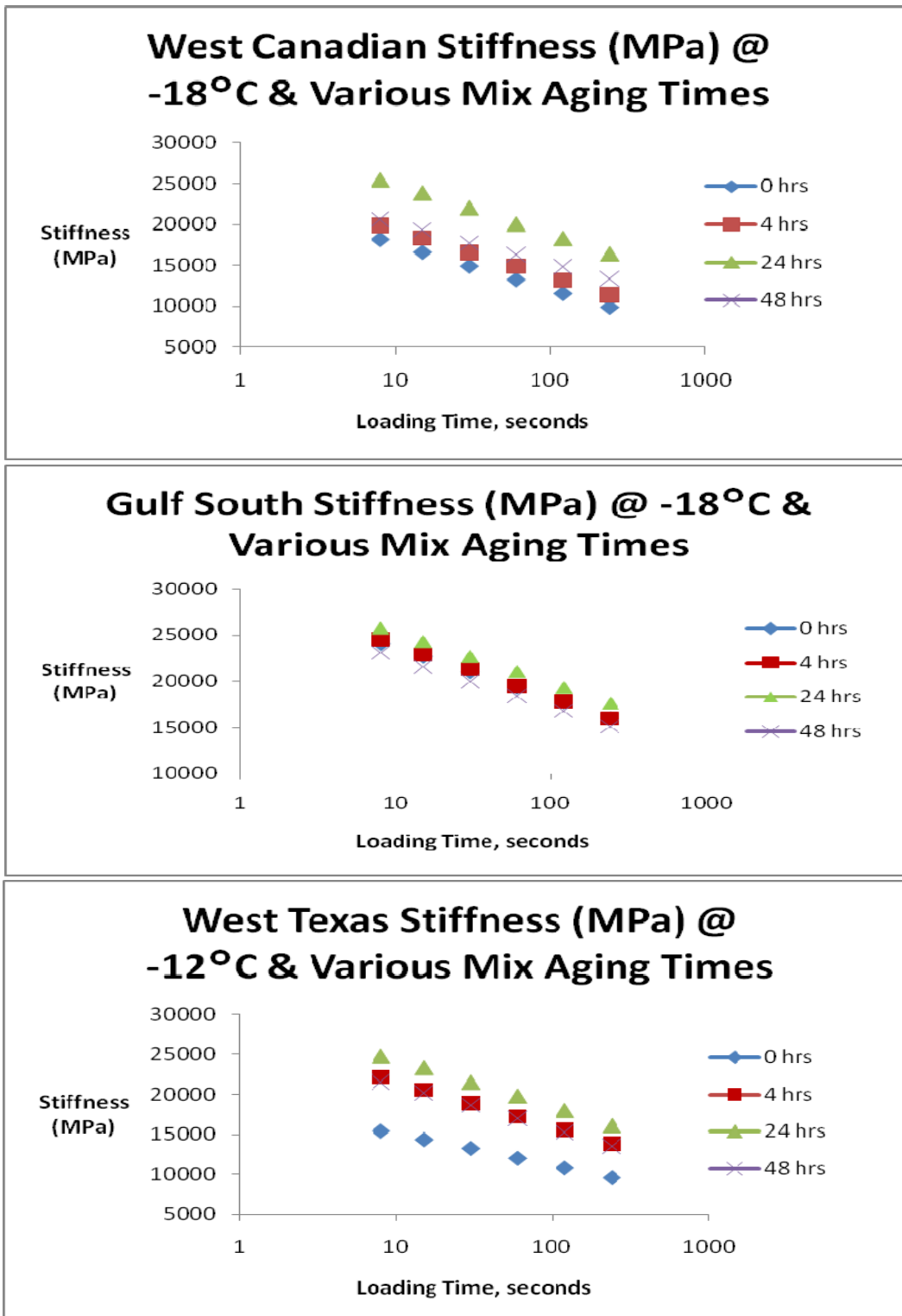


Figure 3.31 BBR Loading curves for mixes below Tcritical (S vs. log time)

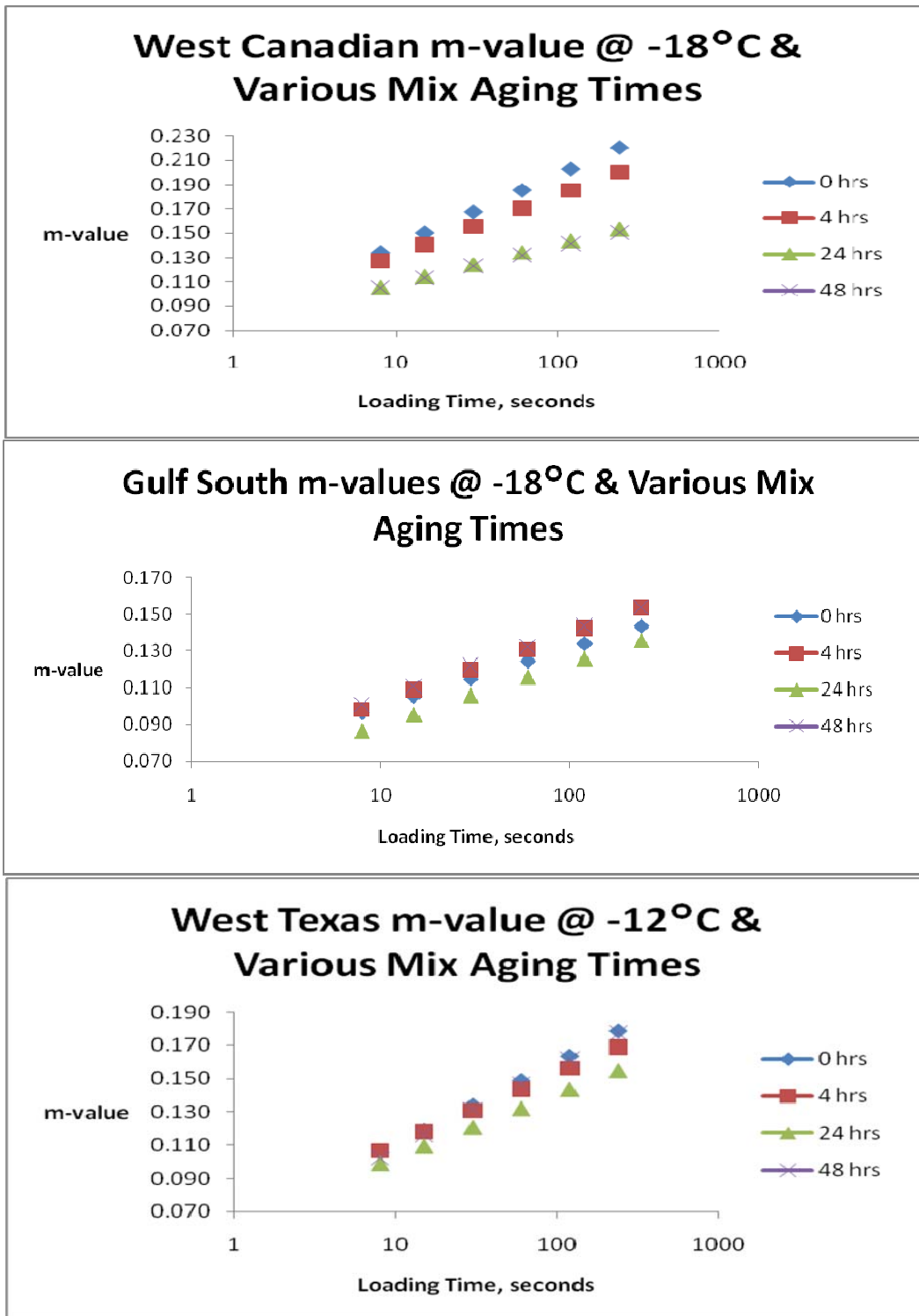


Figure 3.32 BBR Loading Curves for Mixes Below $T_{critical}$ (m-value vs. log time)

These findings lead to one potential solution for predicting the onset of cracking. If a BBR mix specimen cut from a pavement has a stiffness approaching 20,000 MPa and an m-value approaching 0.13 at the lowest predicted pavement temperature for that location and depth, binders properties are within the range where micro cracking is imminent even if the mixture is not confined. Hence, the BBR mixture bending test has great potential as a field test that might be built into timing strategies for pavement preservation. The specific failure limits noted here may need some adjustment for pavement condition and cooling rate. In particular, the mixture stiffness would be expected to have some dependence on aggregate quality and mix characteristics, so these results could be specific to the single mix design used for the laboratory phase of this study. The BBR test specimen represents an unconfined mix that has been cooled at a rate of over 40 degrees Celsius per hour, leaving almost no time for stress relaxation. Some adjustment to this parameter will be necessary to account for cooling rates and mixture confinement. A series of field validation tests on surface mixtures from a variety of pavements with different cracking/raveling severity will be needed to refine conclusions that "m-value" may reflect approaching damage before visible cracks form.

Data needed to determine pavement temperatures and cooling rates at any U.S. location should be available through LTPPBind(6), the software developed by Mohseni, Carpenter and Symons as part of the PG binder grading system. Since many of the weather stations utilized by LTPPBind are located at airports, that data should be particularly appropriate for FAA needs.

Applying the Hirsch Model to Predict Binder Properties from BBR Bending Tests on Mixtures

During discussion of the binder test results earlier in this report, several theoretical approaches for predicting critical cracking temperatures were discussed. Bouldin-Rowe (6) developed thermal stress curves for different cooling rates based upon BBR properties S and m-value. Direct tension tests were run to determine failure strength. They then defined the critical cracking temperature to be the temperature at which the failure strength matched the tensile stress. Shenoy (7) used the Bouldin-Rowe thermal stress curves to directly predict critical cracking temperatures for each cooling rate. Shenoy tried two different approaches, the two asymptote procedure (TAP) and the single asymptote procedure (SAP), both of which yielded similar results. Both methods also provided reasonable agreement with the Bouldin-Rowe approach for standard RTFO/PAV aged binders.

As part of his adaptation of the BBR for mixture testing, Marasteanu (8) used the Hirsch Model to back-calculate binder properties from BBR bending tests on mixtures. One particularly important application for this technique is to predict the effect of cooling rate on the critical cracking temperature of a given mixture using the loading curve from his BBR mixture test. To avoid the need for a direct tension test to determine failure strength, he applied the Shenoy single asymptote method (SAP) to predict Critical Cracking Temperatures at different cooling rates.

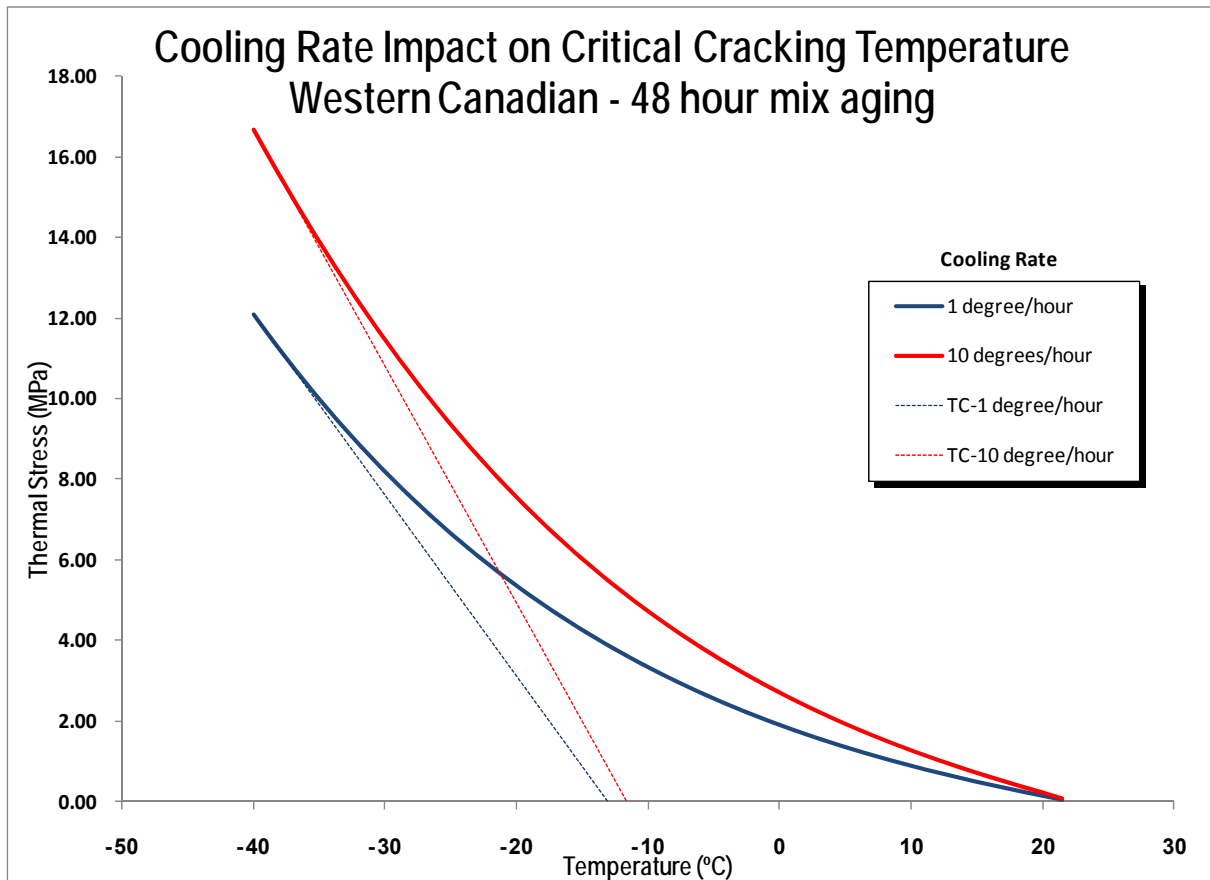


Figure 3.33 BBR Mixture Bending Test

Impact of Cooling Rate on Shenoy's SAP Critical Cracking Temp: WC mix @ 48 hr aging

BBR thermal stress curves were constructed for each mix evaluated in the study, and Shenoy's SAP procedure was applied to predict Critical Cracking Temperature (CCT). Figure 3.33 shows the back-calculated binder tensile stress curves for the 48-hour aged Western Canadian mixture for two cooling rates, and the corresponding predicted CCT. Table 3.20 lists the predicted CCT of all twelve mixes for two cooling rates representing rapid (-10°C/hr) and slow (-1°C/hr) pavement thermal changes. Figure 3.34 represents this same data graphically. Several important observations can be made from these results:

- Mixture aging
 - Aging a mixture for 48 hours @ 135°C increases the CCT by 6-18°C, representing a loss of one to three low temperature PG grades.
 - The rate of change in CCT accelerates with additional aging time.
 - West Texas Sour, the asphalt with poor initial m-control before aging, experiences a much greater loss in CCT after 48 hours aging, losing one PG grade more than the other two asphalts.

- Because previously described results from the mixture BBR tests suggested there may be some damage in the more highly aged specimens as tested at the lowest temperatures, any predictions of CCT taken from BBR tests with m-value near 0.13 may not be valid.
- Cooling rate
 - Increasing the cooling rate from 1°C/hour to 10°C/hour increases the CCT by 2-4°C, representing a loss of less than one PG grade.
 - The influence of cooling rate on the CCT decreases at longer aging times.
 - Mixture aging has a much more negative impact on CCT than cooling rate.

Table 3.20 BBR Mixture Bending Test

Aging Time Hours	West Texas Sour		Gulf-Southeast		Western Canadian	
	Cooling Rate		Cooling Rate		Cooling Rate	
	1°C/hr	10°C/hr	1°C/hr	10°C/hr	1°C/hr	10°C/hr
0	-22.30	-18.35	-21.40	-17.18	-26.78	-23.38
4	-18.21	-14.15	-21.04	-17.05	-25.26	-21.84
24	-15.42	-10.80	-19.72	-15.98	-20.32	-16.60
48	-4.37	-2.39	-12.32	-11.47	-13.12	-11.67

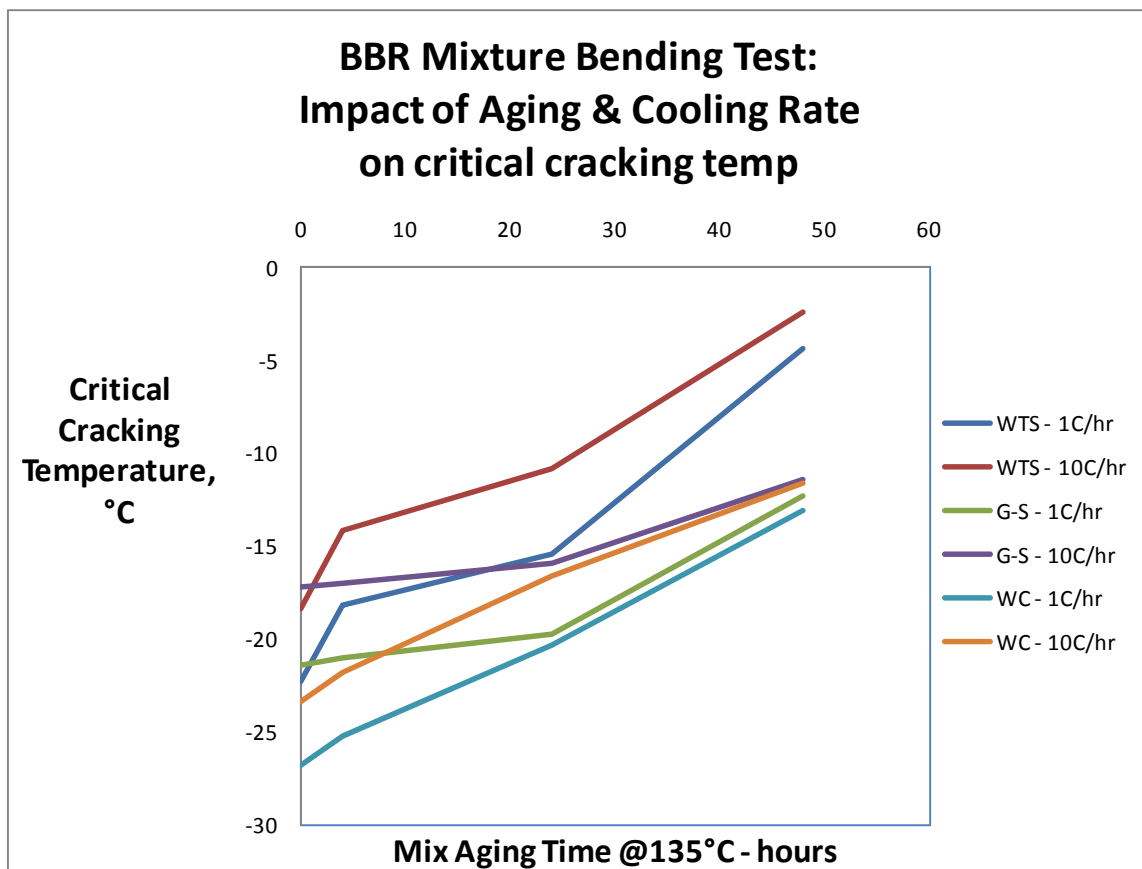


Figure 3.34 BBR Mixture Bending Test

Use of Shenoy's SAP to Predict Critical Cracking Temperatures

It is important to recall that Bouldin-Rowe developed their method to predict single-event thermal cracking, with its assumptions for longitudinal confinement, fairly rapid cooling, and "typical" binder relaxation properties as viewed in Black Space. Furthermore, Shenoy developed his method to get approximately the same CCT predictions without needing to run the direct tension test. Curiously the two predictions begin to diverge as the mixture ages.

At this point it is interesting to analyze how a cracking model based upon 'Limiting Stiffness' concepts might compare to Shenoy's SAP predictions of CCT. Again the tensile stress curves created by Bouldin-Rowe can be applied. But 'limiting stiffness' requires all materials to fail at the same Stiffness. Based BBR fracture tests to be discussed later in this report, fracture strength for the BBR specimens in this study ranged from 4-8 MPa. A failure strength 6 MPa, the mid-point of the experimental range, was selected for further analysis. Bouldin-Rowe derivations predict cracking failure occurs when the failure strength equals the thermal stress. Table 3.21 lists the predicted CCT at which the thermal stress equals 6 MPa for all twelve mixes at two cooling rates representing rapid (-10°C/hr) and slow (-1°C/hr) pavement thermal changes. Figure 3.35 presents this same data graphically.

Table 3.21 BBR Mixture Bending Test

Aging Time	West Texas Sour		Gulf-Southeast		Western Canadian	
	Cooling Rate		Cooling Rate		Cooling Rate	
Hours	1°C/hr	10°C/hr	1°C/hr	10°C/hr	1°C/hr	10°C/hr
0	-30.0	-23.8	-25.7	-21.7	-36.0	-30.3
4	-22.8	-18.4	-25.4	-20.5	-32.1	-27.4
24	-18.2	-13.5	-24.6	-20.6	-25.2	-21.2
48	-17.0	-7.3	-19.9	-13.3	-22.5	-15.0

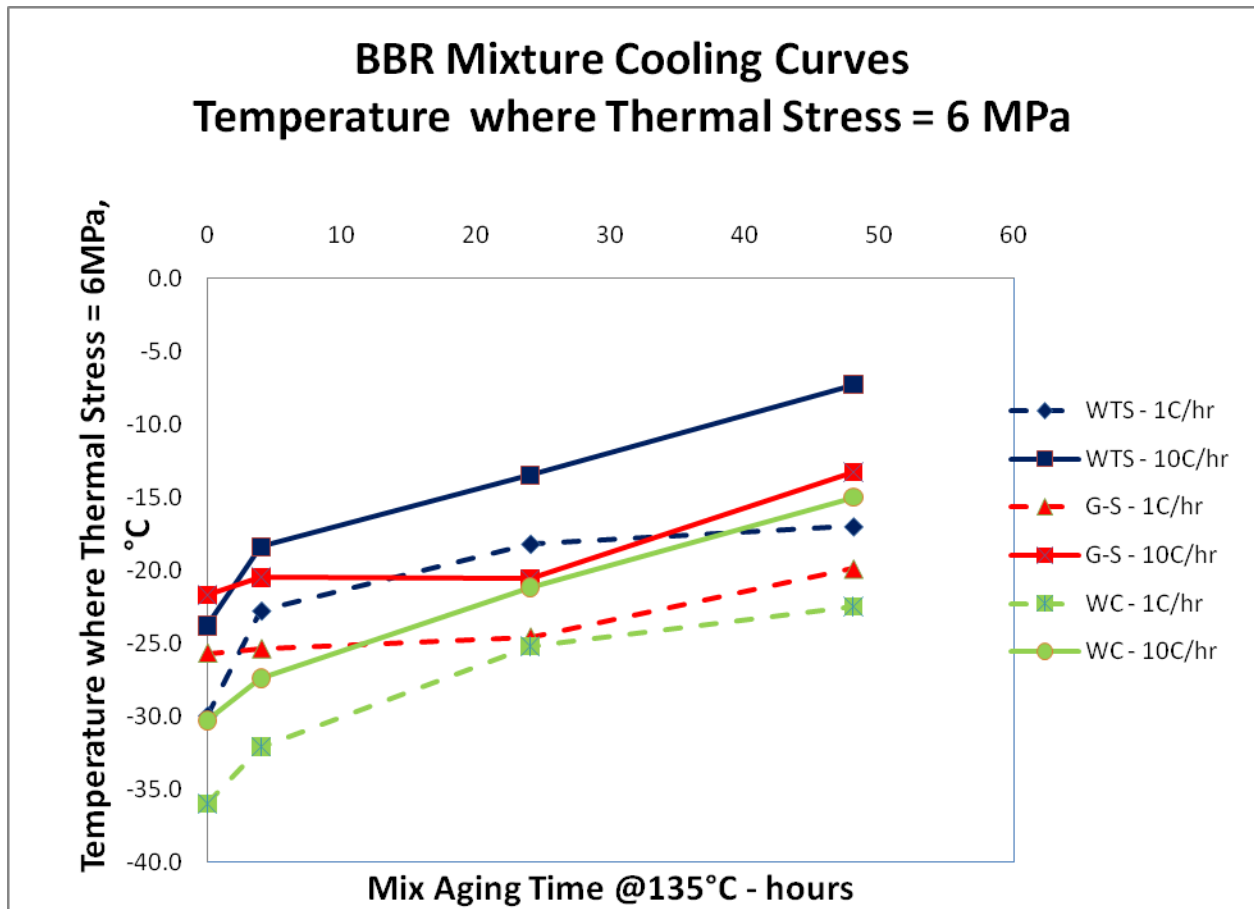


Figure 3.35 BBR Mixture Bending Test

Temperature Where Thermal Stress Curve on Cooling reaches 6.0 MPa

Figure 3.36 uses the unaged WTS specimen to compare the CCT limits for fast and slow cooling rates (10 and 1 degree C per hr), applying both the limiting stiffness methods (6 MPa) and the Shenoy SAP procedure. Figure 3.37 evaluates the same relationships for the 48 hr aged WTS specimen. As would be expected, specimen aging increases predicted cracking temperatures for both prediction methods at all cooling rates. The relationship of the absolute values of CCT is not so important at this time, because the “limiting stiffness” failure temperatures would change significantly for a failure strength of 4 or 8 MPa instead of 6 MPa.

However, as materials age, the ‘limiting stiffness’ and Shenoy’s ‘SAP’ diverge in one very important way. At 6 MPa, or at any other single failure stress, the temperature range between the two cooling curves increases with aging. Just the opposite is true for Shenoy’s SAP parameter. SAP predicts that the cracking temperature is less dependent upon the cooling rate, or relaxation time, after the mixture ages. This trend is consistent with finding from binder and mixture BBR experiments that show strong loss in phase angle or m-value with aging. As the binder phase angle approaches zero degrees, the mix behaves as an elastic solid. At this limit, there is no time dependence to flow, so the cracking temperature would not change as the

cooling rate changes. This finding is a critical element for a thermal cracking hypothesis. The 'limiting stiffness' approach is reported to predict transverse cracking quite well, but Shenoy's SAP prediction of CCT appears to capture the sensitivity of highly aged mixes to block cracking.

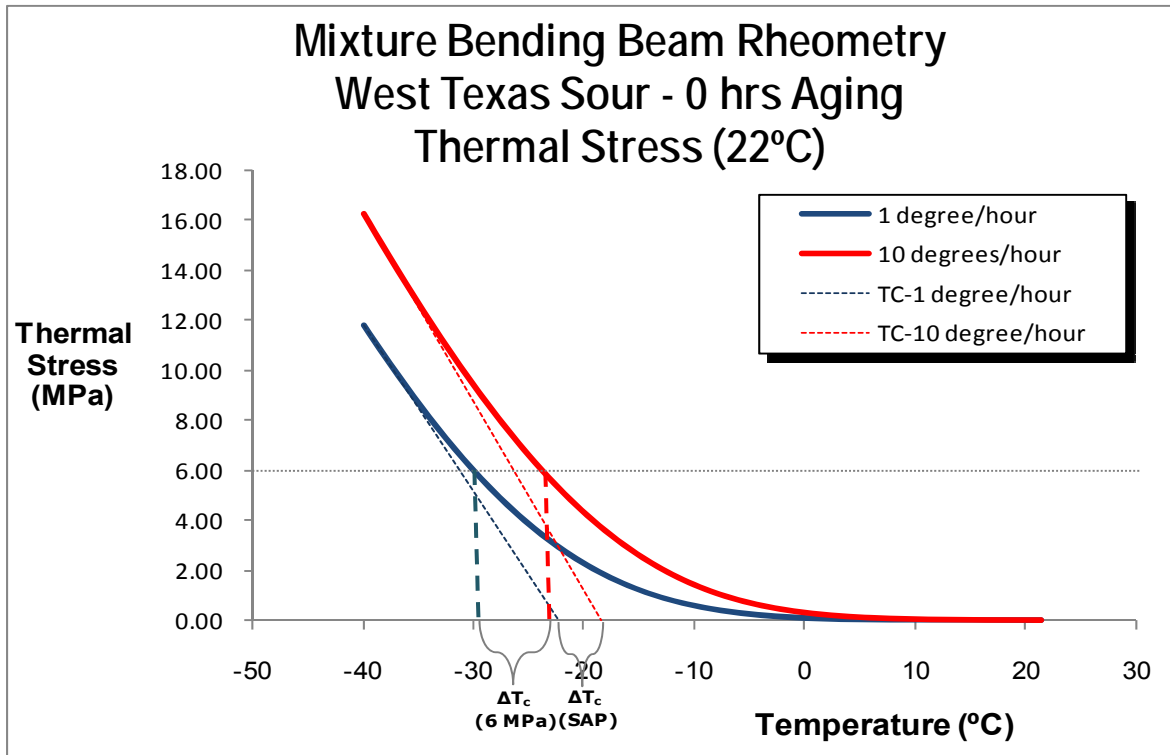


Figure 3.36 Unaged WTS CCT: Shenoy (SAP) vs. "Limiting Stiffness" of 6 MPa

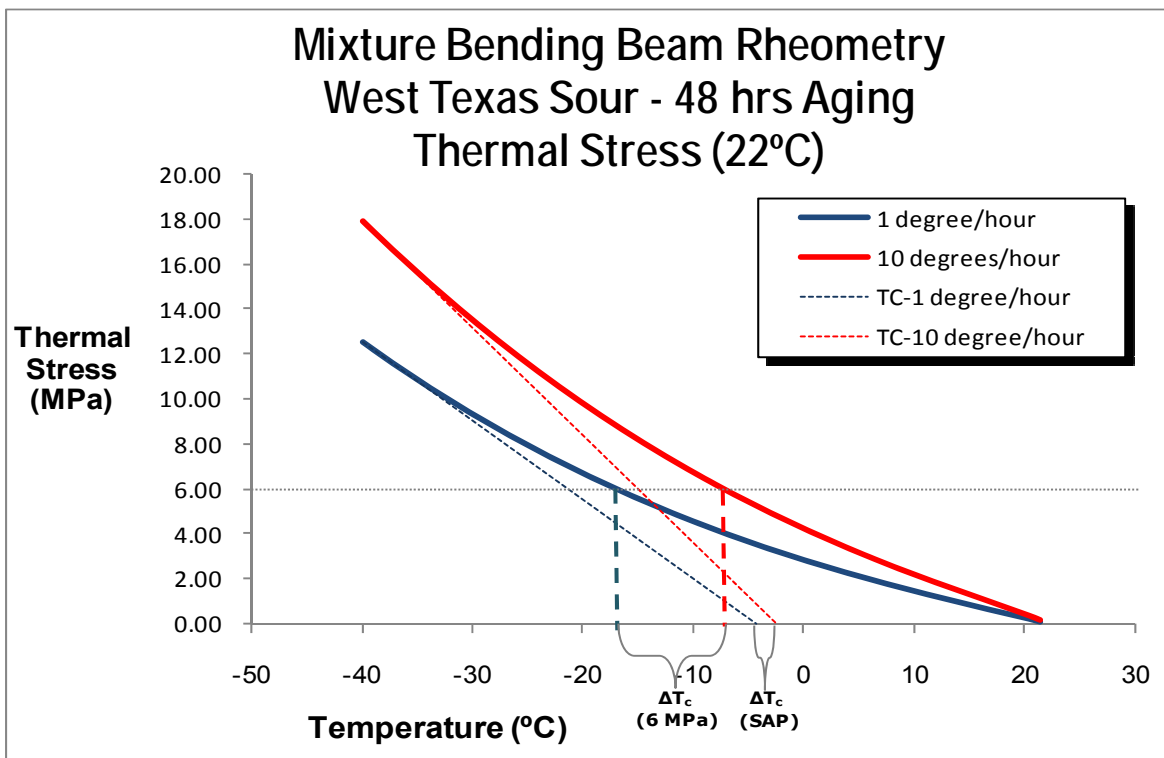


Figure 3.37 48 hr aged WTS CCT: Shenoy (SAP) vs. “Limiting Stiffness” of 6 MPa

BBR Fracture Test on Mixtures

BBR shaped mixture specimens were cut and tested by Dr. Marasteanu using a newly developed technique that enables the BBR to be used as a fracture device. Four replicate specimens were tested at each of the two temperatures as previously selected for the mixture bending tests. Details of the procedure have not yet been standardized, but the method has been published in various research papers previously mentioned (Zofka *et al.* (5)). Current procedures are as follows for sample preparation and testing, Figures 3.38 and 3.39.

1. The 150mm (6in) samples were trimmed to smooth the surface by removing about 4mm from the top.
2. Next 12mm (0.5in) round slices were cut from the sample. (For a pavement core, it may only be possible to cut one 12mm round slice due to pavement surface thickness only being 37mm (1.5in) or less in some pavements.)
3. Every rounded slice was cut vertically to obtain about seven rectangular beams, each beam is about 6 to 8 mm (0.3in) thick.
4. Both ends were cut off in order to achieve 101mm (4.0in) length beams.
5. Samples were then tested in the BBR for the standard 240 sec just as for asphalt binders, except for the following modifications:
 - a. Depending upon the test temperature, higher loads of 4,000mN or 8000mN were applied instead of the standard 981mN.
 - b. A software modification by Cannon increases the resolution of the deflection measurements.

- c. Results at the lowest test temperature are not always reliable because small deflections (5 to 15 microns) are difficult to measure accurately. If the load is too high, the sample can form microcracks.

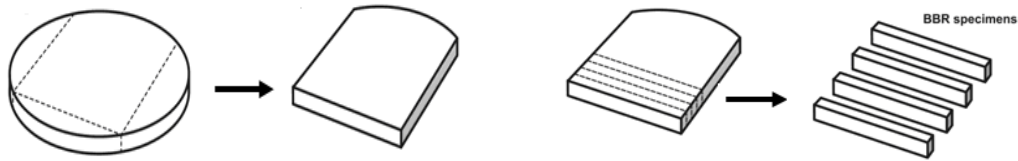


Figure 3.38 Sample Preparation (Cutting) BBR Mixture Beams

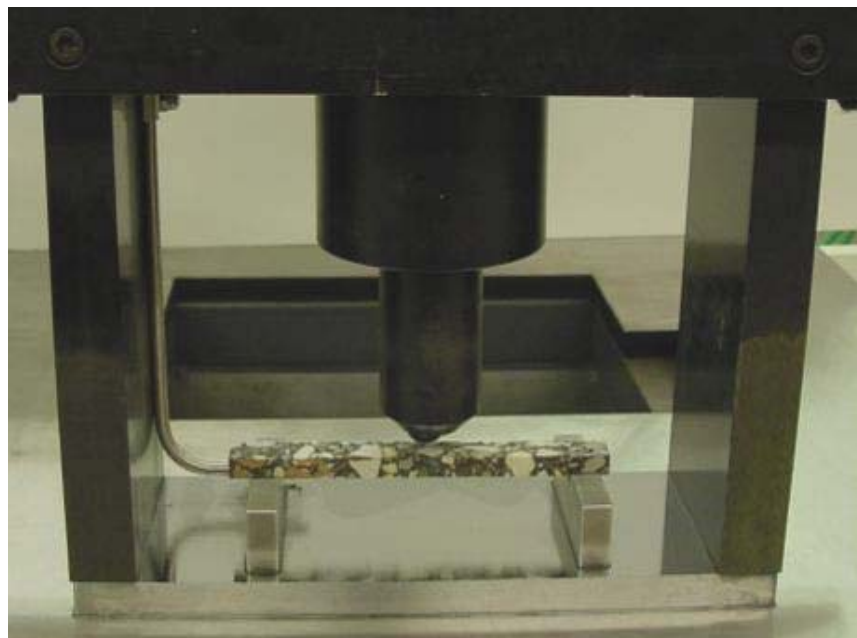


Figure 3.39 Loading BBR Mixture Beams

Table 3.22 Results from BBR Fracture Tests on Aged Mixtures

Aging Time	Fracture Stress (Mpa)					
	West Texas Sour		Gulf-Southeast		Western Canadian	
	-6°C	-12°C	-12°C	-18°C	-12°C	-18°C
Hours						
0	7.3	6.6	6.0	6.9	7.0	7.1
4	7.0	6.7	7.5	6.2	8.7	7.1
24	5.6	6.1	7.0	5.9	6.5	5.7
48	5.7	4.7	4.1	4.7	6.3	4.9

Table 3.23 Statistical Variability for BBR Fracture Tests on Aged Mixtures

		Coefficients of Variation for Fracture Stress Data					
Aging Time		West Texas Sour		Gulf-Southeast		Western Canadian	
Hours		-6°C	-12°C	-12°C	-18°C	-12°C	-18°C
0		4%	18%	15%	7%	12%	15%
4		10%	13%	13%	10%	6%	13%
24		14%	16%	17%	12%	12%	8%
48		23%	14%	21%	13%	9%	8%

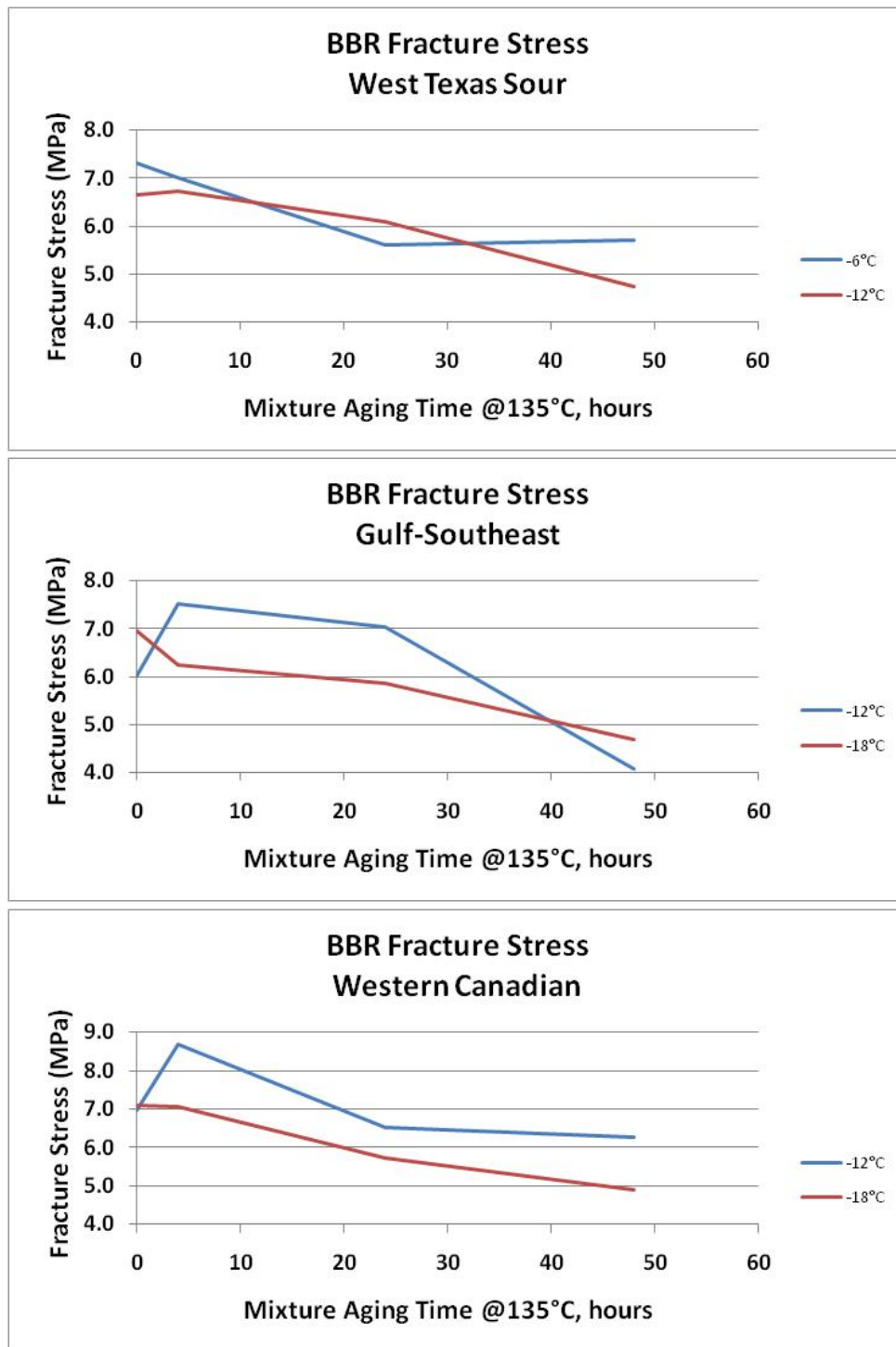


Figure 3.40 BBR Fracture Stress for Three Asphalts After Loose-Mix Aging

Fracture Stress results for each of the twelve specimens as tested at temperatures immediately above and below their low temperature PG grade are reported in Table 3.22, and shown graphically in Figure 3.40. Statistical variability for this data is reported in Table 3.23. As can be

noted on the three graphs in Figure 3.40, the BBR fracture stress of mixtures typically decreases with aging. The only exceptions to this observation are the two better asphalts as they are oven-aged for only four hours. Because both of these binders were S-controlled before aging, it is not unreasonable to expect a small amount of oxidation to stiffen the asphalt in a manner that might even improve fracture properties. Since the asphalt binder should be growing stiffer with aging, failure must be occurring at lower strain, particularly as the asphalt reaches m-control. This finding is consistent with the previously observed loss in binder ductility with aging. Although neither fracture energy nor strain-at-failure data are collected for this test, the binder appears to be exhibiting more brittle-like behavior in tension as the mixture ages. However, data is scattered, and only the Western Canadian mix shows better failure stress at the higher test temperature for all levels of aging. Better fracture strength at lower temperatures is not consistent with most other data that predicts more cracking at colder temperatures. From this data, it does not appear that a maximum failure stress alone is sufficient to predict cracking.

3.3.4 Disk-Shaped Compact Tension [DC(t)] Test

After compaction and trimming to 50mm thickness for testing, all samples for DC(t) prepared at 0, 2, 24, and 48 mix aging conditions were grouped per crude source and aging time, Figure 3.41. During preparation for testing, mechanical problems were encountered with the test frame and device. In order to reduce any steric hardening effects that may have occurred as the samples sat 3 to 5 months at ambient temperature, all compacted specimens were reheated on a metal supporting plate for 1 hour at 60°C (140°F). Also, round metal collars were used as added edge support.



Figure 3.41 Laboratory Samples Prepared for DC(t) Testing from the Three Binder Sources.

Testing

The DC(t) test is similar in concept to the asphalt binder force ductility test and founded on fundamental 3-point beam fracture tests. The Disk-Shaped Compact Tension (DC(t)) test, ASTM D7313, was developed at University of Illinois-Urbana Champaign (UIUC) for the purpose of measuring mixtures properties of the thin core layers. Figure 3.42 shows the Cox and Sons DC(t) device empty and with sample loaded. A sample is pre-cut to initialize the crack zone. A small seating load of not more than 110N (25lbs) was pre-applied, and then the sample was loaded at 1 mm/min until failure. Failure is determined when the load drops below 100N (22lbs). Fracture energy is calculated by measuring the area under the force-displacement curve (i.e. Force x Distance), Figure 3.43. The data is normalized for the samples thickness by dividing by the un-cracked face, which is about 50mm x 80mm = 4000mm² (40cm²). The failure from cracking can be easily seen post-testing, Figure 3.44.



Figure 3.42 Cox and Sons DC(t) Testing Device without sample (left) and with sample loaded (right) and instrumented.

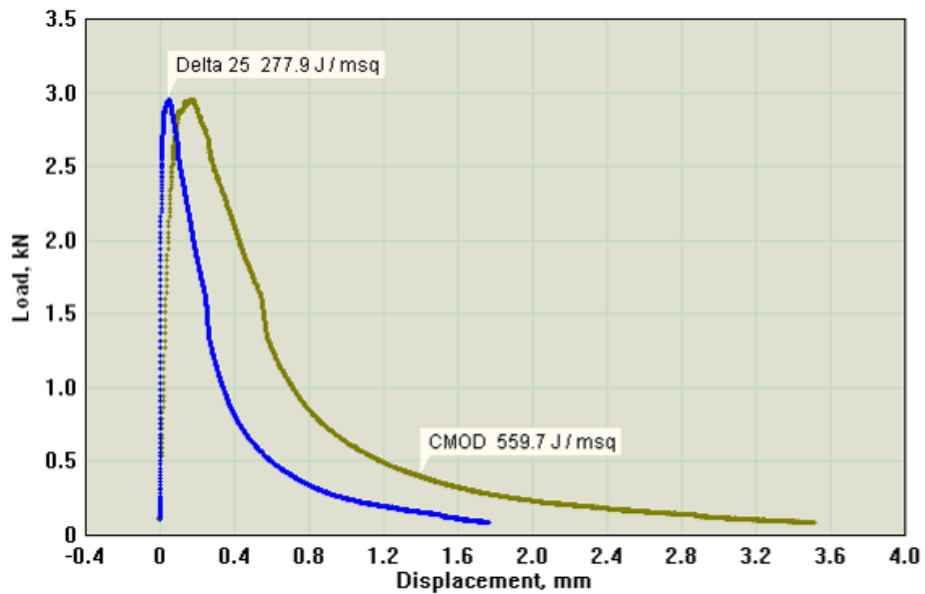


Figure 3.43 DC(t) Loading Showing Peak Load and Fracture Energy for CMOD and Delta 25 Gages.

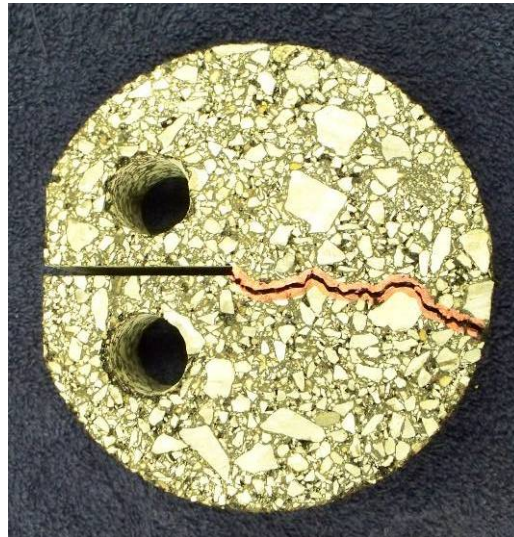


Figure 3.44 DC(t) Sample after Testing Showing Crack Progression.

DC(t) Fracture Energy

The testing at the various temperatures and aging conditions are shown in Tables 3.22 and 3.23 for the CMOD and Delta 25 gage (energy) measurements. The test temperatures were selected based on current recommendations by University of Illinois which is +10°C above the anticipated low temperature PG grade as required for a specific climate. DC(t) testing was also performed at other temperatures in 6°C increments so the data could be overlapped for comparison. The common test temperature was -12°C.

Figures 3.45 through 3.48 are various plots of the CMOD gage data in Table 3.24. Figures 3.49 through 3.51 are various plots of the Delta 25 gage data in Table 3.25. For this study of only neat (non-modified) binders, the CMOD gage data was about 2 times the Delta 25 gage data, which is typical for such materials.

Figure 3.45 plots all of the data in Table 3.24 and shows that as the mixture ages and as the temperature cools, the samples generally fracture with lower applied energies. This is what one would expect to see in pavements. As a pavement continues to age and/or the temperature cools, the potential energy of a pavement should decrease. A few samples show an increase in fracture energy after 4 hours of loose aging. This could possibly be a strength gain in the mixture through asphalt absorption into the aggregates, but is more likely an indication that the binder is still ductile at this condition. The Western Canadian crude at -18.0°C showed an increase until the final aging time and then through the aging and then dropped significantly in energy. This may be testing error or just the behavior of this mixture.

Figure 3.46 through 3.48 illustrate the same data but plotted as isotherm-type graphs or at comparable temperatures to break-down the data in climatic-based plots. Figure 3.46 shows the extreme climatic situation where the data is compared at -6°C less than the expected grade

of these test binders. The climatic working grade of the binders are about -12°C , -12°C , -6°C for the Western Canadian, Gulf Southeast and West Texas crudes. Figure 3.47 is a true isotherm plot where all data is compared at -12.0°C . If all binders were equal in performance, the data in Figure 3.47 would be the same and overlay each other.

Finally, Figure 3.48 may provide the best insight since all data is plotted in to compare energies at the expected climatic grade (like mentioned above) of the binders. As expected, there is a significant difference in the binders (crudes) where the Western Canadian and Gulf Southeast show more potential energy than the West Texas binder. The Western Canadian binder has a slight advantage over the Gulf Southeast binder. The West Texas Sour has much less energy and should have more of a tendency to crack as compared to the other crudes. This data is similar, but not exact, in ranking (and aging) as compared to the binder testing in Figure 3.22.

In Figure 3.45, a suggested minimum limit of 300 J/m^2 is proposed as a minimum energy for a cracking limit. This initial limit seems to be a reasonable per review of University of Illinois-Champaign's data per Braham et al that suggested a minimum limit of 375 J/m^2 in a limited field study. The limit may also make sense because at lab aging times of 24 and 48 hours to simulate years service (maybe 5 and 10 years as a best guess), the West Texas Sour crude may have a potential to crack early. More work should be performed to validate an initial cracking limit. A longer aging time maybe also needed for air field pavement mix. While 24 to 48 hours of aging may be good for highways where the expected surface life is 8 to 15 years for an average pavement, it may not be enough for GA pavements that can see a longer expected service life. For example, 48 hour mix testing maybe similar to 40 hour binder PAV aging. If this is so, it would warrant more loose mix aging time to see a more aged material as in the binder portion of this study like Figure 3.22.

Table 3.24 Fracture Energy from DC(t) Tests on Lab Mixtures using Crack Mouth Opening Displacement (CMOD) Gage

		West Texas Sour Crude			Gulf-Southeast Crude			Western Canadian Crude		
		Test Temperature								
Aging Time, hrs	Sample	0°C	-6°C	-12°C	-6°C	-12°C	-18°C	-12°C	-18°C	-24°C
0.01	1	492.2	425.2	330.9	515.5	381.8	239.1	498.1	349.5	315.9
0.01	2	451.6	352.1	311.1	515.1	385.8	265.6	524.8	418.7	258.2
0.01	3	549.3	449.4	270.8	554.7	515.0	219.1	626.5	388.0	322.1
0.01	Average	497.7	408.9	304.3	528.4	427.5	241.3	549.8	385.4	298.7
	Standard Deviation	49.1	50.7	30.6	22.7	75.8	23.3	67.8	34.7	35.2
	COV	10%	12%	10%	4%	18%	10%	12%	9%	12%

4	1	537.5	370.0	318.6	486.3	559.7	349.1	456.9	450.5	298.0
4	2	548.8	384.9	373.6	525.8	509.0	335.4	493.7	372.2	282.6
4	3	461.3	359.9	367.5	432.7	415.4	333.0	528.7	393.1	268.8
4	Average	515.9	371.6	353.2	481.6	494.7	339.2	493.1	405.3	283.1
	Standard Deviation	47.6	12.6	30.1	46.7	73.2	8.7	35.9	40.5	14.6
	COV	9%	3%	9%	10%	15%	3%	7%	10%	5%

24	1	379.6	320.8	301.1	460.9	436.6	323.0	366.0	398.5	265.3
24	2	402.3	351.8	320.5	441.0	476.5	298.6	475.4	473.7	285.6
24	3	363.6	285.7	336.6	513.7	420.5	339.9	422.6	440.5	270.9
24	Average	381.8	319.4	319.4	471.9	444.5	320.5	421.3	437.6	273.9
	Standard Deviation	19.4	33.1	17.8	37.6	28.8	20.8	54.7	37.7	10.5
	COV	5%	10%	6%	8%	6%	6%	13%	9%	4%

48	1	340.0	310.0	295.9	459.0	478.4	303.4	561.6	366.5	232.2
48	2	333.7	354.8	301.1	388.1	401.3	267.6	491.9	316.1	295.9
48	3	351.6	361.8	258.9	382.7	320.4	317.4	320.4	284.0	221.4
48	Average	341.8	342.2	285.3	409.9	400.0	296.1	458.0	322.2	249.8
	Standard Deviation	9.1	28.1	23.0	42.6	79.0	25.7	124.1	41.6	40.3
	COV	3%	8%	8%	10%	20%	9%	27%	13%	16%

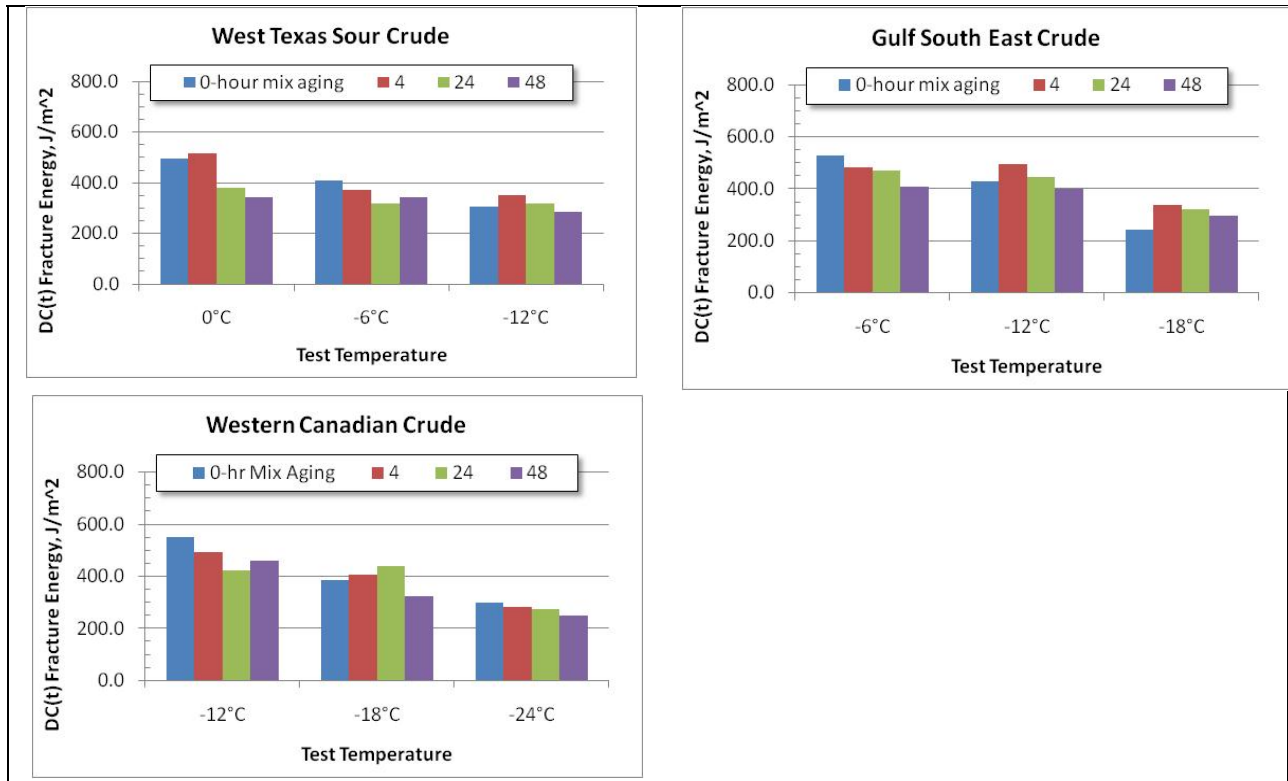


Figure 3.45 DC(t) Testing on Laboratory Prepared Samples from the Three Binder Sources at Three Testing Temperatures with CMOD Gage

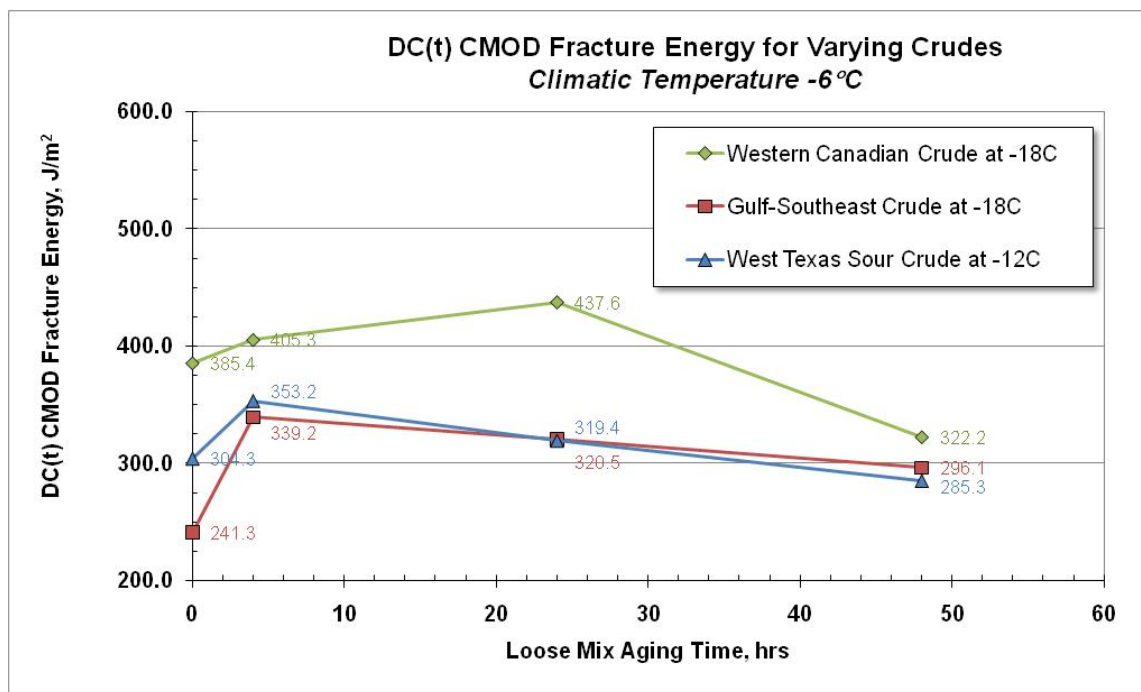


Figure 3.46 DC(t) Testing on Laboratory Prepared Samples from the Three Binder Sources at "Climatic Temp - 6°C" with CMOD Gage

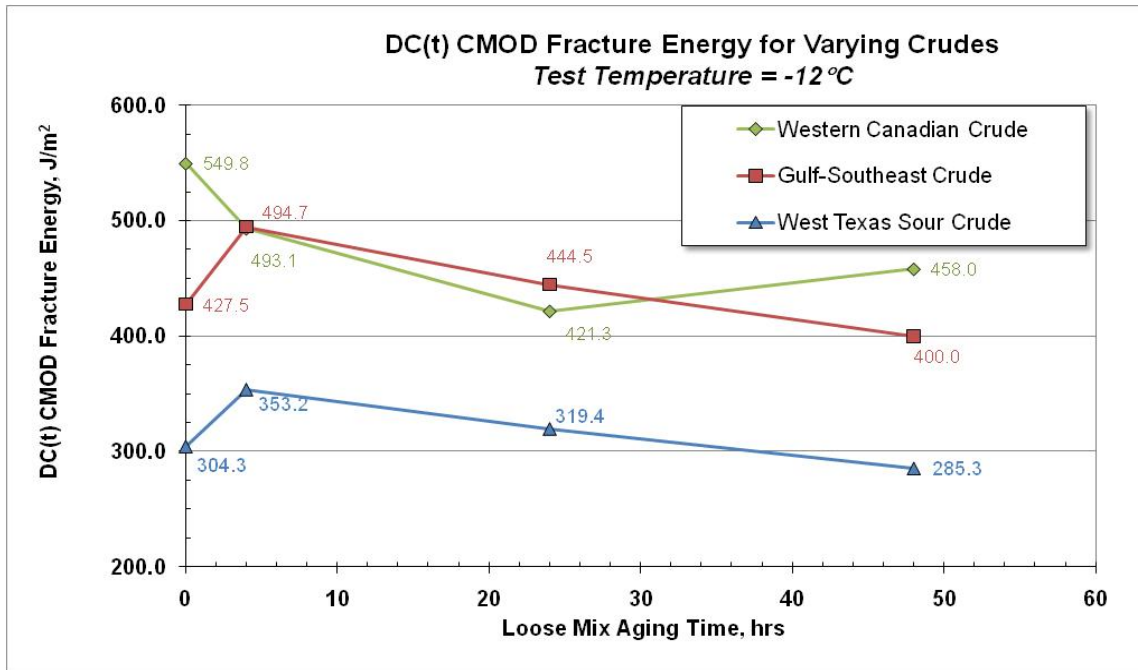


Figure 3.47 DC(t) Testing on Laboratory Prepared Samples from the Three Binder Sources at “Climatic Temp -12°C” with CMOD Gage

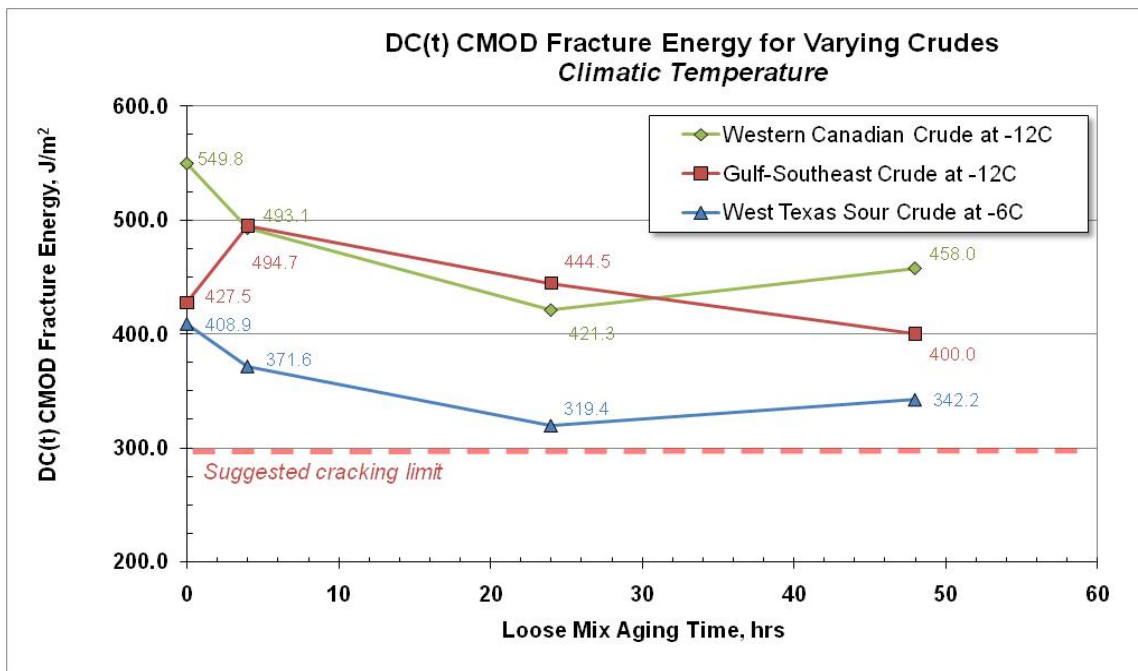


Figure 3.48 DC(t) Testing on Laboratory Prepared Samples from the Three Binder Sources Normalized for the PG Low Binder Grade with CMOD Gage

Table 3.25 Fracture Energy from DC(t) Tests on Lab Mixtures using Delta 25 Gages

		West Texas Sour Crude			Gulf-Southeast Crude			Western Canadian Crude		
		Test Temperature								
Aging Time, hrs	Sample	0°C	-6°C	-12°C	-6°C	-12°C	-18°C	-12°C	-18°C	-24°C
0.01	1	243.2	222.8	169.4	253.0	178.5	128.2	250.1	181.1	150.9
0.01	2	218.1	180.9	159.4	255.2	197.6	135.2	260.4	210.5	130.3
0.01	3	268.7	229.5	143.7	275.2	261.0	113.1	300.7	184.9	163.1
0.01	Average	243.3	211.1	157.5	261.1	212.4	125.5	270.4	192.2	148.1
	Standard Deviation	25.3	26.3	13.0	12.2	43.2	11.3	26.7	16.0	16.6
	COV	10%	12%	8%	5%	20%	9%	10%	8%	11%
4	1	270.1	191.5	164.3	243.1	277.9	163.0	230.3	228.0	154.6
4	2	268.8	198.3	188.2	257.0	242.9	173.3	255.8	195.4	149.9
4	3	236.1	191.8	192.2	218.8	213.5	176.0	259.9	197.8	139.6
4	Average	258.3	193.9	181.6	239.6	244.8	170.8	248.7	207.1	148.0
	Standard Deviation	19.3	3.8	15.1	19.3	32.2	6.9	16.0	18.2	7.7
	COV	7%	2%	8%	8%	13%	4%	6%	9%	5%
24	1	193.6	167.3	163.2	232.2	198.6	165.9	189.8	199.9	137.5
24	2	207.9	183.3	167.1	232.1	226.1	157.6	242.2	246.5	148.2
24	3	185.8	157.8	170.8	248.6	221.8	172.1	204.6	220.5	143.2
24	Average	195.8	169.5	167.0	237.6	215.5	165.2	212.2	222.3	143.0
	Standard Deviation	11.2	12.9	3.8	9.5	14.8	7.3	27.0	23.4	5.4
	COV	6%	8%	2%	4%	7%	4%	13%	11%	4%
48	1	173.5	159.8	153.4	238.7	245.9	156.3	283.4	195.5	118.0
48	2	174.9	182.5	160.3	199.8	203.8	143.2	257.3	167.4	149.4
48	3	178.1	172.3	135.5	195.2	163.7	169.6	166.2	.	110.8
48	Average	175.5	171.5	149.7	211.2	204.5	156.4	235.6	181.5	126.1
	Standard Deviation	2.4	11.4	12.8	23.9	41.1	13.2	61.5	19.9	20.5
	COV	1%	7%	9%	11%	20%	8%	26%	11%	16%

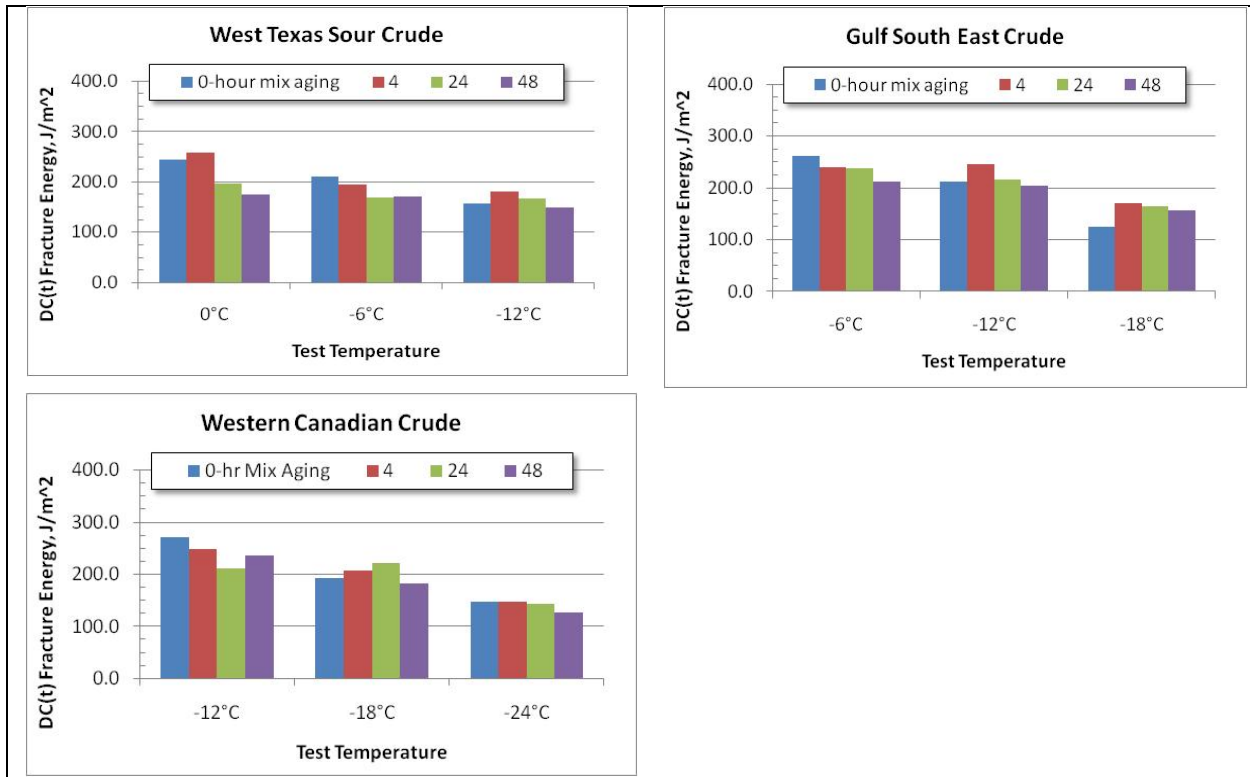


Figure 3.49 DC(t) Testing on Laboratory Prepared Samples from the Three Binder Sources at Three Testing Temperatures with Delta 25 Gages

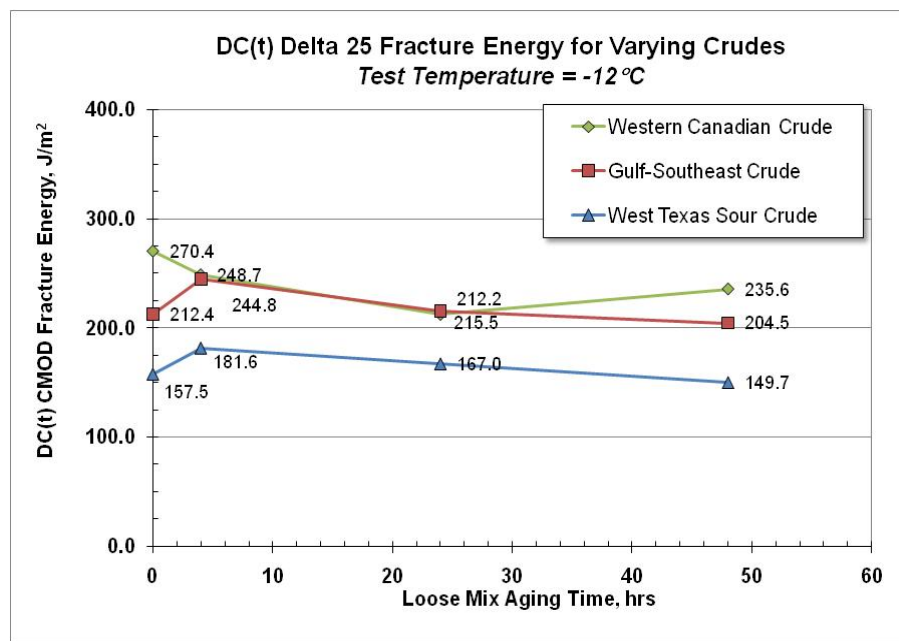


Figure 3.50 DC(t) Testing on Laboratory Prepared Samples from the Three Binder Sources at "Climatic Temp -12°C" with Delta 25 Gages

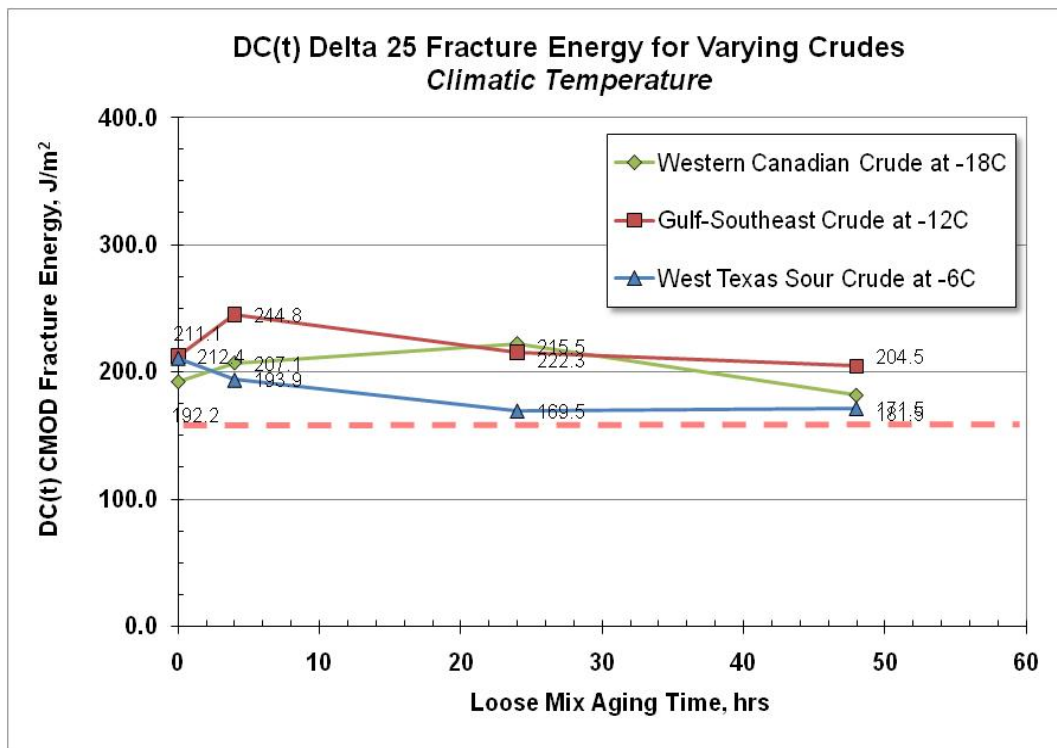


Figure 3.51 DC(t) Testing on Laboratory Prepared Samples from the Three Binder Sources Normalized for the PG Low Binder Grade with Delta 25 Gages

Peak Load

Table 3.26 contains the peak load data that is also derived from the DC(t) test. The data is simply the point of peak load from the example data trace in Figure 3.43. Figures 3.52 through 3.55 are various plots of the data in Table 3.26. Figure 3.52 plots all data in Table 3.26 as bar graphs, while Figures 3.53 through 3.55 are isothermal plots which break-down the data by climate-based performance.

Peak load does not seem to be affected by loose mix aging. While peak load is useful in predicting critical transverse cracking temperatures of a mixture as in AASHTO T322 using the Indirect Tension (IDT) test, it does not seem to as pertinent at the higher test temperatures. The DC(t) is run +10°C above the critical cracking temperature, so peak load was not expected to be a significant response in this test. Most of the small differences in peak load can be accounted for by test error. Figure 3.54 may be the most meaningful, as it ranks the West Texas Sour binder lower than the other binders as one would expect. The West Texas Sour binder is a PG xx-16, as compared to the other binders at PG xx-28 and xx-22.

DC(t) is similar to Indirect Tensile Strength (IDT) test and applies a rapid load with little time for relaxation, it is reasonable to assume product rankings may be more consistent with classic transverse cracking of brittle pavements at lower pavement temperatures.

Table 3.26 Peak Load from DC(t) Tests on Lab Mixtures

		West Texas Sour Crude			Gulf-Southeast Crude			Western Canadian Crude		
		Test Temperature								
Ageing Time, hrs	Sample	0°C	-6°C	-12°C	-6°C	-12°C	-18°C	-12°C	-18°C	-24°C
0.01	1	2418	2658	2658	2620	2448	2463	2556	2577	2987
0.01	2	2588	2370	2370	2716	2600	2900	2450	2828	2673
0.01	3	2558	2696	2451	2869	2553	2708	2732	2902	2920
0.01	Average	2521	2575	2493	2735	2534	2690	2579	2769	2860
	Standard Deviation	91	178	148	126	78	219	143	170	166
4	1	2660	2729	2821	2444	2961	2911	2611	2969	2942
4	2	2672	2727	2747	2658	2710	2867	2943	2550	2978
4	3	2444	2720	2950	2389	3032	2520	2924	2934	2878
4	Average	2592	2725	2840	2497	2901	2766	2826	2818	2933
	Standard Deviation	128	5	103	142	169	214	186	232	51
24	1	2466	2786	2718	2735	3010	2822	2509	3106	2964
24	2	2587	2516	3043	2699	2961	2734	3088	3111	2781
24	3	2509	2594	2757	2790	2801	2997	2796	3104	2993
24	Average	2520	2632	2839	2741	2924	2851	2798	3107	2912
	Standard Deviation	61	139	178	46	109	134	290	4	115
48	1	2515	2819	2939	2798	3414	2847	3059	2818	2880
48	2	2351	2627	2601	2736	2513	2722	2855	2754	2933
48	3	2472	3049	2830	2702	2898	3073	2906	2806	3013
48	Average	2446	2831	2790	2745	2942	2881	2940	2793	2942
	Standard Deviation	85	211	172	48	452	178	106	34	67

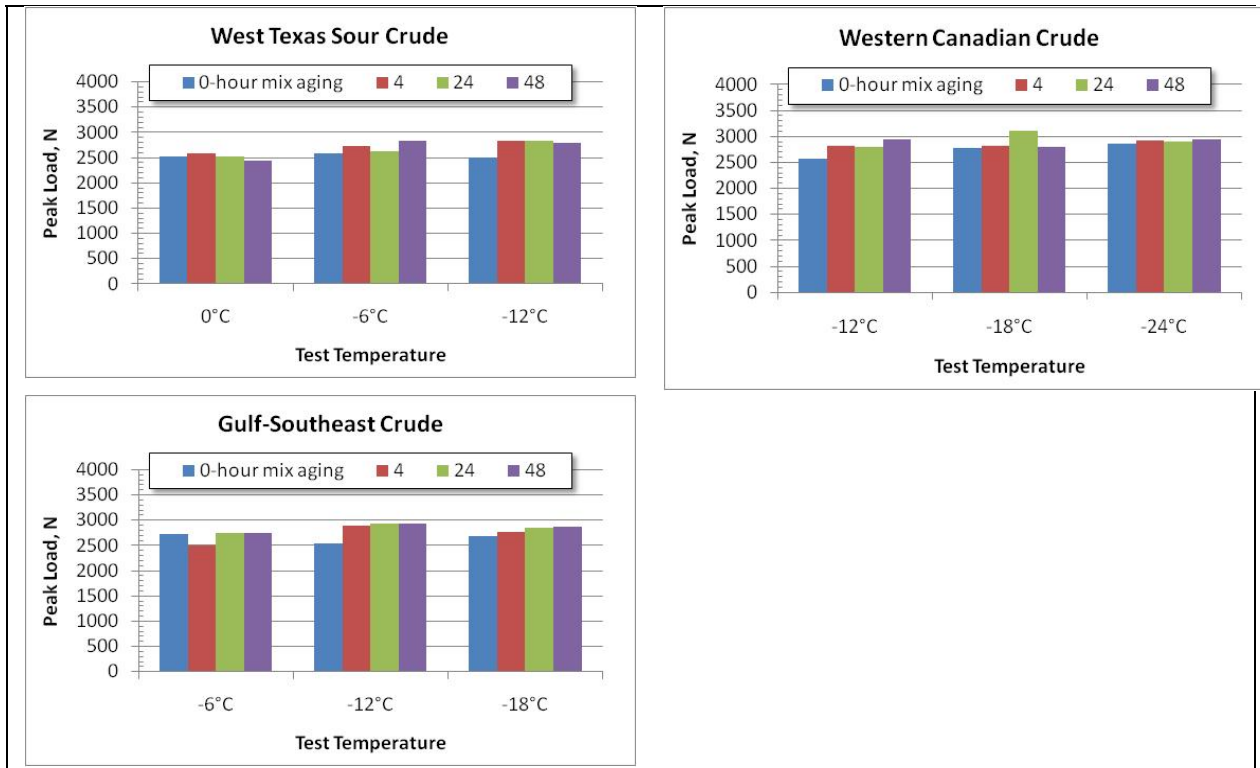


Figure 3.52 Peak Load using DC(t) Testing on Laboratory Prepared Samples from the Three Binder Sources

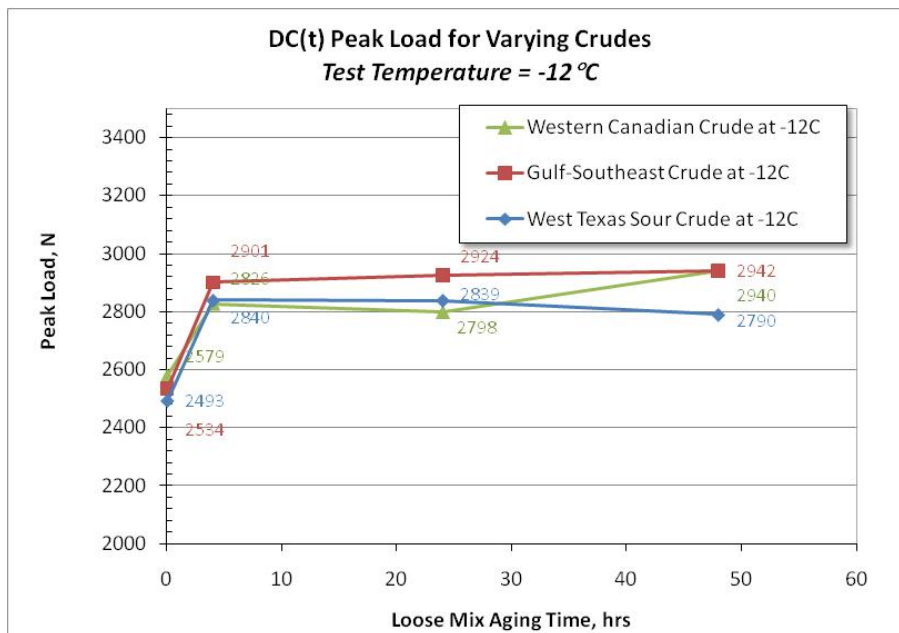


Figure 3.53 Peak Load using DC(t) Testing on Laboratory Prepared Samples from the Three Binder Sources at -12 °C

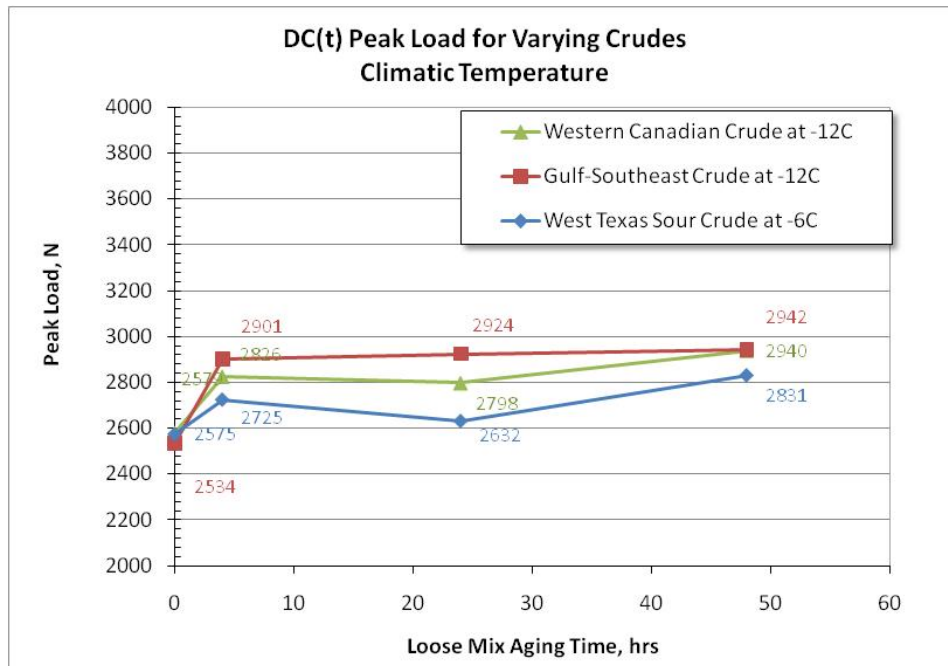


Figure 3.54 Peak Load using DC(t) Testing on Laboratory Prepared Samples from the Three Binder Sources at Climatic Temperature

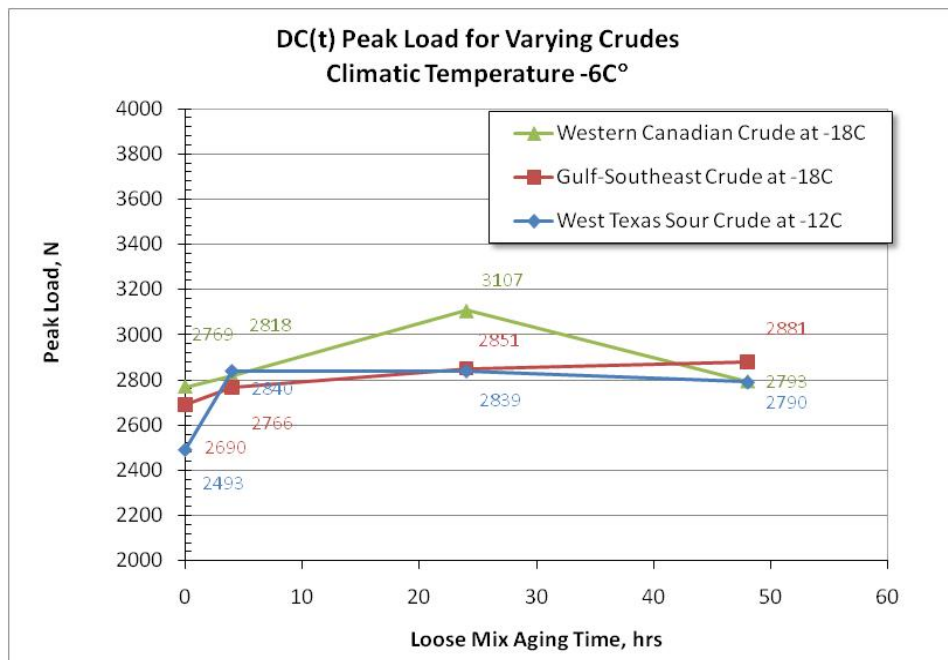


Figure 3.55 Peak Load using DC(t) Testing on Laboratory Prepared Samples from the Three Binder Sources at "Climatic Temp -6 °C"

CHAPTER 4.0 FIELD STUDY

4.1 INTRODUCTION

Cores were gathered from two of the three climatic locations identified in the original testing plan as outlined in Chapter 3.2. These locations are shown in Figure 4.1. Samples photos of cores taken from two of the three climatic locations are shown in Figure 4.2. As mentioned earlier, the airport manager would not be able to permit coring of the Hazard Airport pavements in Kentucky.

It was difficult to find general aviation (GA) sites where both cracked and non-cracked pavements existed in the same location since GA airports are smaller and tend to pave or treat all areas (taxiway and runway) in a single year. This was the case for both New Mexico and Montana sites.

In New Mexico, two airports were cored to obtain cracked and non-cracked surfaces. In Montana, the older pavement was badly cracked and had been treated with a fabric and overlaid, Figure 4-left photo. So cores were taken to capture both the old surface overlay and the new surface.

About 4mm was trimmed from each core to even the surface. The next 25mm was then cut for testing. The remainder of the cores will be retained in case further testing is needed.

A sampling of specimens tested in the DC(t) was then extracted for binder testing so that laboratory and field phases of the study could be compared. The number of field specimens identified in the research plan was limited, and the loss of Hazard airport further reduced the size of the field validation effort. However, the field testing phase did yield valuable data that generally supports findings made in the earlier laboratory experimental design.

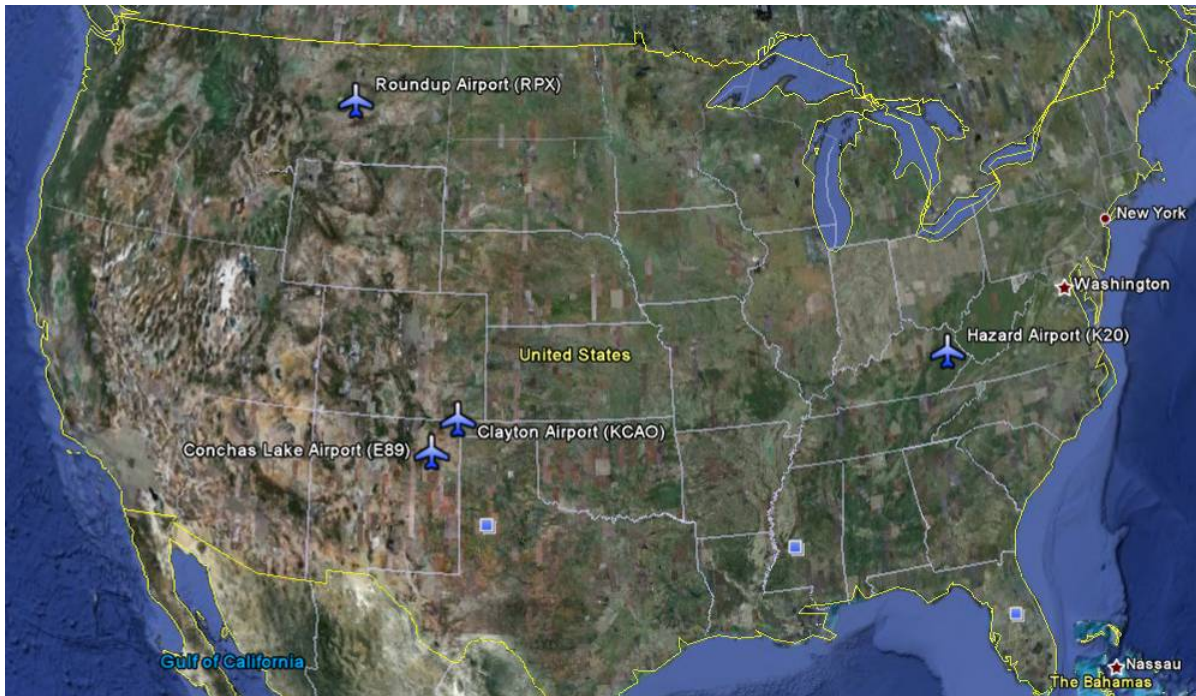


Figure 4.1 Planned Coring Sites for Cracked and Non-Cracked Surfaces (Hazard was not cored.)



Figure 4.2 Samples Cores from Roundup, MT (RPX) and Conchas Lake, NM (E89)

4.2 PAVEMENT CONDITION AT TIME OF CORING

Cores were taken from three airport projects representing four in-service pavements. In Montana, cores were taken from one airport – identified as Roundup – that had recently received an overlay of an older, cracked pavement. These cores were split into layers with the upper layer representing the new pavement (Roundup Top) and the lower layer representing the older pavement (Roundup Bottom). Delineation between the two layers was very clear, as can be seen on the first picture in Figure 4.2.

4.2.1 Roundup Airport, MT (RPX)-Top Lift (Newer pavement) and Bottom Lift (older pavement)

The Roundup airstrip is located about 55 miles north of Billings. Based on the visual inspection made on August 17th, 2009, the general condition of the runway, taxi way, and apron is deemed good. The estimated age of the pavement is 12 to 15 years old. There are a number of cracks that that have been previously routed and sealed. Based on the condition of the sealant, it is estimated that this was done 5-8 years ago. New cracks are forming, and old cracks continue to propagate from their previously sealed lengths. The cracks are mainly at construction joints or transverse thermal cracks. No structural cracking was seen, nor was there other evidence of structural problems. Other evidence of maintenance includes application of coal tar sealants in the fueling area and parking locations on the apron as well as past fog sealing. A fog seal applied in 2007 is showing signs of wear. There was also some raveling in limited locations.

The lower layer, representing the older pavement from the same site, was covered about 12 to 15 years ago. No pictures are available of this pavement other than the core layer photos in the Appendix. This older surface layer was reported to have been badly cracked before overlay, but little other information is available. Core thickness details are in Table 4.1 and 2009 photos are in Figure 4.3.

According to LTPPBind software version 3.2 using 98 percent reliability, the pavement temperature would range from a 58°C high temperature to -32°C (-34°C if rounded to the nearest 6°C increment) low temperature. For comparing non-load cracking in the DC(t), a temperature of -24°C (+10°C higher than the -34°C low temperature) was used. Additional data at -18°C and -12°C was collected in order to overlap data with the other pavement sections in New Mexico.

Table 4.1 Pavement Layer Thicknesses for Roundup Airport

Sample	Surface Thickness, mm	Middle (fabric interlayer) Thickness, mm	Bottom Thickness, mm	Comments
1	47	1	52	
2	48	2	32	
3	37	2	55	
4	45	2	55	
5	41	2	49	
6	79			Appears to be only surface lift
7	90			Appears to be only surface lift
8	87			Appears to be only surface lift
9	48	2	50	
10	64	3	40	
11	49	2	60	

Sample	Surface Thickness, mm	Middle (fabric interlayer) Thickness, mm	Bottom Thickness, mm	Comments
12	52	3	47	
13	46			Middle and bottom layers in bad shape
14	47	3	48	
MEAN	55.7	2.2	48.8	
MAX	90	3	60	



Figure 4.3 Roundup Pavement surface (top layer) Condition at Time of Coring

4.2.2 Clayton Airport, NM (KCAO)-Newer Pavement

In New Mexico, cores were taken from the Clayton airport and the Conchas Lake airport. Site reports for the Clayton airport indicate that it was paved in 2004 using a standard 85-100 penetration asphalt binder from a local supplier (likely using West Texas Sour). Some low severity longitudinal cracking and raveling was identified. Core thickness details are in Table 4.2 and 2009 photos are in Figure 4.4.

According to LTPPBind software version 3.2 using 98 percent reliability, the pavement temperature can range from a 59°C high temperature to -22°C low temperature. For comparing non-load cracking in the DC(t), a temperature of -12°C (+10°C higher than the -22°C low temperature) was used. Additional data at -6°C and 0°C was also collected.

Table 4.2 Pavement Layer Thicknesses for Clayton Airport

Sample	Surface Thickness, mm
1	54
2	61
3	62
4	52
5	51
6	57
7	36
8	57
9	61
10	51
11	68
12	48
13	44
14	32
15	42
MEAN	51.7
MAX	68



Figure 4.4 Clayton Airport Condition at Time of Coring

4.2.3 Conchas Lake, NM (E89)-Older Pavement

Site reports from the Conchas Lake airport indicate that it was paved in 2001 using a standard 85-100 penetration asphalt binder from the same local supplier (again, likely using West Texas Sour). Some low-to-moderate severity raveling was identified over most of the paved area and will need sealing. According to the report, the pavement surface appeared slightly oxidized. Core thickness details are in Table 4.3 and 2009 photos are in Figure 4.5

According to LTPPBind software version 3.2 using 98 percent reliability, the pavement temperature would can range from a 64°C high temperature to -19°C (-22°C if rounded to the nearest 6°C increment) low temperature. For comparing non-load cracking in the DC(t), a temperature of -12°C (+10°C higher than the -22°C low temperature) was used. Additional data at -6°C and 0°C was also collected.

Table 4.3 Pavement Layer Thicknesses for Conchas Lake Airport

Sample	Surface Thickness, mm
1	85
2	73
3	69
4	73
5	62
6	68
7	68
8	71
9	66
10	68
11	62
12	75
13	76
14	82
15	81
MEAN	71.9
MAX	85



Figure 4.5 Conchas Lake Airport Condition at Time of Coring

4.3 LABORATORY TESTING OF AIRFIELD PAVEMENT CORES

4.3.1 Asphalt Binder

Binder Extraction from Cores

After mix testing was completed, several cores from each project were heated and combined for further testing. Extraction and recovery testing was then conducted for each set of field cores. Extraction testing was conducted following ASTM D2172, *Quantitative Extraction of Bitumen from Bituminous Paving Mixtures*, Method A, using toluene as the extraction solvent. After the extraction procedure was complete, the effluent was recovered following ASTM D5404, *Recovery of Asphalt from Solution Using the Rotary Evaporator*.

Testing

The recovered asphalt binder was then tested using the two most promising procedures from the lab experiment: (1) determination of $G'/(η'/G')$ at 15°C and 0.005 rad/s (DSR mastercurve procedure); and (2) determination of $ΔT_c$ – the difference between $T_{c,m(60)}$ and $T_{c,S(60)}$ from the BBR.

To determine $G'/(η'/G')$ at 15°C and 0.005 rad/s, the recovered asphalt binder sample was tested in the DSR using a temperature-frequency sweep procedure. Three test temperatures (5, 15, and 25°C) and 31 testing frequencies (from 0.1 to 100 rad/s) were used to generate the mastercurve at a reference temperature of 15°C. Once the mastercurve was developed, $G'/(η'/G')$ was calculated at a loading frequency of 0.005 rad/s.

To determine $ΔT_c$, the recovered asphalt binder sample was tested in the BBR at two test temperatures. The critical temperature where $m(60)$ is exactly 0.300 – $T_{c,m(60)}$ – and the critical temperature where $S(60)$ is exactly 300 MPa – $T_{c,S(60)}$ – was determined by interpolation. The difference between the two critical temperatures was then determined.

Results

Figure 4.6 presents data from the mastercurve analysis at a reference temperature of 15°C. The graph shows that the recovered Conchas Lake asphalt binder is the stiffest at all loading frequencies followed by the Roundup Bottom asphalt binder. The least stiff asphalt binder is the Roundup Top asphalt binder with the Clayton asphalt binder behaving similarly.

Figure 4.7 shows Black Space data for each of the four recovered asphalt binders. All the asphalt binders appear similar in terms of their relationship between G^* and phase angle. Table 4.4 shows the data from the BBR and the determination of the critical temperatures.

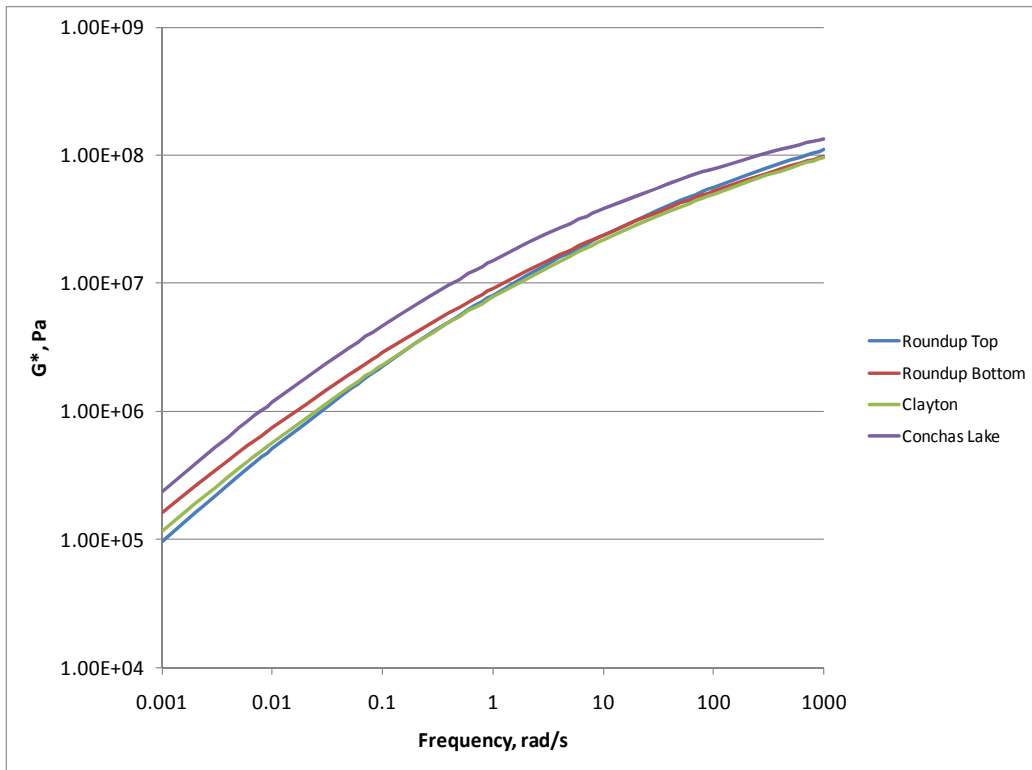


Figure 4.6 Recovered Asphalt Binders – Mastercurves at 15°C

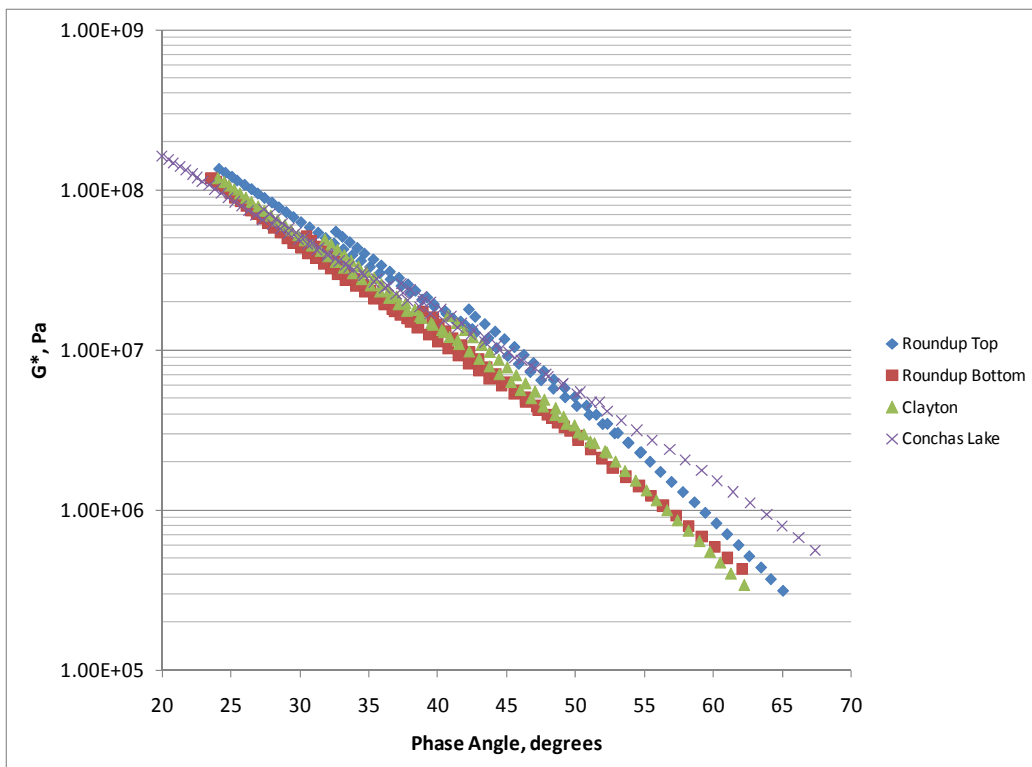


Figure 4.7 Recovered Asphalt Binders – Black Space

Table 4.4 BBR Data for Recovered Asphalt Binder

		Airport Project			
		Roundup Top	Roundup Bottom	Clayton	Conchas Lake
S(60), MPa	-6°C				
	-12°C	172	173	155	272
	-18°C	360	345	304	458
	T _c , S(60), °C	-26.5	-26.8	-27.9	-23.1
m(60)	-6°C				
	-12°C	0.337	0.316	0.330	0.280
	-18°C	0.282	0.265	0.281	0.230
	T _c , m(60), °C	-26.0	-23.9	-25.7	-19.6
	Δ T _c , °C T _{c,m(60) – T_{c,S(60)}}	0.5	2.9	2.2	3.5

Table 4.5 presents a comparison of the durability parameters using data from the recovered asphalt binders. In addition to $G'/(η'/G')$ and $ΔT_c$, the ductility at 15°C and 1 cm/min. is predicted using the equation in Figure 3.3 that relates ductility to $G'/(η'/G')$.

Table 4.5 Comparison of Durability Parameters for Recovered Asphalt Binder Data

	Roundup Top	Roundup Bottom	Clayton	Conchas Lake
$G'/(η'/G')$¹, MPa/s	3.28E-04	6.80E-04	4.65E-04	6.66E-04
ΔT_c, °C	0.5	2.9	2.2	3.5
Predicted Ductility², cm	7.8	5.7	6.7	5.7

¹ Determined at 15°C and 0.005 rad/s.

² Ductility predicted using $G'/(η'/G')$ and equation in Figure 3.3

The data in Table 4.5 indicates that the Roundup Top asphalt binder appears to be the most “durable” according to both the $G'/(η'/G')$ and $ΔT_c$ data. Since this is the newest of the four airfield asphalt pavements, the data makes sense. Likewise, the Roundup Bottom asphalt binder appears to be one of the least “durable” based on the $G'/(η'/G')$ and $ΔT_c$ data. Again, this makes sense as it was the pavement that was overlaid by the Roundup Top mixture.

Of the two New Mexico airfield pavements, the Conchas Lake asphalt binder appears to be less “durable” than the Clayton asphalt binder. Based on site reports this also appears to be rational since the Conchas Lake pavement is approximately 3 years older than the Clayton pavement and has shown some “low-to-moderate severity raveling” with a pavement surface that “appeared slightly oxidized”.

To place the data in context, the recovered asphalt binders were plotted on the same graph as the laboratory aged asphalt binders shown in Figure 4.7. The recovered asphalt binder data

points are shown in Figure 4.8 as open circles. Figure 4.9 presents the same data, but on a magnified scale to better see the data and suggested cracking warning and cracking limit lines.

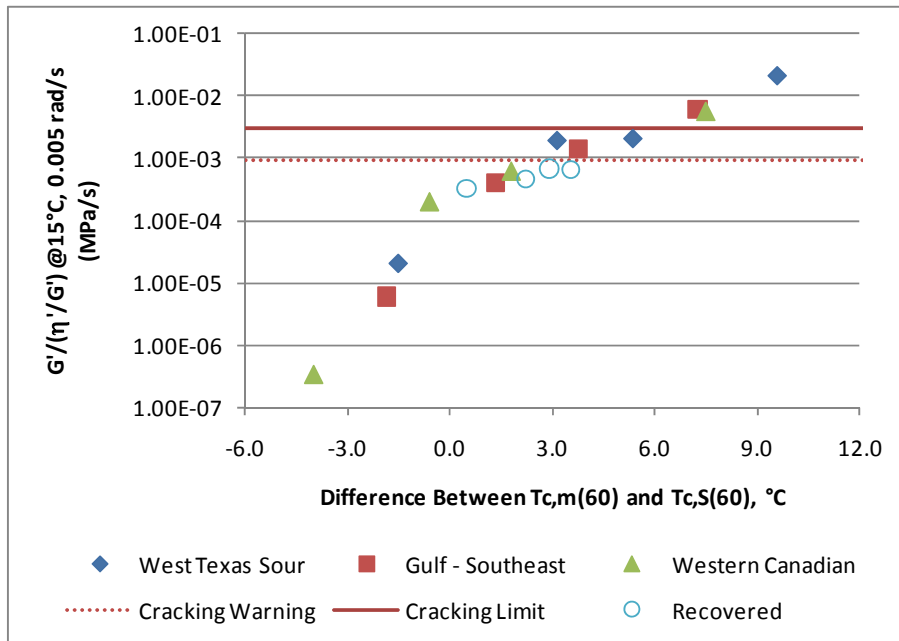


Figure 4.8 Relationship Between $G'/(η'G')$ and ΔT_c – with Recovered Asphalt Binders

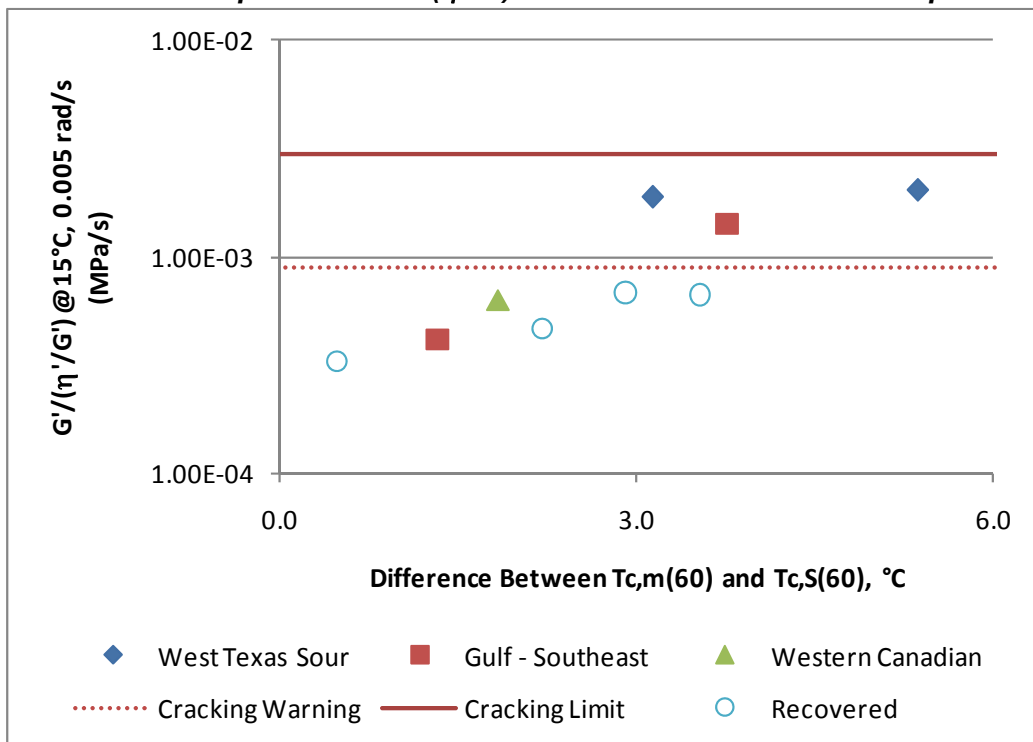


Figure 4.9 Relationship Between $G'/(η'G')$ and ΔT_c – with Recovered Asphalt Binders (Magnified)

As shown in Figures 4.8 and 4.9, the data from the recovered asphalt binders fit in fairly well with the data from the laboratory aged asphalt binders. Two data points – Roundup Bottom and Conchas Lake – are close to the “Cracking Warning” line. Since both airfield pavements have experienced some distress, the suggested value to identify the onset of cracking – $G'/(η'G')$ equal to $9.00E-04$ MPa/s – this may need to be adjusted when additional data from other research projects becomes available. Also as noted earlier, this Glover fatigue parameter is determined at 15°C. Some adjustment may still need to be made so that failure limits reflect climate temperature.

As can be seen from data in Table 4.5, predicted cracking results from ΔT_c were even more encouraging. The older, cracked Montana pavement and the older New Mexico pavement at Conchas Lake both showed values above the hypothesized limit of 2.5 where damage begins. Even with its less than ideal West Texas Sour-like asphalt, the Clayton binder fell a bit below 2.5. The relatively new pavement in Montana with its Western Canadian-like asphalt was well below this limit. Four data points do not validate a performance test method, but results are indeed consistent with projections from the laboratory phase of the study. So long as the standard BBR low temperature grade is supplied, this parameter should be automatically adjusting for climate.

4.3.2 Asphalt Mixture Testing

Much like lab mixture specimens, field cores were trimmed and cut for mixture BBR and DC(T) testing, and then some DC(T) specimens were extracted for binder testing. Again, care was taken to only smooth the core surface and consistently test the remaining top 25mm from each core to best represent the aged surface.

Mixture Bending Beam Rheometer (BBR) Testing

Two cores from each test site were sent to Dr. Marasteanu at University of Minnesota for BBR mixture testing in both bending and fracture modes. After smoothing the core surface by removing approximately 4 mm, nine BBR specimens were cut from each core, so that six replicates were run for each location at each of three test temperatures.

Figure 4.10 shows replicates for S and m-value as measured for all test specimens at -12°C. As can be noted from the individual graphs, some results show high variability, particularly when material properties are near conditions where damage develops in the specimens. However, the loading curves were always straight lines, indicating no further damage occurred as the specimen was loaded in the BBR. For each set of six replicates, the specimens with the highest and lowest stiffness were discarded, and the remaining four results were averaged for further analysis. The average results for each location at all BBR test temperatures are shown in Figure 4.11.

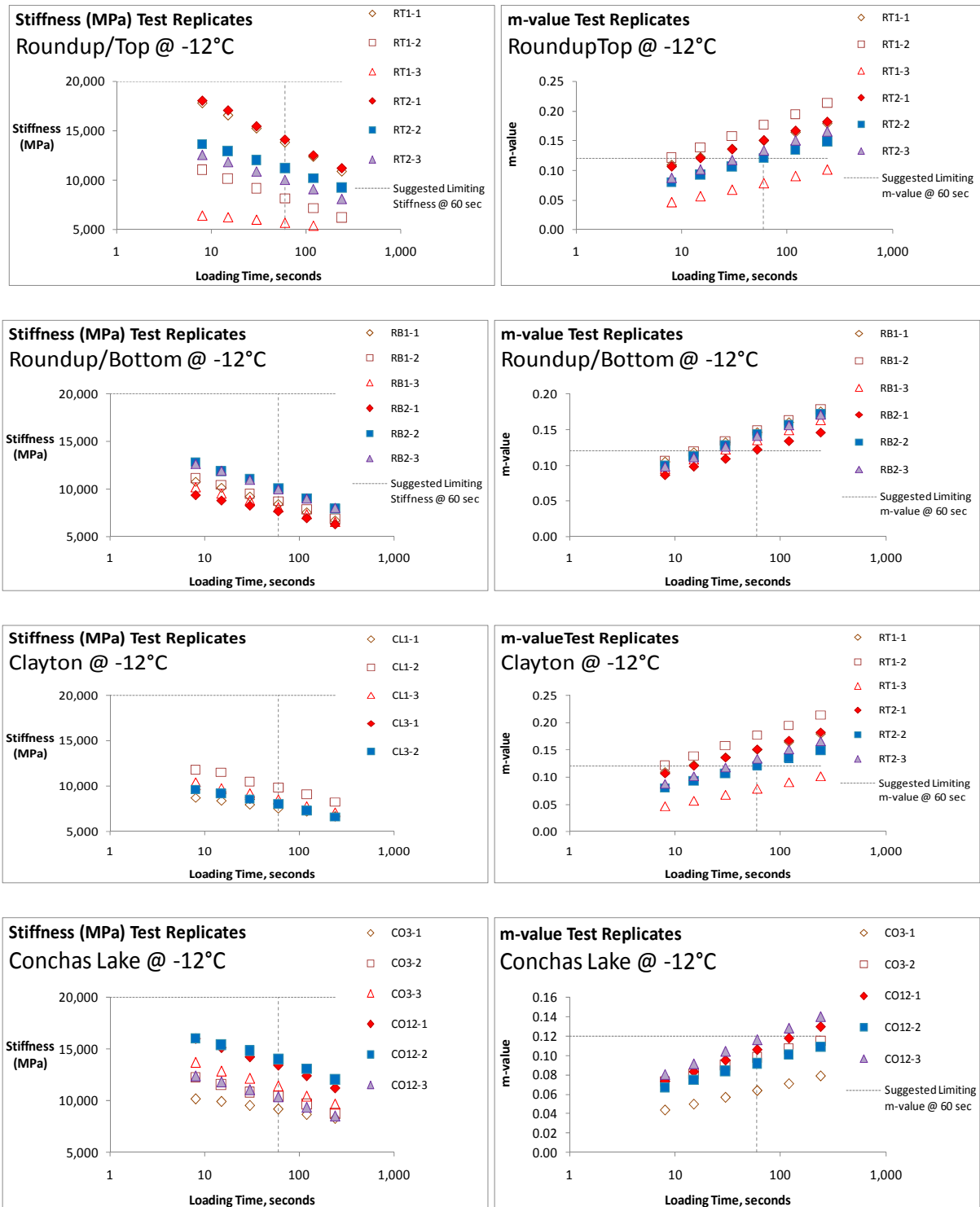


Figure 4.10 Replicate Results for S and m-value for All Field Specimens Tested @-12°C

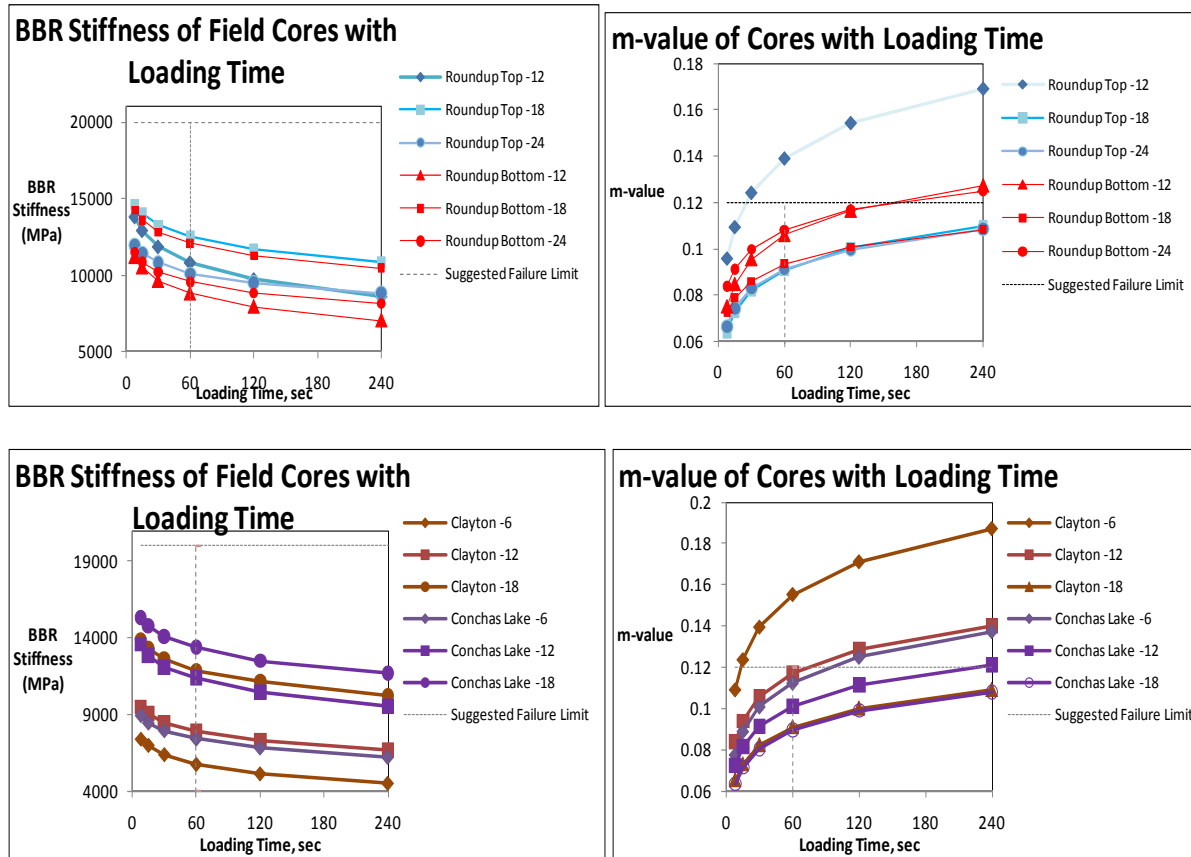


Figure 4.11 Average BBR Mixture loading Curves for All Field Mixes at Three Temperatures

During the laboratory testing phase as described in section 3.3.3, it was noted that mixture stiffness increases and m-value decreases with aging up to some critical limit, and then the onset of damage causes these trends to reverse with additional aging. For the laboratory mix, this reversal occurred as the m-value approached 0.13 and the mixture stiffness approached 20,000 MPa. Figure 4.12 consolidates all of the stiffness data for the standard 60 second loading time into a single chart, and Figure 4.13 does the same for m-value.

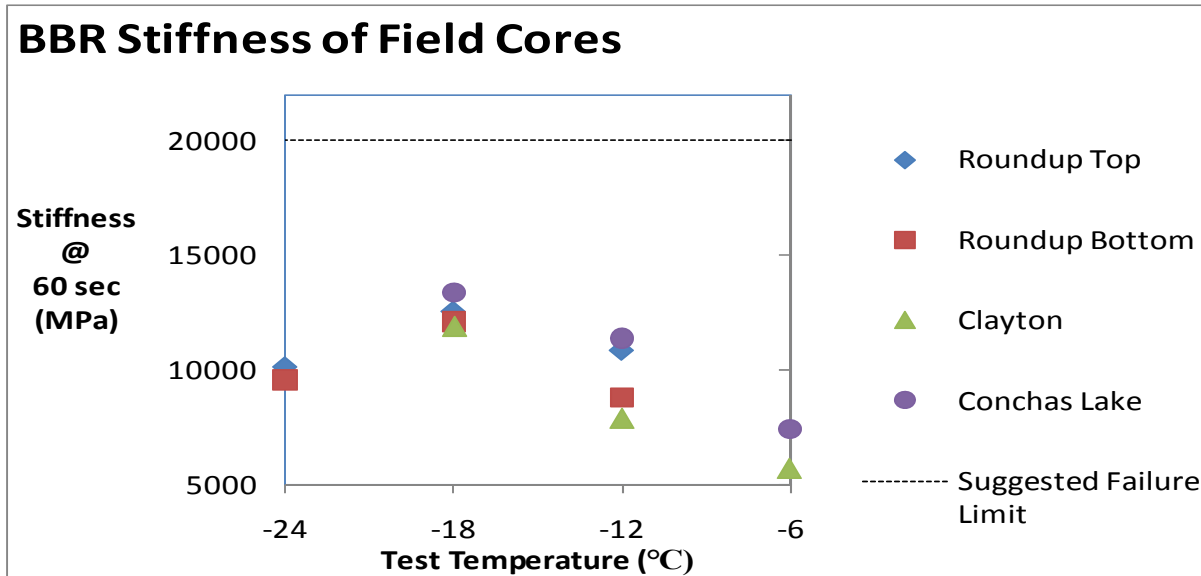


Figure 4.12 BBR Stiffness for Field Cores – 4 Locations

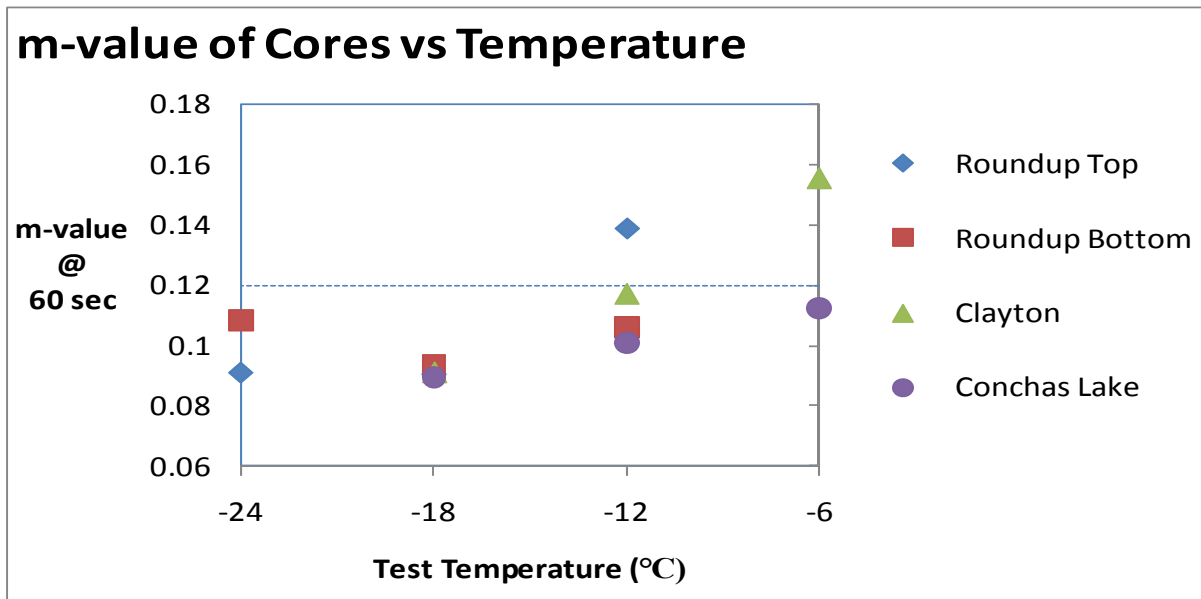


Figure 4.13 BBR m-value for Field Cores – 4 Locations

Here there are no different aging times for each specimen, but the samples do show a damage anomaly with decreasing temperature that is similar to that observed in the laboratory specimens with increased aging. That is, once some critical material property has been reached through the combined effects of increased aging and low temperature, the stiffness and m-value reverse as if some specific amount of damage has occurred within the specimen. However, the reversal in stiffness for the lab mix occurred at 20,000 MPa, whereas the reversals here appear

to occur much earlier. Since mixture stiffness is aggregate dependent, this difference was not unexpected. The minimum m-value is also lower, approaching 0.09 and then reversing as opposed to 0.13 for the lab experiments. However, the m-value results do seem to fall in line with reported damage from field observations at these sites.

Since the mixture m-value varies with temperature, the lowest local temperatures must be known as part of the mixture prediction model based upon a limiting m-value. LTPPBind Version 3.1 was used to estimate temperatures for the three airports. Using 98% reliability, results were as shown in Table 4.6. It is important to remember that the BBR test temperature is offset by +10°C from the low pavement temperature.

Table 4.6 Low PG Climate Temperatures for the Airport Field Sites (98% reliability)

	Roundup, MT	Clayton, NM	Conchas Lake, NM
PG – High Temp °C	57.4	58.6	61.5
PG – Low Temp °C	-32.7	-21.1	-19.6

Given the previously defined limits on mixture m-value, and assuming the binder's low temperature stiffness is appropriate for the climate, it is now possible to make some predictions on the damage state of the various field sites.

The Conchas Lake specimen is taken from a moderate climate in northeast New Mexico. However, the very poor m-value even at -6°C indicates that this mix is highly aged and probably cracked if low pavement temperatures reach the corresponding -16°C. Since the LTPPBind low pavement temperature for Conchas Lake is -19.6°C, m-value predicts significant but probably not severe non-load associated damage related to surface cracking and raveling.

The Clayton specimen should not be damaged if the pavement temperature remains above -16°C, but will be on the brink of cracking at -22°C, and damaged at -28°C. Given a low temperature climate of -21.1°C, Clayton's runway should not show significant visible damage, but it is definitely a candidate for immediate preservation action. In equal New Mexico climates, Clayton should exhibit significantly less cracking than Conchas Lake, but is likely at the point where damage will begin to accumulate without healing.

Roundup/Top has the best relaxation properties as measured by m-value, but this airport is located in a much colder Montana climate requiring a low temperature PG grade of -32.7°C or better. The new surface (Roundup/Top) is clearly less aged than the underlying oxidized mix (Roundup/Bottom) that was cracked and overlaid. However, in the colder Montana climate, even the surface mix may exhibit some damage if the PG grade temperature is reached, and should be treated quickly. The old overlaid surface should have cracked significantly if exposed to surface temperatures before overlay. These predictions taken from mixture m-values appear to be fairly consistent with field observations of damage. More field data is clearly needed to broaden the database and refine conclusions. However, existing data does support a warning that a preservation treatment should be applied as the mixture m-value approaches 0.12.

There is also some question as to whether these observations should use the 98% reliability values (one year in 50) or the 50% reliability values (one year in 2).

BBR Bending Tests – Thermal Stress Curves and Shenoy Parameters

As discussed in section 3.3.3, Shenoy uses thermal stress curves derived from BBR loading curves to predict critical cracking temperatures based upon cooling rate. These properties were calculated with two replicates for each of the four field sites, as noted in Table 4.7.

Table 4.7 Low Temperature Cracking Predictions from Shenoy Method

Cooling Rate	-1°C/hr		-10°C/hr	
Site	Replicate 1	Replicate 2	Replicate 1	Replicate 2
Clayton	-21.1°C	-23.5°C	-18.5°C	-20.9°C
Conchas Lake	-7.8°C	-20.6°C	-5.8°C	-17.3°C
Roundup/Top	-15.4°C	-7.8°C	-13.6°C	-6.4°C
Roundup/Bottom	-19.8°C	-22.8°C	-17.6°C	-20.1°C

The results for the Shenoy predictions were very disappointing. A long extrapolation is required to determine the failure temperature, and the high variability in the BBR tests was magnified when applying Shenoy’s methods. Even replicate samples varied in predictions by 12°C, or two full PG grades. Results also did not correlate with other lab findings, or with field observations. Intuitively, the Shenoy approach makes sense, but the method can only be applied if the BBR data is very accurate and consistent. Given the variability observed for the field specimens, this does not appear possible at this time. Shenoy’s parameter as taken from back-calculated mixture BBR properties is probably not a viable predictive tool for cracking

BBR Bending Tests – Binder vs. Mixture

As discussed previously in this section, BBR bending tests were also run on binders extracted from these four field mixes. Figure 4.14 compares trends for binder vs. mixture stiffness, and Figure 4.15 compares results for binder vs. mixture m-value.

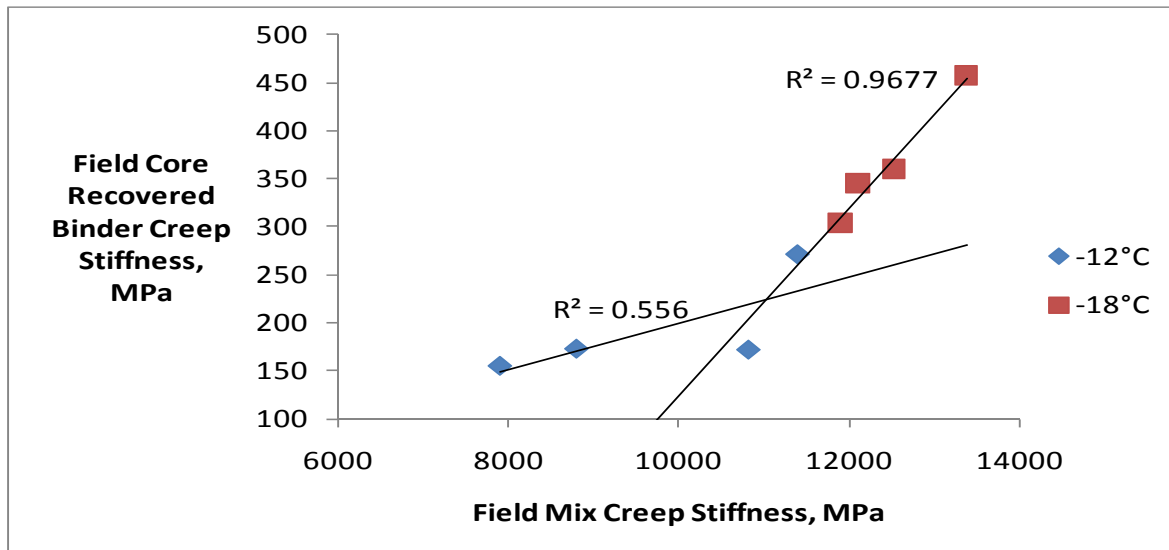


Figure 4.14 Comparison of Binder vs. Mixture Stiffness for 4 Field Sites

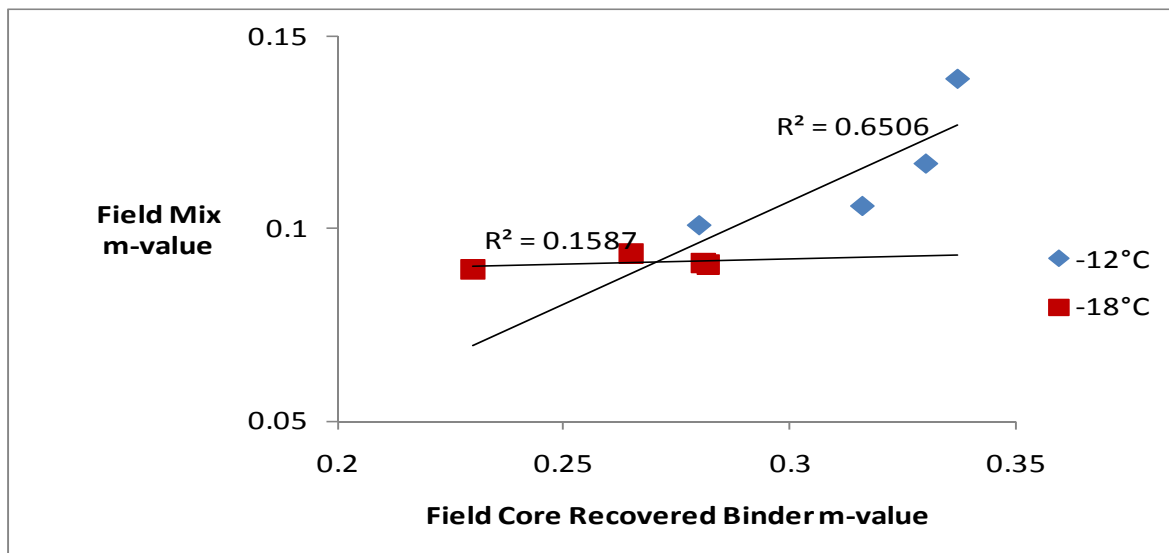


Figure 4.15 Comparison of Minder vs. Mixture m-value for 4 Field Sites

Regardless of mix design for the four mixes, there appears to be a fairly good correlation between binder and mixture stiffness, with no clear reversal at higher mixture stiffness up to 14,000 MPa. Recall from section 3.3.3 that the reversal in stiffness in the lab study did not occur until the mixture stiffness reached 20,000 MPa. However, the m-values for the mixture clearly plateau at an m-value near 0.1, even though the binder m-value continues to decrease with age or lower temperatures. These graphs further support the idea that a minimum m-value trigger for the mixture should be a reasonable indicator of impending damage, but there is no equivalent

minimum m-value for the binder. Instead, any binder trigger should depend upon a location in a black diagram.

Although not useful for identifying a trigger, it is also interesting to view comparative binder and mixture physical properties on a single graph. Figure 4.16 show such data for cores taken from the Clayton airport pavement. Figure 4.17 views this same comparison of binder and mixture properties for data from all four field sites.

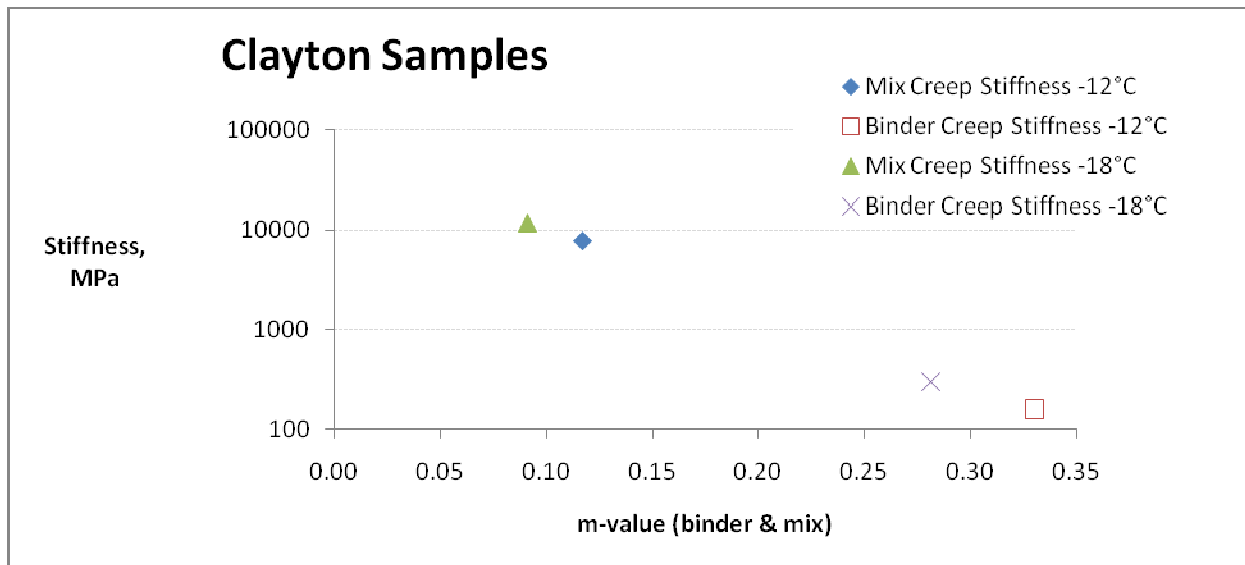


Figure 4.16 Binder and Mixture Physical Properties for BBR Bending Tests – Clayton

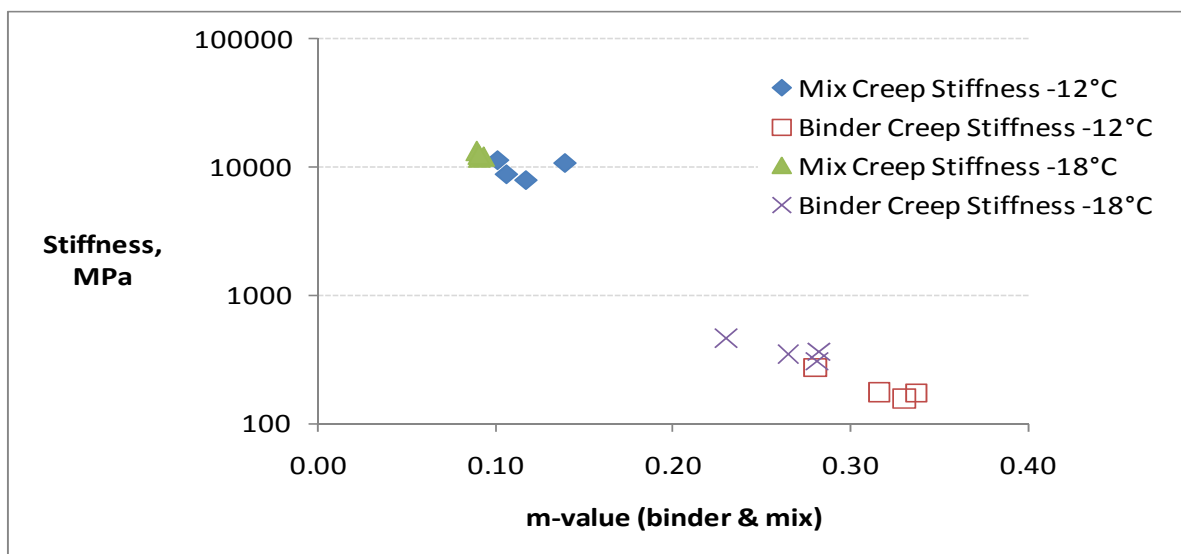


Figure 4.17 Binder and Mixture Physical Properties for BBR Bending Tests – 4 Field Sites

Recalling the following relationships for BBR ΔT_c from Table 4.6 as reported earlier in this section, and comparing these to the limits of 2.5 (onset of damage) and 5.0 (significant damage) as proposed from the laboratory phase of the study described in section 3.3.3, Roundup Bottom and Conchas Lake should exhibit visible damage, Clayton should be very near the critical point for damage initiation, and Roundup Top should still be in good condition, as depicted in Table 4.8. These predictions have a built in assumption that the original binders were selected to have stiffness appropriate for the PG grade needed in that local climate.

Table 4.8 Using ΔT_c , °C as a Cracking Predictor

	Roundup Top	Roundup Bottom	Clayton	Conchas Lake
ΔT_c , °C	0.5	2.9	2.2	3.5

It is interesting to note that these predictions of surface condition are very similar to those expressed above when using mixture m-value in combination with the local climate temperature. Although only 4 sites were tested, both predictive methods appear to be consistent with visual damage surveys of the respective pavements.

Because poorly constructed longitudinal joints typically have a high percentage of interconnected air voids, oxidation should occur most rapidly in these areas. Raveling or cracking in these joints or in other segregated areas may be a pre-indication of imminent damage, and might also be used to trigger aggressive preservation actions.

BBR Fracture Test

BBR Fracture tests as described in section 3.3.3 were also run on field specimens. Figures 4.18 through 4.21 show results for 3 replicates run at each of three different test temperatures (-6°C, -12°C, -18°C) for one core from Clayton airport. The four Figures show curves for results as represented on different axes. The failure stress results for the Clayton specimens are listed in Table 4.9.

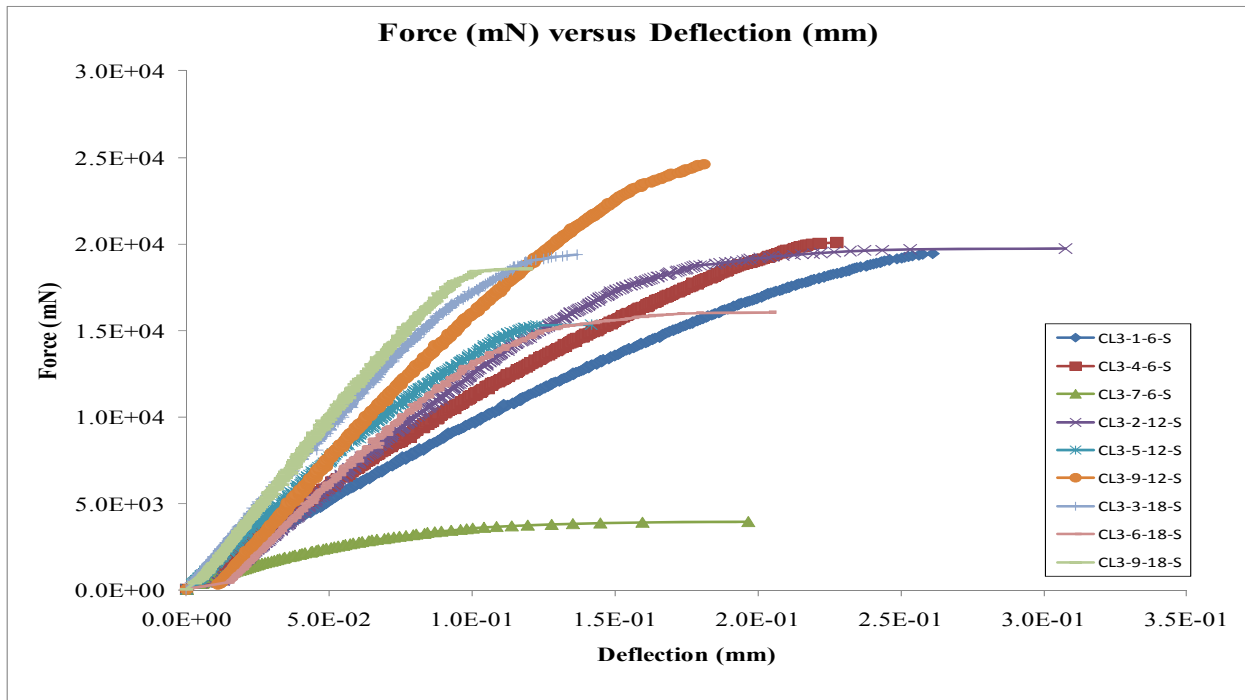


Figure 4.18 BBR Fracture Test: Force vs. Deflection for Clayton (3 temps, 3 reps)

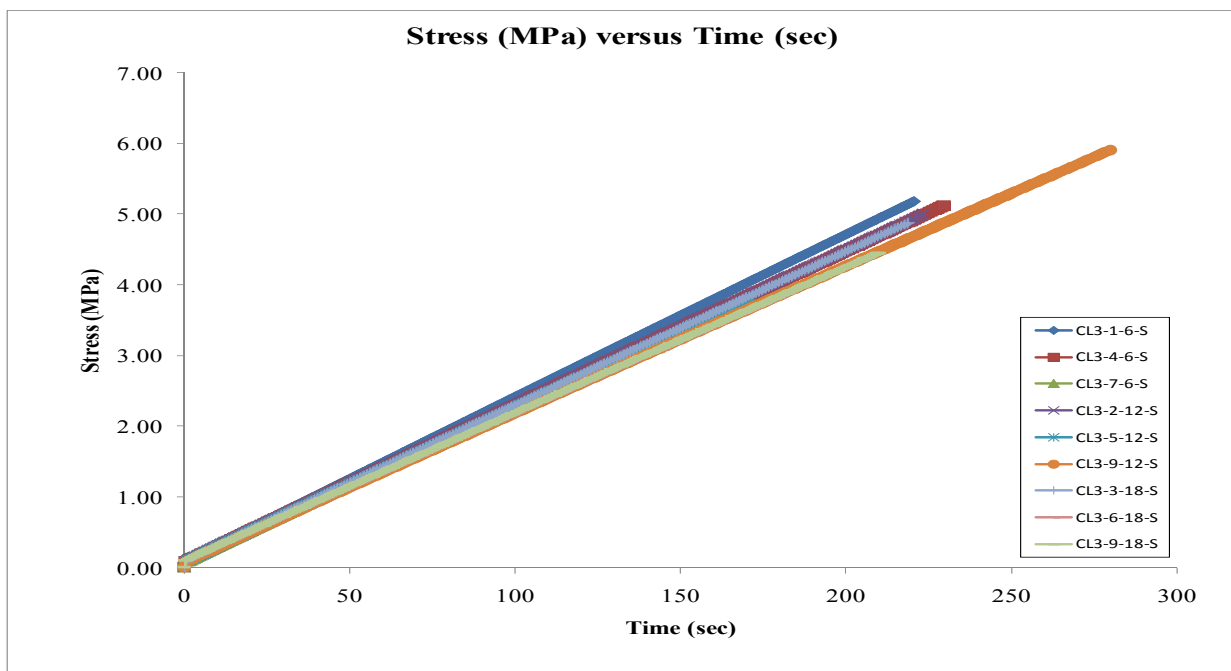


Figure 4.19 BBR Fracture Test: Stress vs. Time for Clayton (3 temps, 3 reps)

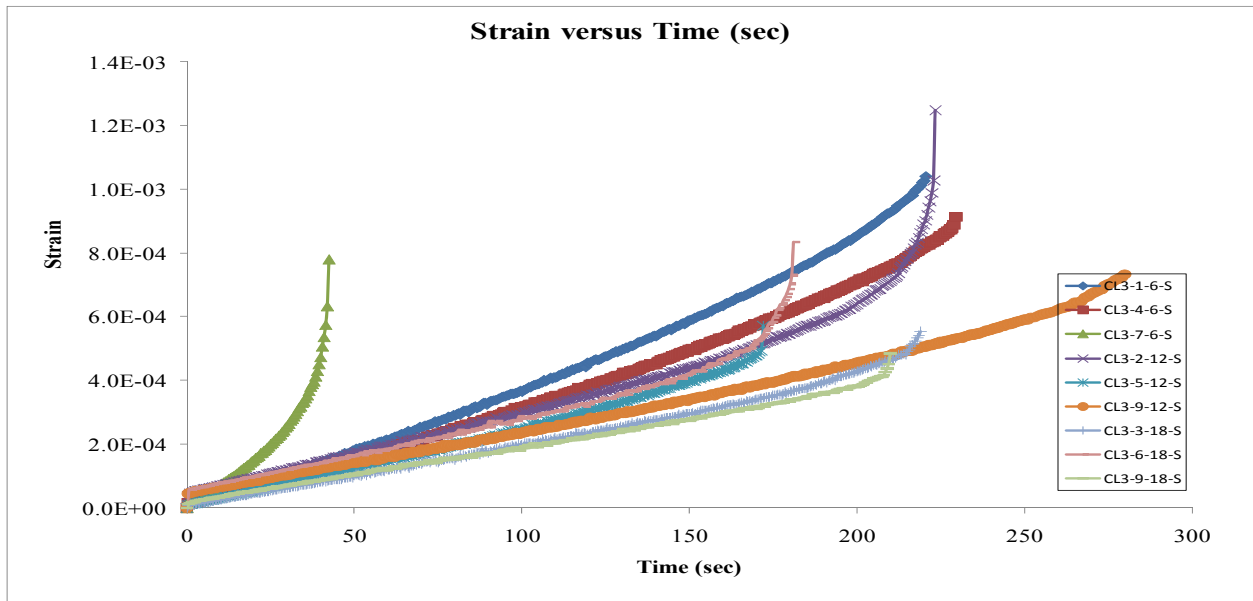


Figure 4.20 BBR Fracture Test: Strain vs. Time for Clayton (3 temps, 3 reps)

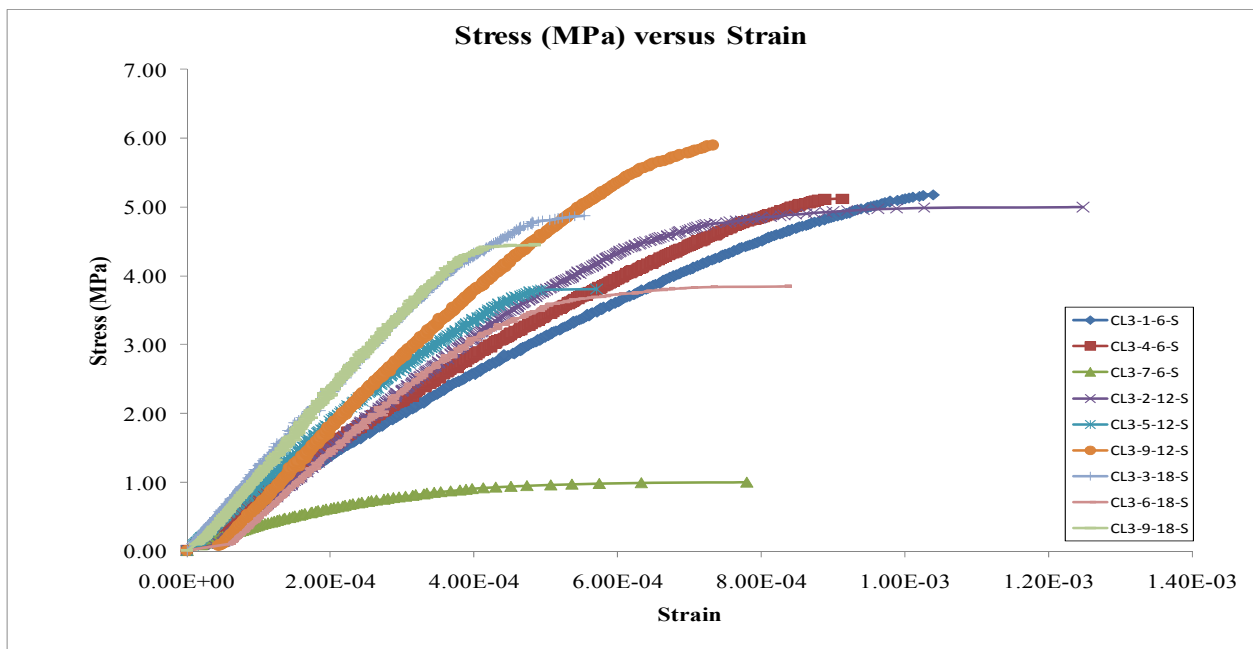


Figure 4.21 BBR Fracture Test: Stress vs. Strain for Clayton (3 temps, 3 reps)

Table 4.9 BBR Failure Stresses (MPa) for Clayton Airport Cores

Clayton Airport Replicates	Temperature		
	-6°C	-12°C	-18°C
1	5.18	5.00	3.85
2	5.12	5.90	4.45
3	3.42	4.42	4.76
4	4.74	4.14	4.08
Average	4.62	4.87	4.29

As with the lab prepared specimens, there was a great deal of variability in all test results for failure stress as compared to any differences with temperature, even after throwing out the high and low values from six replicates. There are no obvious trends from the BBR fracture tests that fit with observed field results for surface raveling or cracking.

Disk-Shaped Compact Tensions Test (DC(t))

Fracture energy from the DC(t) test on the cores is shown in Tables 4.10 (CMOD measurement) and 4.11 (Delta 25 measurement). The CMOD data is about two times more than the Delta 25 gage data as expected and seen with the lab portion of this study. Further analysis will just focus on the CMOD gage data. Figures 4.22 and 4.23 are plots of the data from the CMOD gage data in Table 4.10 from the New Mexico and Montana airfield pavement sites. As might be expected, test variability was higher for field cores than for lab compacted specimens. Also, a few data cells in the Tables were not completed due to testing difficulties. Since all cores were trimmed to the top 25mm, the fracture energy per m² calculation was adjusted to account for the thinner samples. As in the lab study, all samples were about 150mm in diameter.

All data revealed lower fracture energies than in the laboratory study except for the Conchas Lake (older) pavement. Lower fracture energies were expected in the older pavement cores, but it is confusing to also find low fracture energies in the newer pavement sections. It was even more surprising to find key predictions seemingly reversed from expectations. Figure 4.22 shows that at the test temperature of -12°C (10°C above the low PG climate grade), the fracture energy for the Conchas Lake specimen was almost twice as high as for the newer Clayton pavement. Moreover, based on the 300 J/m² minimum limit suggested by the laboratory study, the Conchas Lake pavement should not be cracked, and Clayton should exhibit significant damage.

Predictions for the two Roundup specimens are also reversed at -24°C (10°C above the low PG climate grade), although these two values are probably within experimental error. Also, the Roundup core bottom was the most limited on data and only had one test sample. According to

DC(t) data for Roundup, both sections should be ready to crack. In this case, the new surface was fairly new and in good condition, whereas the lower layer was assumed to have to have been cracked before overlaying. Photos in Figure 4.5 indicate a Conchas Lake pavement with some longitudinal cracking, but not much block or environmental cracking. There is no visual record of the condition of the Roundup pavement that was covered.

It is also important to note that the field mixes have lower fracture energies than the lab-aged mixtures. Harsher lab mixture aging, perhaps 72 hours or 96 hours at compaction temperature, may be needed to match lab and airport pavement fracture energies. It might also be possible to laboratory age specimens at a higher temperature to reduce oven time. This should be done with caution since small increases in oven temperature greatly increased mixture/binder aging.

Given the lack of response and significance of DC(t) peak load in the lab study, that data was not analyzed for the field cores.

Table 4.10 DC(t) Fracture Energy Measured from Crack Mouth Opening Displacement (CMOD) Gage

		West Texas Sour Crude Clayton Airport, NM			Western Canadian Crude Roundup Airport (top), MT		
		Test Temperature					
Pavement Condition	Sample	0°C	-6°C	-12°C	-12°C	-18°C	-24°C
Good, very few to no cracks	1	349.7	304.9	143.8	236.9	348.7	237.0
	2	208.3	215.3	211.4	193.6	267.5	205.2
	3	341.2	281.3	265.2		256.9	241.3
	Average	299.7	267.2	206.8	215.3	291.0	227.8
	Standard Deviation	79.3	46.4	60.8	30.6	50.2	19.7
	COV	26%	17%	29%	14%	17%	9%

		Conchas Lake Airport, NM			Roundup Airport (bottom), MT		
Pavement Condition	Sample	0°C	-6°C	-12°C	-12°C	-18°C	-24°C
Older with some cracks but may be good pavement	1	306.8	335.6	388.9	202.4	224.6	
	2	330.1	288.2	267.7	229.4	309.0	250.9
	3	270.4	302.2	448.8			
	Average	302.4	308.7	368.5	215.9	266.8	250.9
	Standard Deviation	30.1	24.4	92.3	19.1	59.7	Insufficient Data
	COV	10%	8%	25%	9%	22%	Insufficient Data

Table 4.11 DC(t) Fracture Energy Measured from Delta 25 Gages

		Clayton Airport, NM			Roundup Airport (top), MT		
		Test Temperature					
Pavement Condition	Sample	0°C	-6°C	-12°C	-12°C	-18°C	-24°C
Good, very few to no cracks	1	141.8	136.9	68.2	116.2	178.7	124.6
	2	96.7	94.5	105.3	97.3	132.1	99.7
	3	152.6	128.1	129.7		128.1	126.0
	Average	130.4	119.8	101.1	106.8	146.3	116.8
	Standard Deviation	29.7	22.4	31.0	13.4	28.1	14.8
	COV	23%	19%	31%	13%	19%	13%

		Conchas Lake Airport, NM			Roundup Airport (bottom), MT		
		Test Temperature					
Pavement Condition	Sample	0°C	-6°C	-12°C	-12°C	-18°C	-24°C
Older with some cracks but may be good pavement	1	143.3	164.1	192.5	100.9	101.1	189.5
	2	161.7	131.0	130.6	114.0	161.7	132.6
	3	131.3	146.3	222.0			
	Average	145.4	147.1	181.7	114.0	131.4	161.1
	Standard Deviation	15.3	16.6	46.6	Insufficient Data	42.9	40.2
	COV	11%	11%	26%	Insufficient Data	33%	25%

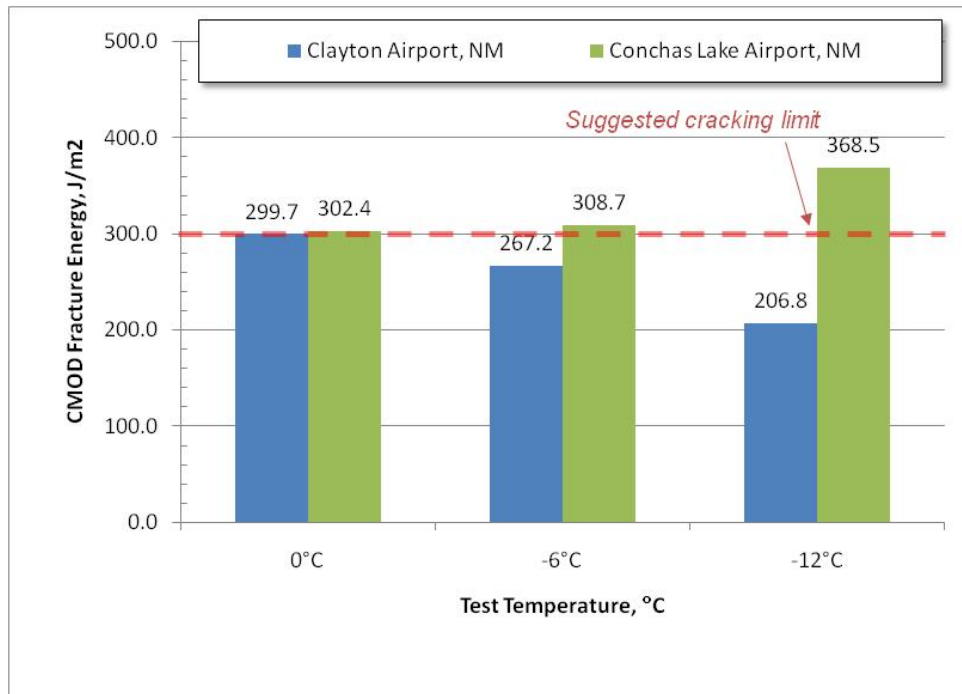


Figure 4.22 CMOD Fracture Energies for Pavement Cores with Suggested Cracking Limit, New Mexico Sites

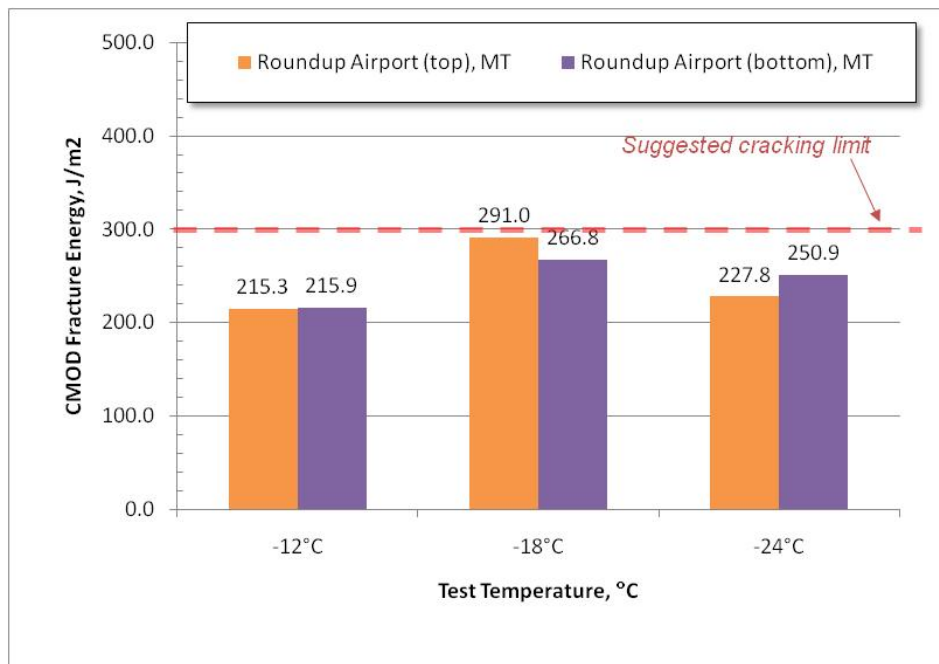


Figure 4.23 CMOD Fracture Energies for Pavement Cores with Suggested Cracking Limit, Montana Site

Table 4.12 DC(t) Fracture Energy Comparing Good to Cracked Sites at Climate Temperature Using CMOD Gages

Location	98% Low Temperature PG to Use for Low Temp. Performance	Shifted +10 Degrees C	CMOD Average Value for Temperature Specific Target- <u>Good</u> Pavement, J/m ²	CMOD Average Value for Temperature Specific Target- <u>Older</u> Pavement, J/m ²
NE New Mexico	-22	-12	206.8	368.5
Central Montana	-34	-24	227.8	250.9
Average Energy for Climatic Temperature			217.3	309.7

Table 4.13 DC(t) Fracture Energy Comparing Good to Cracked Sites at Climate Temperature Using Delta 25 Gages

Location	98% Low Temperature PG to Use for Low Temp. Performance	Shifted +10 Degrees C	Delta 25 Average Value for Temperature Specific Target- <u>Good</u> Pavement, J/m ²	Delta25 Average Value for Temperature Specific Target- <u>Older</u> Pavement, J/m ²
NE New Mexico	-22	-12	101.1	181.7
Central Montana	-34	-24	116.8	161.1
Average Energy for Climatic Temperature			108.9	171.4

CHAPTER 5.0 LABORATORY TOOLS FOR PREDICTING TRANSVERSE AND BLOCK CRACKING

The primary objective for this study was to identify simple binder and/or mixture tests which can predict imminent cracking or raveling so that pavement preservation strategies can be timed to delay or prevent damage. Secondary objectives were to advance the theoretical knowledge of thermal cracking mechanisms, first by validating the assumptions discussed above, and then by proposing a universal hypothesis that might guide future research (See Appendix A).

5.1 EXISTING PAVEMENT

Cores should be taken from the pavement so as to obtain a representative sample of the existing condition. Care should be taken so that the top 25mm (1") is intact. As mentioned in the previous chapters, the top of the core should only be trimmed to smooth the surface and remove end debris. Next, a 25mm (1 inch) specimen should be cut to represent material properties as close as possible to the pavement surface. These samples should then be trimmed for mixture testing and/or the binder extracted and recovered for binder testing.

5.1.1 Binder Tools to Rank Propensity for Cracking

To rank binder quality in cracking situations, tools must be able to capture both the relative quality of neat asphalts and the deterioration of relaxation properties that occurs with aging.

Transverse Cracking

- BBR, with separate controls for S and m-value – Continue to use current BBR standards as defined by PG specifications. Transverse cracking should be dominated by the stiffness measure.
- Direct Tension Test (DTT) - Used in combination with BBR for Table II PG specifications

Block Cracking

The two key binder properties for ranking resistance to block cracking are binder modulus and phase angle at the lowest pavement temperatures. Unfortunately, direct measurements currently require DSR torsion bar geometry and expensive research grade instruments. Western Research Institute (WRI) recently reported that 4mm plates can be used for low temperature testing, so long as machine compliance corrections are made. Significant laboratory and field data will be needed to develop and validate experimental methods, and then define failure curves in two-dimensional Black Space, and later in three-dimensional extensions of Black Space to include cooling time (See Appendix A). However, several simple binder tools can rank binders for their resistance to age related cracking so long as their moduli fall within a similar range.

- BBR ΔT_c - The most straightforward choice is ΔT_c from continuously-graded BBR data. This parameter is defined from both established BBR failure limits, and its relationship to Black Space is easy to understand. It is both a direct measure of binder quality, and can also be used as an aging shift factor. Furthermore, it is measured at low temperatures where block cracking occurs, and the reference point of 300 MPa and 0.30 m value is well established as a condition where cracking should not occur via any mechanism. Because binders are selected to specifically satisfy these parameters at the low pavement temperature, the requirement that stiffness remain within a fairly narrow range is reasonably well satisfied. Test equipment is already available, and the only additional testing would be a second BBR test temperature so that continuous grades could be calculated for both S and m-value.
 - RECOMMENDED BINDER PARAMETER
 - As a tool for timing preservation strategies. Recommend action as ΔT_c approaches 2.5°C.
 - As a parameter for binder specifications to differentiate binder quality, require $\Delta T_c \leq 2$ after standard RTFO/PAV aging. This limit is subject to further discussion and refinement, as it would eliminate strongly m-controlled asphalts from PG binder pools.
- DSR Parameter - The parameter $G'/(η'/G')$ as calculated using the mastercurve method at 15°C and 0.005 rad/sec shows a reasonable correlation with ΔT_c . Because it was developed as a fatigue cracking parameter, it is less clear whether the parameter location in Black Space falls near the failure temperature for block cracking, nor whether the modulus will fall within a narrow range. But it does appear to rank binder quality for cracking resistance, again so long as binders have comparable moduli. Adjustments for climate temperature need to be developed and included in any specifications based upon this concept.
 - Texas A&M's simplified approach using a single DSR measurement at 44°C and 10 rad/sec does not appear to correlate well with ΔT_c and can't be recommended at this time.
- Ductility @ 15°C and 1 cm/min – When evaluating research data from a prior era, the use of ductility at the designated test conditions appears to rank materials similarly to ΔT_c . Again, quality rankings can only be made when moduli are similar.

5.1.2 Mixture Tools to Predict Cracking

Transverse Cracking

- TSRST – The thermal stress restrained specimen test is the most direct method to determine the transverse cracking temperature at various cooling rates for fully confined specimens.
- IDT – The indirect tension test accurately predicts transverse cracking; cooling rate models are well defined, and the tool is well accepted as SuperPave performance test of choice.

Block Cracking and Surface Raveling

- DC(t) – The Disk-Shaped Compact Tension [DC(t)] fracture energy test measures fracture energy in tension. The test geometry offers a long fracture face to pure tension loads, and physical properties are very suitable to finite element modeling. This tool has become the method of choice to predict reflective cracking, especially for overlays on JCP. However, loading times are relatively rapid, and fracture energy alone does not correctly rank materials for block cracking. Further modeling will be needed to make this tool applicable to cracking mechanisms that occur over very long loading times.
- BBR Mixture Bending Test – Because phase angle, or m-value, is so important to material performance over very long periods of time, the BBR bending test on mixtures seems to be a good choice. Specimens are small, so numerous replicates are needed to get statistically valid results. Several parameters can be determined, and some combination of these may ultimately prove useful. Although field validation results are limited, findings to date are:
 - Mixture Stiffness – Aggregate structure is a very important component of mixture stiffness, even at low temperatures. Mixture stiffness alone can therefore not identify binder properties as they approach critical limits.
 - Mixture m-value – Relaxation properties at low temperatures appear to be strongly related to binder properties. The reversal in mixture m-value as the mix exhibits early stages of internal damage provides a very clear indication that preservation action should be taken within a fairly narrow range of m-values as measured at the lowest pavement temperature.
 - RECOMMENDED MIXTURE PARAMETER
A mixture m-value of approximately 0.12 is probably a good trigger for preservation, although further field validation of this property is needed.

Shenoy Parameters – The Shenoy parameter determine by extrapolating the thermal cooling curves to a failure temperature deserve further analysis. However, field data from this study was not consistent enough for accurate extrapolations. Use of Shenoy's Parameter is not recommended as a preservation trigger at this time.

5.2 TESTS FOR DESIGN AND SPECIFICATION - ACCELERATED LABORATORY AGING PROCEDURES

The test recommendations for design and specification are the same as previously listed except that the binder and mixture must be conditioned to simulate an aged pavement.

5.2.1 Binder

During the laboratory design phase, project asphalt binders should be selected that meet the appropriate low temperature grade for the climate specified. In addition, the value of ΔT_c should be determined from continuously-graded BBR data and compared to recommended limits in this report. At this time, no changes in long-term aging procedure (AASHTO R28) are recommended.

5.2.2 Mixture

After mixing the aggregate and asphalt binder, the mixture should be loose-mixed aged for further mechanical property testing in accordance with AASHTO R-30. The mixture is placed in a pan 25 to 50 mm (1 to 2 inches) thick and the pan is placed into a forced draft oven at compaction temperature. Different than AASHTO R-30, the loose mixture should be aged for 48 ± 1 hour to better simulate the pavement surface after several years of service. It is not practical to stir the loose mixture every hour.

Once the mixture is removed from the oven, the mixture is transferred to the Superpave Gyrotory Compactor (SGC) for preparation of 150mm cylinders. The cylinders are then trimmed, cored, and instrumented for testing in accordance with ASTM D7313, "Standard Test Method for Determining Fracture Energy of Asphalt-Aggregate Mixtures Using the Disk-Shaped Compact Tension Geometry".

CHAPTER 6.0 CONCLUSIONS AND RECOMMENDATIONS

Thermally induced cracks open in response to stresses that develop as pavement materials shrink upon cooling. Depending upon material properties and environmental conditions, these cracks may follow different paths, with extremes ranging from single-event full-depth transverse cracking to severe block cracking visible only near the pavement surface. Transverse cracking has long been associated with binder stiffness at low pavement temperatures, whereas block cracking is prevalent on older oxidized pavements.

Thermal stresses build more quickly when binders are unable to flow. Hence, thermally induced cracking mechanisms typically cause more damage at the lowest pavement temperatures where the binder phase angle is at its lowest. Any ranking of binder quality must then include three key parameters, binder modulus, phase angle, and the time over which the stresses build and relax.

Although often incorrectly referred to as “age hardening”, the primary impact of oxidation is to reduce the phase angle of the binder by destroying molecular degrees of freedom. The BBR stiffness does get harder with aging, but not appreciably. After oxidation, the low binder phase angle causes thermal stresses to last longer. As a result, the dominant cracking mode changes from transverse to block cracking.

This study’s hypothesis for thermal cracking proposes that thermal stress be evaluated as the difference between two functions; the amount of stress that would build under given environmental conditions if the material were completely elastic minus the amount of stress that is relieved through fluid flow over the given time interval for cooling. The interesting outcome of this hypothesis is that the ranking of material quality depends upon the time interval for cooling. That is, there is no single ranking of binder quality with respect to cracking, because a change in the time interval for relaxation changes the relative performance of different binders. For example, rapid cooling events favor transverse cracking via mechanisms dominated by binder stiffness. Very slow cooling greatly increases the influence of binder phase angle and contributes more to block cracking, but only after the aging binder can no longer relieve building stresses through flow.

Because block cracking is so closely tied to pavement aging, laboratory binder and mixture aging studies were conducted to better characterize the evolution in low temperature rheological and fracture properties. Evaluations included numerous test procedures proposed in the literature, as well as simple new tools envisioned by this study to be practical indicators of impending cracking damage in an aging pavement. Based on these laboratory aging studies, more promising test methods were carried forward to evaluate four mixes collected from previously identified airfield pavements. Although field sites were limited, tentative conclusions favor one binder parameter and one mixture test that might be used to identify in-place pavements that have aged to the point where surface cracking and raveling is imminent.

Binder Parameter

ΔT_c , defined as the difference in temperature where a continuously-graded binder reaches its BBR limiting temperature for Stiffness and m-value respectively:

$$\Delta T_c = T(S=300 \text{ MPa}) - T(m\text{-value} = 0.300)$$

The results of this study suggest that if $\Delta T_c \geq 2.5$ then surface cracking/raveling is imminent and surface treatment is recommended. If $\Delta T_c \geq 5.0$ then surface damage should already be significant and other forms of pavement rehabilitation, such as mill and replace, should be considered.

Mixture Parameter

Minimum m-value using BBR mixture bending test

The results in this study suggest that if the m-value from the mixture BBR test is approximately equal to 0.12 then surface damage is imminent and surface treatment is recommended.

It should be noted that, because internal specimen damage causes the m-value to increase rather than continue to decrease, it is important to catch the m-value near its minimum before it starts to rise again.

Although a rheological failure parameter should be a function of both S and m-value, asphalt binders selected using PG grading criteria should have similar stiffness at low pavement temperatures. Since aging does not have a large impact on the initial stiffness but does dramatically impact relaxation properties, the mixture m-value serves as a reasonable surrogate for predicting block cracking. Because gradients in binder properties accrue with advanced aging, the ability to test thin mixture specimens cut from near the surface is a distinct advantage. Although the binder test is preferred, extracting enough asphalt from thin surfaces for BBR continuous grading requires multiple cores, leading to expensive test results and swiss-cheese pavements. Newly developed DSR procedures using 4-mm plates for low test temperatures will offer the opportunity to test small samples of extracted bitumen from a single core, while also providing direct measures of modulus and phase angle for Black Diagrams. More research is needed to extend the BBR results to these newer DSR binder testing protocols.

Using fracture tests to rank materials for thermally-induced cracking presents a complicated set of issues that are not easy to address, particularly for simplified test methods as requested for this project. First, the BBR mixture fracture test measures fracture stress, while the DC(t) test provides fracture energy. The problem here is that there is no single correct ranking of materials for cracking, because the cooling rate and time changes everything. Even though the DC(t) is an excellent test method for fracture energy, the resulting material ranking and predicted performance are only valid if results can be modeled in the context of changing binder relaxation

properties and cooling time. This may be possible with elegant finite element and other theoretical modeling, but this approach is not simple. There also appears to be some variability in the data as measured by coefficients of variation. It is probably easier to use fracture data in combination with thermal stress curves from rheological data to define critical cracking temperatures, much like Bouldin and Rowe did when adding the direct tension test to Table II binder specifications. However, requiring both a rheological test and a fracture test would be - expensive and time-consuming, and beyond the scope of the simple methods requested in this project.

6.1 STUDY LIMITATIONS AND FUTURE RESEARCH NEEDS

This study has several limitations that could affect its general use. First, only three asphalt binders were evaluated in the laboratory studies and they may or may not represent the range of expected aging performance of asphalt binders in the United States. Second, no modified asphalt binders were evaluated. The relationships found between physical properties and aging of unmodified asphalt binders may not be valid for modified asphalt binders (N.B. modified asphalt binders may not be routinely used in GA airport asphalt pavements, rendering this last limitation somewhat irrelevant). Third, only four airport asphalt pavements were studied in the field validation portion of the study from three airports in two sets of environmental conditions. Unfortunately, none of the four pavements exhibited high levels of cracking needed to validate the proposed parameters. Further field validation is needed. Lastly, the recommended use presumes that an airport manager will have the desire, time, and resources to conduct testing and analysis throughout the pavement's life. It would be advantageous if prequalification testing of the asphalt materials could be used to identify the risk for early cracking and provide a general time frame when preventative maintenance should occur (e.g., "Early cracking expected; suggested preventative action in 3-5 years" or "Early cracking possible, but not expected; suggested preventative action in 6-8 years"). To accomplish this goal will require significantly more study and performance modeling.

Additional work is needed to fully validate the assumptions and hypotheses used in the report. We do know that the parameters discussed in the report seem to be related to aging based on the laboratory studies and that there is enough promising data to suggest an approach for additional validation work.

ACKNOWLEDGMENTS

The authors would like to thank the following individuals and organizations:

- Dave Johnson (Asphalt Institute) and John Tenison (AMEC) for coordinating efforts to obtain cores and reports on site conditions.
- Jason Coleman, Wes Cooper, Shay Emmons, and Jonathan Oepping of the Asphalt Institute for conducting much of the laboratory testing.
- Dr. Mihai Marasteanu (University of Minnesota) for coordinating the mixture BBR testing and analysis.
- Dr. William Buttlar (University of Illinois) for conducting testing and providing support on the DC(t) testing.
- Dr. Geoffrey Rowe (Abatech) for his assistance with software development and analysis.
- Bill Criqui (Road Science) for his assistance with the DC(t) sample and test set-up

Finally, the support of the Member Companies of the Asphalt Institute is gratefully acknowledged. Without their continued active interest and support, the work conducted by the AI staff could not have been accomplished.

CHAPTER 7.0 PRIMARY REFERENCES

1. Bell, Chris A. "Aging of Asphalt Aggregate Systems," Prepared for the Strategic Highway Research Program, National Research Council, SR-OSU-A-003A-89-September 1989.
Bell, Chris A. "Aging of Asphalt Aggregate Systems," Prepared for the Strategic Highway Research Program, National Research Council, SR-OSU-A-003A-89-September 1989.
2. Asphalt Institute. Superpave Performance Graded Asphalt Binder Specifications and Testing. 3rd ed. Superpave Series No. 1. Lexington, Kentucky. 2003.
3. Hanson, Douglas I., King, G., Buncher, M., Duval, J. Blankenship, P., and Anderson, M. Techniques for Prevention and Remediation of Non-Load Related Distresses on HMA Airport Pavements (Phase I, 05-07), Airfield Asphalt Pavement Technology Program (AAPTP). Final report, September 30, 2008.
4. Braham, A. F., Buttlar, W.G., Clyne, T. R., Marasteanu, M. O., and M. I. Turos, "The Effect of Long Term Laboratory Aging on Hot Mix Asphalt Fracture Energy," Journal of the Association of Asphalt Paving Technologists, 2009.
5. Zofka, A, Marasteanu, M, Clyne, T, Li, X, Hoffmann, O; "Development of a Simple Asphalt Test for Determination of Asphalt Blending Charts", MNDOT report MN/RC 2004-44, 2004, 100 pages.
6. Bouldin,, M., Dongre, R. Rowe, G, and Sharrock, M.J. "Predicting Thermal Cracking of Pavement from Binder Properties – Theoretical Basis and Field Validations", AAPT, V. 69, 2000, pp. 455-496
7. Shenoy, Aroon; "Single-Event Cracking Temperature of Asphalt Pavements Directly from Bending Beam Rheometer Data", J. of Transportation Engineering, Sep/Oct 2002, pp. 465-471.
8. Marasteanu, M., Basu, A., Hesp, S., & Voller, V.; "Time-Temperature Superposition and AASHTO MP1a Critical Temperature for Low-temperature Cracking", International Journal of Pavement Engineering, Vol 5 (1), March, 2004, pp. 31-38.

APPENDIX A

A UNIVERSAL HYPOTHESIS FOR NON-LOAD INDUCED CRACKING

APPENDIX A

A UNIVERSAL HYPOTHESIS FOR NON-LOAD INDUCED CRACKING

1.0 INTRODUCTION

Transverse cracking and block cracking represent two very different forms of pavement damage, both of which are thought to be caused by temperatures changes in the pavement, Although transverse cracking can be fairly well characterized as damage primarily related to the stiffness of the binder at the lowest pavement temperatures, the sources of stress causing block cracking have remained elusive. Before definitive test methods or predictive mathematical models can be developed as predictive tools for non-load associated cracking, a universal hypothesis is need to bridge the gap between the two very different failure mechanisms. Unfortunately, no such universal cracking theories exist.

1.1 A Universal Theory for Gravity

As the story goes, one day an apple fell from a tree. Not a particularly auspicious event had it not hit the head of a curious young man. After further experimentation, Isaac discovered that a falling brick hurt more than a feather, and so Newton's theory of gravity was born, including an equation with a constant for the earth's gravitational field. When physicists further recognized that gravity depends upon the mass of two different bodies as they interact through the distance separating them, Newton's equation was extended to a Universal Theory of Gravity. This fortunate extension of gravitational theory enabled Neil Armstrong to lift the Eagle off of the moon's surface without rebuilding Saturn 5. An age-old story perhaps, but how will a few bites from Newton's apple help us understand non-load associated cracking?

1.2 A Universal Theory for Thermally-Induced Cracking: Learning by Analogy

Classic transverse cracking is too often equated with thermal cracking, so much so that most textbooks define the term "transverse thermal cracking" as though this cracking pattern were the only one to develop as pavements cool. By analogy to Sir Isaac, that definition locks science into a view of gravity from the earth's surface. His equations can't be extended to movement of other bodies in a broader universe because the mass of one body has been arbitrarily fixed. To relieve this bottleneck which inhibits a more universal perspective on cracking as induced by changes in temperature, the concept of thermally-induced cracking must first be separated from classic transverse cracking in the same way that a solution for a universal theory of gravity had to move away from the earth to recognize that the second body can have a continuum of masses. Newton's early equations for gravity on earth were not wrong, as our many theories and tools to predict transverse cracking are not wrong. However, this myopic view with its limiting assumptions does not shed any light on other types of cracking that might also be caused by thermally induced stresses. For example, block cracking has proven much more difficult to isolate and predict, although it is generally accepted that this damage mechanism occurs only after significant binder oxidation, often referred to as age hardening. The field survey accompanying this study revealed that serious block cracking can occur on older airfield pavements that have been closed for twenty years, so this damage mechanism must also be caused by environmental stresses.

But solving block cracking independently would be like creating a second theory for gravity on the moon. It would likewise be correct, but only for a second body with mass = moon. As the universal solution for gravity works for any two bodies in space, a universal solution to thermally-induced cracking should predict propensity for damage given any pavement temperature change occurring over any period of time. If the solution is clever enough, even the location and pattern of those cracks will be predicted with some modest level of accuracy. But what other physical parameters (akin to second-body-mass and inter-body distance for gravity) can extend the principles already exploited for single-event transverse cracking to a much broader cracking universe?

2.0 BRINGING VISCOELASTICITY INTO A “LIMITING STIFFNESS” WORLD

The answer to the search for a second variable should be obvious to fundamental theoreticians. Concepts predicting cracking at some “limiting binder stiffness” have long provided the underpinnings for predicting transverse cracking. However, asphalt cement is viscoelastic, it can flow or stress-relax on some time-dependent regime to relieve building stress. Hence, the rheology of asphalt must always depend upon two parameters, the hardness as measured by complex modulus (G^*) and the rate of stress relaxation as defined by phase angle (δ). Like the two-body problem for gravity, there is no unique relationship between G^* and δ , but neither can cracking be predicted from either one independently. As the earth’s mass was concealed in Newton’s initial gravitational constant, some assumption for phase angle must be concealed in crack predictions based only upon stiffness. The importance of these two parameters was recognized by Anderson and coworkers during development of new SuperPave binder specifications, and a function of both ($G^*/\sin \delta$) was appropriately applied to predict high temperature distresses related to permanent deformation. However, a comprehensive solution for cracking was not found, so the SuperPave binder specification used BBR to set two independent material limits for cracking, one based upon low temperature stiffness ($S \leq 300$ MPa) and a second based upon relaxation rate, or m-value ($m \geq 0.30$). Although it was known at the time that these two variables do not operate independently, the lack of a universal solution led to a compromise. Although not theoretically sound, the separate limit for m-control was adopted as a practical way to prevent the overuse of highly oxidized roofing asphalts that were reported by CalTrans to crack prematurely when used in thin pavement surface mixtures. But if phase angle represents the “second body” in our cracking universe, could there also be a third independent variable akin to distance between the bodies?

Any driver knows that speed alone doesn’t predict how far he travelled. Knowing distance requires a second variable, the travel time. Like speed, phase angle is a rate. It quantifies how fast a material can relax stress, but does not define how much relaxation has occurred. Hence, the third independent variable important to cracking must be the time available for relaxation to occur. Rheologists usually address the time variable by discussing loading time, test frequency, or even relaxation time. In the context of thermally-induced cracking, stresses come from the environment, not from loads. It is more appropriate to view the time axis as the total period the material remains under stress, perhaps better described as the total time available for molecular relaxations to relieve stress. Slower cooling allows more time for liquid flow, resulting in lower ultimate thermal stresses and more healing of micro cracks.

Because environmental changes occur over a much longer time-scale than traffic loading events, molecular relaxation becomes an essential component of damage prediction. One way to view the problem is by asking two questions.

1. How much thermal stress would be created in the pavement for a given temperature change if the binder were elastic (phase angle = 0)?

If the materials are confined within the pavement, the induced stress, without relaxation, should be a function of the volume change in the aggregate and the modulus of the binder, with volume change being the product of the temperature change (ΔT) and the coefficient of thermal expansion (α) of the mix. The latter can be further separated into thermal expansion coefficients for the aggregate and the asphalt mastic respectively.

2. How much of that building stress can be relieved through fluid flow?

The reduction of these building stresses over time must be a function of the modulus and the amount of relaxation, with the latter depending upon both the relaxation rate δ and the time over which the cooling event occurs (t_{cool}). It is important to note that this time variable is not equivalent to “relaxation time” as defined for dynamic rheological measurements made under load.

With a simple assumption that the net stress is the difference between the stress created in an elastic body minus the stress lost through flow, these observations can be reduced to the following equation:

$$\text{Eq. 1: Thermal stress} = f(\Delta T, \alpha_{agg}, \alpha_{mastic}, G^*) - f(G^*, \delta, t_{cool})$$

Yet another assumption from the transverse cracking world also needs to be challenged. Given the observation that blocks cracks continue to get smaller, damage must be driven by localized differential volume changes or stiffness gradients even when materials are not fully confined. Another question comes to mind.

3. How rapidly do thermal stresses build during cooling if the pavement is already cracked (partially unconfined)?

The Thermal Stress – Restrained Specimen Test (TSRST) is a common tool for predicting transverse cracking temperatures at various cooling rates. This test applies the classic assumption that a pavement is continuous, so the asphalt mixture cannot shrink in the direction of confinement. Under this assumption, any changes in aggregate volume must apply tensile strains to the binder. Without confinement, aggregates move closer to each other as the mixture shrinks. Ultimate binder stress should be lower, because not all of the aggregate volume change applies tensile strain to the binder. In a universal cracking model, building stresses must be reduced when an unconfined mixture shrinks. The thermal stress equation must now include another parameter which is much more difficult to measure or model, the state of confinement for the mix in a cracked pavement.

The source of stress creating damage in an unconfined mix is not obvious, nor does the literature effectively answer this question. At least three possibilities are worth exploring further:

- Aggregate and mastic have different expansion coefficients, causing localized stresses within the mix.

The observation that unconfined BBR specimens exhibit damage at very low temperatures might be explained by this source of stress. The fact that the BBR damage is not propagated during loading suggests that distress must be localized and stable, as it could be if differential volume changes between the aggregate and mastic are the source of damage.

- Thermal gradients with depth in the pavement cause materials to bend.

Pavement thermal gradients are a well-documented cause for curling stresses which cause damage in long PCC pavement slabs. As the phase angle of the asphalt drops with aging, the asphalt mix may also become susceptible to bending stresses caused by thermal gradients.

- Stiffness gradients with depth in the pavement cause differential response to thermal changes.

As asphalt oxidizes, it stiffens. But oxidation is not uniform with depth. After four years in a desert climate, the binder $G^*/\sin \delta$ in the top 1/2" of the pavement can be three to four grades harder than for comparable mix buried three or more inches in the same pavement.

And so the complexity of a universal cracking hypothesis expands again:

$$\text{Eq. 2: Thermal stress} = f_1(\Delta T, \alpha_{\text{agg}}, \alpha_{\text{mastic}}, G^*, \text{State of confinement}) - f_2(G^*, \delta, t_{\text{cool}})$$

Not many crack predictions will be made from such a generalized equation, but it does serve as model from which to design and analyze laboratory and field experiments. Although the two functions for equation 2 are not yet known, the following hypothesis fits experimental data collected to date:

From function 1, more thermal stress is created when:

- the net temperature change is greater
- the aggregate's coefficient of thermal expansion is higher
- the binder/mastic modulus is higher
- all materials are totally confined (long, wide pavement with no cracks)
- a large difference exists between the coefficients of thermal expansion for the aggregate and the binder mastic respectively (Note: any differential volume changes within heterogeneous materials become relatively more important if the mix is unconfined. This source of building stress could be unimportant for transverse cracking, but the dominant cause for stresses leading to block cracking)
- the thermal gradient in the pavement is high
- the stiffness gradient in the pavement is high

From function 2, more thermal stresses can be relieved through fluid flow when:

- the binder modulus is lower
- the binder phase angle is higher

- Binder is S-controlled and unaged
- Temperature is higher
- the cooling time is longer
 - Slower cooling
 - Longer time between temperature changes

Any thermal stress model must measure or make assumptions about each of these key variables. Because assumptions are sometimes hidden in the mathematics, resulting conclusions may only be valid for a narrow range of conditions.

Bouldin-Rowe further challenged earlier assumptions by noting that all binders, particularly when modified with elastomeric polymers, do not fail in tension at the same tensile strength. Hence, a crack occurs when the building thermal stresses reach the unique failure strength for a given binder or mix. This observation does not change the thermal stress analysis, but adds the complication that any crack prediction model may need to include a tensile failure strength test in addition to the thermal stress analysis. Such an analysis is not as straightforward as it might seem, because a direct tension test has a strain rate (loading time) which must be physically or mathematically adjusted to the strain rate of the binder/mastic in the cooling pavement.

3.0 A RHEOLOGIST'S PERSPECTIVE ON AGING

As noted from binder experiments discussed earlier, aging increases the modulus at any temperature. But oxidation's most powerful impact is to reduce the rate of molecular relaxation (δ). High levels of oxidation must therefore cause enough change in the relative magnitude of the two terms in the generalized equation 2 so that cracking patterns evolve preferentially towards block cracking as pavements age. Because the binder tests showed oxidation to have a much more dramatic impact on phase angle than modulus, it seems logical that deteriorating binder performance will be dominated by relaxation, all of which is captured in the second function of the thermal stress equation 2.

As physics expanded Newton's theory of gravity from a "single body falling to earth" problem to the universal theory of gravity as a "two bodies attracting each other" phenomenon, it is time to reanalyze thermally-induced cracking from a set of experimental observations and assumptions that collectively recognize there is no fixed relationship between G^* and phase angle for all binders, nor is cracking a function of either parameter individually. Furthermore, stress relaxation is an important time-dependent function within the pavement temperature range where cracks develop.

The remainder of this appendix will review the experimental findings from this study in the context of refining the generalized equation so that it might eventually become part of a predictive model. Failure data for transverse cracking is available elsewhere, and models are well developed. But very little performance data is available for other forms of thermally-induced cracking, so we're still stuck at the earth's surface trying to peer into the universe. This study had very limited resources to evaluate field specimens, so specific failure criteria and limits cannot be proposed at this time for anything beyond transverse cracking. However, it is hoped that a generalized hypothesis for non-load induced cracking may point out hidden limiting assumptions and guide further laboratory and field experimentation so that accurate predictive models can be developed.

3.1 Building a Hypothesis

Thermal stresses originate when cooling causes materials to shrink, and cracks form when the building stresses exceed the tensile strength of the binder. Older oxidized pavements crack more readily, sometimes so badly that it is difficult to understand why cracking continues even without the confinement that logically seems a critical element for building thermal stresses.

Two types of damage are commonly attributed to thermal stresses, transverse cracking and block cracking. As described by FHWA's Distress Identification Manualⁱ:

- Transverse Cracking: Cracks that are predominantly perpendicular to pavement centerline.
- Block Cracking: A pattern of cracks that divides the pavement into approximately rectangular pieces. Rectangular blocks range in size from approximately 0.1 m² to 10 m².

Reports from field surveys for this projectⁱⁱ suggest that these two distresses are not interdependent. Even when local environmental conditions are identical, pavements may exhibit either type of crack independently, or both forms of distress to differing degrees. Block cracks are typically found in older pavements, whereas transverse cracks may occur as early as the first winter.

Observation #1: Thermal stresses build and create damage as asphalt pavements cool.

Every material has a coefficient of thermal expansion. With few exceptions, both liquids and solids shrink as they cool, with the volume change being determined as the product of the temperature change and the expansion coefficient. Aggregate makes up 95% of the composite mixture, but rocks cannot flow to accommodate the changing volume. No expansion joints are built into an asphalt pavement, so aggregate shrinkage puts the binder in tension. When the developing stresses in the binder equals its tensile strength, the binder fractures. If the strain applied throughout the binder were uniform, visible cracks would occur quickly. However, the binder/mastic film thickness in a heterogeneous asphalt mix may vary by orders of magnitude from aggregate contact points to interstices filled with mastic. The true tensile strain applied to the binder as the aggregate shrinks likewise varies by orders of magnitude. Hence, micro-cracks may form at the aggregate interfaces where the binder film is thin and true strains are high. As this occurs, the mix is weakened or damaged because the aggregate particles are no longer bonded near their respective contact points. However, much higher tensile strains are needed to fracture the mastic located within the aggregate interstices. Given enough time or higher temperatures, fluid flow may enable the thinnest binder films to reconnect across these micro cracks, and damage is reversed. If the bulk mastic finally fails, the micro cracks quickly coalesce into a visible crack that displaces aggregates. Healing across continuous cracks becomes impossible, so strength loss is severe and damage is permanent.

This micro cracking phenomenon is exemplified by the BBR binder and mixture bending studies described in the experimental sections of this report. The binder continues to stiffen with advanced ageing as the relaxation rate as defined by m-value continues to deteriorate. However, as the mixture approaches some critical limiting stiffness (20,000

MPa) and m -value (0.12), the magnitude of both parameters reverses direction. The mixture beam has no visible cracking, nor does the BBR loading curve show any anomalies that suggest a continuous crack has formed. How can the mixture appear to be softer with advanced aging when the binder is clearly getting harder? The logical explanation supports the explanation above that micro cracking begins within the mixture sometime before these limiting values are met, even though the BBR specimen size is quite small and there is no confinement preventing shrinkage. Although the specimen is weakened by micro cracking, there is no obvious propagation of that damage during the BBR's 240 second loading time. Because this type of damage would accumulate over time and seems to require no confinement over long distances, BBR mixture bending tests support observations consistent with block cracking. In all three binders, this damage was not observed until the loose mix had been oven-aged for more than 24 hours, and the BBR results only showed damage in test specimens run six degrees colder than the critical cracking temperature determined from the PG binder grading scheme. It should further be noted that BBR specimens are cooled from ambient temperature to a very cold testing temperature with a conditioning time of one hour. Hence, built into the BBR test are some assumptions pertinent to the cracking hypothesis as expressed by equation 2 earlier:

1. The extremely fast cooling rate, the relatively fast loading rate, and the low test temperature all limit opportunities for relaxation. Material behavior should be more elastic.
2. Beam specimens are small and unconfined, so mixture shrinkage should reduce any thermal stresses building within the specimen.
3. Without confinement, micro cracks appear to be forming in the mixture, but not in the binder under similar test conditions. Those micro cracks appear to be formed before loading begins, and do not appear to propagate significantly under load during the bending test.
4. Micro cracks remain relatively stable at constant temperature under test conditions that favor elastic behavior (low temperature, very rapid cooling, short loading and relaxation times).

Note here that volume change is only a function of changing temperature (ΔT), the singular driver for all thermally-induced cracking. All differences in crack location and patterns will be related to the rate at which micro cracks form, and whether they continue to propagate or have time to heal.

Observation #2: Time-temperature superposition is valid for any single binder.

Time-temperature superposition is a fundamental component of viscoelastic theory. For a liquid to satisfy this principle, the phase angle will always be the same when the liquid reaches a given complex modulus, regardless of the temperature and frequency at which that modulus is measured. The most direct way to validate this property is to graph a rheological mastercurve for a range of temperatures and frequencies on plots of G^* vs δ , commonly called Black Diagrams. Without any shifting as would be needed for plots of G^* vs temperature, all data must fall on one unique curve. Hence, for that liquid, the relationship between G^* and δ is fixed, such that either can be immediately found from the Black Diagram if the other is known.

- *It is important to note that time-temperature superposition no longer applies when high applied stresses and strains push the material into the non-linear region. Any assumptions for time-temperature superposition must come from measurements that fall on the true Black Diagram mastercurve.*
- *Exception to Assumption #2: Not all asphalts exhibit time-temperature superposition. Any phase transition occurring within the temperature range of the Black Diagram mastercurve alters the unique relationship between G^* and δ . This is particularly true when amorphous or microcrystalline waxes pass through a solid/solid or solid/liquid transition. Such a change alters the fundamental properties of molecular relaxation for that liquid, changing its shape in Black Space uniquely for that temperature. As an added complication, the stiffness of asphalt changes as wax molecules transform from amorphous to microcrystalline solids at low temperatures over a period of several days. This time dependent behavior should cause stresses to build, not relax over time. Therefore, waxy asphalts will not satisfy fundamental assumptions for superposition, and may need to be excluded from predictions postulated hereafter.*

Observation #3: Each binder has its own unique curve in Black Space.

Although not usually recognized, any theory basing crack prediction upon a limiting stiffness concept must have an implied assumption that there is a constant relationship between G^* and phase angle such that relaxation at any G^* will always be the same. As one example, assuming a phase angle of 90 degrees would imply that all binders would always behave as elastic solids at low temperatures, with no flow to relax stresses. A second more common, yet equally confining assumption is that all viscoelastic materials have exactly the same relationship in Black Space, such that all binders overlay a single unique mastercurve. For this to be true, time-temperature superposition would require exactly the same shift factors when G^* vs T mastercurves were plotted for all binders. To see beyond this limiting assumption, one must first recognize that time-temperature superposition only holds for a single binder. The unique relationship between G^* and δ changes with the relaxation properties of the individual asphalt molecules. Binders exhibiting a lower phase angle for a given modulus cannot flow to relieve stresses as quickly, and should therefore develop higher internal stresses during cooling (ΔT).

To more clearly demonstrate the importance of this variable relationship between G^* and δ , the binder's for this study were not selected to be good or bad in accelerated laboratory aging tests such as RTFO or PAV. Rather, the objective was to isolate binders of similar modulus with fast, intermediate, and slow relaxation properties as defined by distinctly different mastercurve locations in Black Space.

Aging of a single binder (Western Canadian) can be similarly followed to monitor how the Black Space mastercurve shifts as the binder oxidizes. (see Figure A.1).

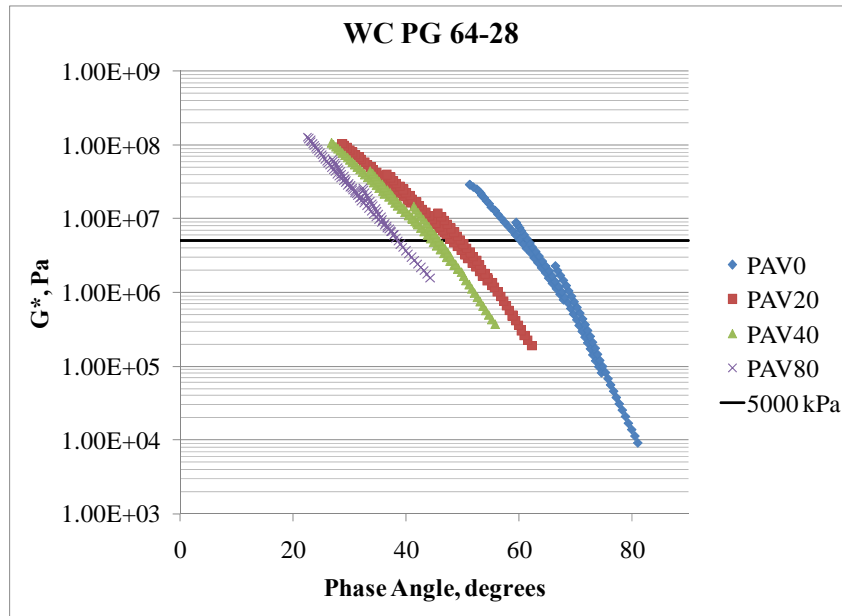


Figure A.1 Black Space Diagram for WC Asphalt Binder

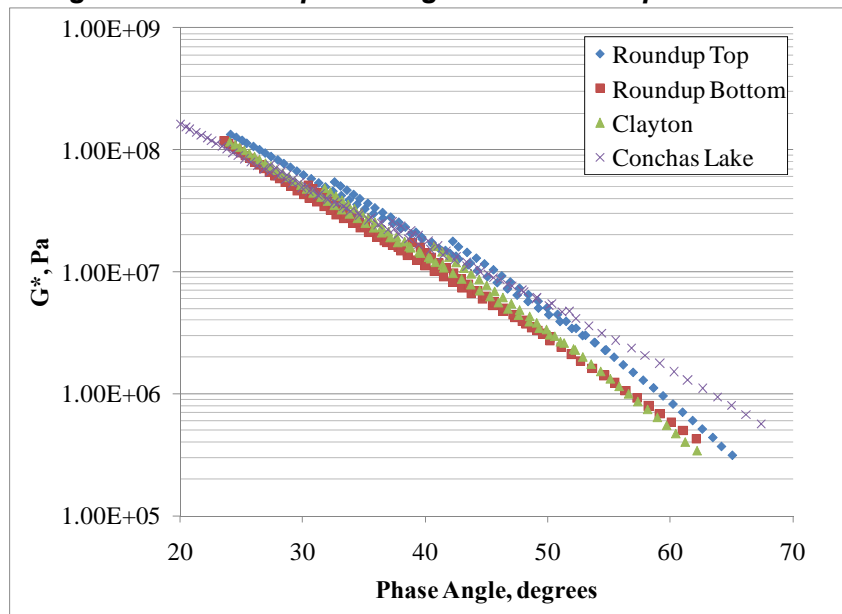


Figure A.2 Black Space Diagrams for Binders Recovered from 4 Runway Pavements

Figure A.2 shows binders extracted from four runways. Surface raveling and surface or block cracking appear to be more severe as the curves shift left in the direction of poor inherent molecular relaxation properties.

It is important to note that this dramatic shift in phase angle with age hardening represents a very different rheological change than would be expected if this same binder had been made harder by distilling it under harsher temperature/vacuum conditions in the refining process. The consequences of this finding have serious implications regarding blending of aged RAP materials with virgin binders or rejuvenators. Softening

is not enough. The low temperature relaxation properties must also be restored to make the aged binder in the RAP perform as a virgin binder.

Because BBR is more typically used for low temperature binder testing, these same trends can be monitored by viewing relative changes in BBR stiffness and m-value, which serve nicely as surrogates for G^* and δ . Hence, the experimental design asked for binder's with a ΔT_c of -3, 0, and +3. The Western Canadian, Gulf-Southeast, and West Texas Sour asphalts used in the study fall close to these three targeted values. The following three tables show how the relative loss in molecular relaxation after oxidation can be captured by the increasing BBR m-control as measured by the temperature difference between the two BBR critical cracking temperatures for S and m-value respectively.

Table A.1 BBR Data for WTX Asphalt Binder

		PAV0	PAV20	PAV40	PAV80
S(60), MPa	0°C		67	77	115
	-6°C	72	140	141	206
	-12°C	198	306	336	363
	T_{c,s} °C	-24.4	-21.9	-21.2	-20.0
m(60)	0°C		0.405	0.388	0.304
	-6°C	0.479	0.335	0.298	0.252
	-12°C	0.371	0.258	0.261	0.217
	T_{c,m} °C	-26.0	-18.7	-15.9	-10.4
	T_{c,m} – T_{c,s} °C	-1.5	3.1	5.4	9.6

Table A.2 BBR Data for GSE Asphalt Binder

		PAV0	PAV20	PAV40	PAV80
S(60), MPa	-6°C	41	100	116	151
	-12°C	140	229	249	264
	-18°C	355	451	464	505
	T_{c,S} °C	-26.9	-24.4	-23.8	-23.2
m(60)	-6°C	0.553	0.381	0.338	0.300
	-12°C	0.421	0.312	0.282	0.253
	-18°C	0.314	0.246	0.236	0.207
	T_{c,m} °C	-28.8	-23.1	-20.0	-15.9
	T_{c,m} – T_{c,S} °C	-1.9	1.3	3.8	7.3

Table A.3 BBR Data for WC Asphalt Binder

		PAV0	PAV20	PAV40	PAV80
S(60), MPa	-6°C		47	58	94
	-12°C	42	118	147	183
	-18°C	147	260	298	347
	T_{c,s} °C	-31.4	-29.1	-28.1	-26.7
m(60)	-6°C		0.453	0.397	0.319
	-12°C	0.552	0.377	0.335	0.283
	-18°C	0.439	0.317	0.286	0.253
	T_{c,m} °C	-35.4	-29.7	-26.2	-19.1
	T_{c,m} – T_{c,s} °C	-4.0	-0.6	1.8	7.5

Observation #4: Cracks are less severe when pavements cool slowly.

Fluid flow is a time-dependent function. Modulus and relaxation rate are key variables, but the final thermal stress can't be known without defining a cooling time. Just as universal gravitation must be defined in three-dimensional space (m_a , m_b , r), so too must cooling time (t_{cool}) be added as a third dimension to Black Diagrams of G^* vs δ in order to understand how flow relieves stresses. Hence, there should be some function, $f(G^*, \delta, t_{cool})$, that defines stress relaxation during any cooling event. If temporary damage occurs in the form of micro cracking, a similar function should be applicable to healing.

The proverbial 'Blue Norther' cools the pavement so fast that there is little time for molecular relaxation on the time scale defined for cold binders with a low phase angle. Under these rapid cooling conditions, t_{cool} is so short that differences in δ as measured in Black Space have little relevance. The second term in equation 2 is small, so G^* dominates cracking. Cracks propagate quickly as though a single event. The vector for the highest stresses must be in the horizontal direction of the pavement where confinement is greatest, because the pavement cracks consistently in the transverse direction. And so is born a "limiting stiffness" theory for transverse cracking.

Although confinement in the transverse direction is not as great, it may be sufficient to cause weak areas such as poorly constructed longitudinal joints to open prematurely via this same mechanism.

When the pavement cools more slowly, there is more time for molecular relaxation to relieve the building thermal stresses in the binder. Reduce the cooling rate from -10°C/hr to -1°C/hr , and the time for molecular relaxation increases by a factor of ten for a given ΔT . Small differences in binder phase angle can now have a significant impact upon the ultimate binder stress as measured when the lowest temperature is finally reached. As discussed in section 3.3.2, Bouldin & Rowe used several models to create thermal stress cooling curves from BBR loading curves. Shenoy then extrapolated these curves to predict theoretical cracking temperatures for binders when subjected to -10°C/hr and -1°C/hr respectively. This same analysis was done for BBR mixture bending tests, as discussed in section 3.3.3.

Observation #5: Asphalt oxidation slows molecular relaxation.

Over the years, Petersen and others have defined the change in chemical functionality that occurs with asphalt oxidation. In all cases, molecules lose degrees of freedom, a physical chemist's way of saying that atoms or molecules are no longer as free to move around with respect to each other. A physical chemist would view this as a loss in molecular relaxation as might be measured using Nuclear Magnetic Resonance (NMR), while a rheologist would view this same change in relaxation phenomena by reporting a loss in phase angle. Over the years, many test methods have been applied to describe the rheological changes occurring during oxidation, including penetration, viscosity, ductility, softening point, and combinations of the above as described by Van Der Poel's Nomograph. With the advent of SuperPave tools, aging has often been described by changes in the shape of the rheological mastercurve. The shape-parameter R describes time-dependency in the Christensen-Anderson-Marasteanu (CAM) model which fits shifted rheological mastercurves plotted for G^* versus either temperature or frequency. Glover's parameter ($G^*/(\eta'/G')$) offers still another rheological approach to characterize binder aging. Perhaps a return to Black Diagrams can offer insight into fundamental changes in the relationship between G^* and δ that might be brought on by aging.

Observation # 6: Asphalt oxidation can be defined by a shift in Black Space.

As previously noted in Figure 3.3.3.25, aging causes Black Space mastercurves to shift dramatically in the direction of lower phase angles for any given modulus. After extended aging, binder phase angles are so low that relaxation rates are extremely slow near minimum pavement temperatures. The second term in equation 2 becomes small, and rheological behavior becomes nearly elastic, even for slower cooling rates.

Although Shenoy's method to predict thermal cracking temperatures was developed to replicate the Bouldin-Rowe critical cracking temperatures without running Direct Tension Tests, both binder and mixture BBR bending tests indicate Shenoy's approach diverges from those of Bouldin as binders are oxidized. The difference, at least in part, appears to be in the importance each gives to the time for relaxation.

One observation from the results using Shenoy's procedure on aged binders and mixes is compelling. As binder's become highly aged, the cooling rate has much less impact on the predicted cracking temperature. This finding is consistent with equation 2 as the second function drops in magnitude. In a limit of no relaxation, the time-dependent function 2 is zero, so all materials of the same modulus build to the same thermal stress, regardless of cooling rate. It no longer matters whether pavements cool quickly or slowly. If relaxation cannot occur within the timeframe of pavement cooling and heating cycles, cooling rate becomes irrelevant. The binder phase angle is approaching that of an elastic solid which exhibits no flow. Stresses build as the volume changes. With no relaxation, cracking occurs after the same net temperature/volume change regardless of cooling rate. While the binder remains in this elastic state, micro cracks cannot heal. Thermal expansion and contraction from both rising and falling temperatures continues to accelerate damage until micro cracks coalesce.

Again by analogy, visualize a single cooling event to fracture by considering the force required to break a coat hanger by pulling it in tension. Are you strong enough to do that with your bare hands? Now visualize thermal cycling to be more like bending the coat

hanger until it breaks. Each bend requires much less energy than a single pull to failure, but damage continues to accumulate with each bending cycle until the metal fails. But damage only accumulates in the bending mode because the metal cannot flow to relieve building stresses. Similarly, an aged binder with a poor δ flows too slowly to relieve accumulating stresses from many small volume changes. Even without confinement it finally breaks, even though it never saw a single cooling event strong enough to break it in tension.

Given the coat hanger analogy, tensile fracture tests run to failure under rapid loading conditions should simulate conditions which predict single event transverse cracking. The Indirect Tension Test (IDT) predicts failure temperatures by creating thermal stress curves on cooling, and then determining the fracture strength. The Disc-Compaction Test (DC(t)) predicts cracking from mixture fracture energies in tension. And the search for the perfect testing geometry goes on, with semi-circular bending, hollow cylinder, etc. Each test method has advantages and problems. The real dilemma is that pavements with block cracking may not have transverse cracking, or vice versa. There can be no single ranking of materials from good to bad in our cracking universe, because relative material performance changes. For any test method to be applicable to cracking events beyond classic transverse cracking, it must deliver results for a continuous range of G^* , δ , and cooling times. This can be done by slowing cooling rates, allowing rest periods for healing, or preferably by developing rheological models which automatically adjust crack predictions as material properties or environmental conditions change. Sections 3.3.3 and 3.4.3 show Disc-Compaction Test results for the aged mixtures evaluated in this study. As might be expected, the maximum tensile strength appears to provide little differentiation for block cracking. This was also noted when evaluating binder force ductility curves. Because aging increases binder modulus as it reduces failure strain, fracture energy should be a much better predictor of cracking when appropriate loading conditions are applied. It is interesting to compare the DCT fracture energies to BBR stiffness and m-values, particularly for test temperatures 6°C below the PG grade where the BBR parameters reversed with additional aging. At -18°C, both the Gulf-Southeast and the Western Canadian mixes show increasing stiffness and increasing fracture strength up to 24 hours of aging, and then both stiffness and fracture strength fall with 48 hours aging. This result appears to confirm the micro cracking theory, and support the use of BBR bending as an appropriate tool to predict possible onset of block cracking. On the other hand, it would be difficult to predict the onset of cracking from the fracture test alone, because there is not much difference in failure energy between the unaged and highly aged specimens. For the West Texas Sour mix at -12°C, the fracture energy fell off after 24 hours of loose mix aging, and then increased again for the 48 hour specimen. This anomaly might be explainable by the fairly high variability in test results. It is important to note that the standard DCT procedure applies a 1 cm/min strain at the crack-opening. This relatively high loading rate should not be expected to capture the damaging effects of thermal cycling analogous to bending the coat hanger rather than pulling it. Significant modeling beyond the skills of the research team will be needed to convert the measured material properties from DCT into crack predictions for block cracking.

Since oxidation always causes the phase angle to deteriorate, it should be possible to define aging shift factors by plotting Black Diagrams for a given asphalt binder at different levels of aging. Aging shift factors were recently proposed by researchers at Western Research Institute (WRI), but their proposals recommend shifting $G^*/\sin \delta$ at high temperatures. Based on the findings from this study, aging shift factors for cracking should be defined at low pavement temperatures. Furthermore, they should identify, or at least correlate with, the changing relationship between G^* and δ in Black Space as binders oxidize.

Interestingly, there are many ways to quantify an aging shift factor that correlates with a shift in Black Space. Applicable test procedures seem to cover a fairly broad range of temperatures and loading rates. For example, as described in the binder test section 3.3.3, BBR bending tests on aged specimens indicate that the critical temperature for m-value (0.30) deteriorates faster than the critical temperature for Stiffness (300 MPa). The parameter ΔT_c was defined as the temperature difference between these two critical BBR temperatures, and it was hypothesized that block cracking is more likely to occur as ΔT_c increases upon aging. Since BBR Stiffness and m-value are closely related to G^* and δ respectively, any change in ΔT_c requires a shift in Black Space. Hence, the change in ΔT_c , or $\Delta(\Delta T_c)$ can be used as an aging shift factor.

In figure 3.3.2.24, ΔT_c was shown to have a very high correlation with Glover's parameter $G'/(η'/G')$ as determined at 15°C and 0.005 rad/sec using the mastercurve approach. Although reported to be a fatigue cracking parameter, the change in this function should likewise be an aging shift factor directly correlated with shifts in Black Space.

And Glover shows that his parameter closely correlates with ductility at 15°C and 1 cm/min. Change in ductility may then also be an aging shift factor that can be correlated with changes in Black Space.

The shape factor R from the CAM modelⁱⁱⁱ increases with aging. Values for R and correlations of R with ΔT_c and Glover's parameter were previously discussed in the binder section. R can also be considered an aging shift factor that correlates with shifts in Black Space. If the phase angle is arbitrarily selected to be 45°C when evaluating the evolution of R in Black Space as binders age, the change in R relates to the change in modulus for the arbitrarily fixed phase angle. The Black Space shift in R could also be evaluated by fixing the modulus and monitoring the change in phase angle with aging.

Parameters that might be used as aging shift factors:

1. A shift in Black Space mastercurves as might be measured by
 - a. ΔG^* at a constant phase angle
 - b. $\Delta \delta$ at a constant G^*
 - c. a directional shift of the mastercurve that includes changing both G^* and δ , such as shifting on a line perpendicular to the mastercurve
2. $\Delta(\Delta T_c)$ from BBR tests on binders.
3. $\Delta G'/(η'/G')$ at 15°C and 0.005 rad/sec
4. $\Delta(\text{Ductility})$ at 15°C and 1cm/min
5. ΔR , with R being the shape factor from the CAM model

Observation 7: If two binders are placed in the same paving environment and they have the same stiffness, then the binder with poorer relaxation properties will accumulate more thermal stress during cooling.

The important thing to remember for crack prediction is that **only the location in Black Space (G^* , δ) will define relaxation properties**. The relationship between these two parameters will depend upon both the initial asphalt quality and the degree of aging. An aging shift factor does not define a location in Black Space; it only quantifies the directional change in location towards more elastic behavior. The magnitude of the aging shift factor for any given binder should correlate with the level of carbonyl formation, but carbonyl content cannot capture the relative quality of different unaged binders. For any given binder, though, a higher shift factor or increasing carbonyl content indicates more aging, rising modulus, poorer relaxation, and much higher probabilities for cracking.

But the initial quality of the each unaged binder is also defined by a unique curve in Black Space. One could also compare the relative quality of different binders by defining an “asphalt quality” shift factor in Black Space. **A binder that starts with better relaxation properties can age more, or experience a greater shift in Black Space before it cracks**. Some of the parameters discussed above can be used to create aging shift factors, but they also capture the combined effects of aging and original asphalt quality in a manner that can locate the phase angle in Black Space if the stiffness is known. Consider the parameter, ΔT_c , as defined by the difference in the two BBR critical cracking temperatures. On a plot of S vs m-value, by definition, an asphalt with a $\Delta T_c = 0$ must pass through the point $S = 300$ kPa and $m = 0.30$. After converting S and m to G^* and δ , $\Delta T_c = 0$ defines one specific point in Black Space. A negative value defines an S-controlled binder with good relaxation properties, and a positive number defines an m-controlled binder that will be more sensitive to cracking. Aging any binder will increase ΔT_c , so $\Delta(\Delta T_c)$ can be used as an aging shift factor. However, the absolute value of ΔT_c represents the combined effects of initial binder quality and aging in a manner that defines a phase angle when the modulus is approximately 300 kPa. **If two binders with the same modulus and same failure strength are put in the same paving environment, the material with the higher ΔT_c should always crack first**. Furthermore, **increasing the cooling time by slowing the cooling rate will accentuate the difference in performance of the two materials**.

Likewise, each virgin asphalt has a unique R value that establishes the relative ability of that material to stress relax over time. As materials age, R increases substantially. Hence, the R value itself is a measure of quality, capturing both the relative performance of the unaged binder and the deleterious impact of oxidation. However, using R as a predictive parameter for cracking presents some problems, as can be noted by from figure A.3. Although R decreases with aging, changes in R at the crossover frequency (phase angle = 45°) do not correlate well with the other aging parameters evaluated in this study (ΔT_c , $G''/(\eta'/G')$, ductility @ 15°C).

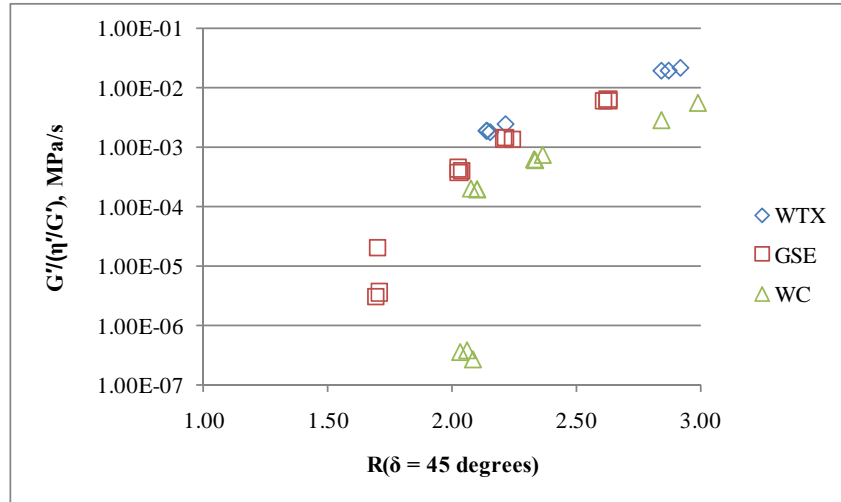


Figure A.3 Relationship between $G'/(η'/G')$ and R (15°C , $\delta = 45^\circ$)

Although both parameters come from the mastercurve in Black Diagrams, they are determined at very different locations. Referring back to figure A.2, it is clear that the mastercurves for extracted binders from field specimens do not just shift laterally in Black Space, they also have different slopes. That is, the ranking of materials for relative phase angle changes as the modulus changes. The glaring example is the binder from Conchas Lake. At higher temperatures, relaxation properties of this binder are considerably better than the others. However, at a modulus of 100 MPa, this binder has the poorest relaxation properties of the four binders. If one continues to extrapolate this curve beyond 300 MPa to the failure range for thermally induced cracking events, it is easy to understand why the Conchas Lake binder exhibits significant cracking damage in the field. ΔT_c essentially ranks the phase angles of binders at 300 MPa, whereas the CAM model from which R value is calculated is only deemed applicable down to phase angles of 20° . If Black diagrams are to be used to rank potential for age related damage, a new parameter other than R value must be found. It would be worthwhile to develop a new model fitting mastercurves in Black Space from which to determine shift parameters. Because the two asymptotes are approximately linear, a hyperbola function might be a good choice.

As noted earlier, the absolute value of ΔT_c shows high correlations with both Glover's parameter ($G'/(η'/G')$) and ductility when measured at appropriate conditions. By inference, it would appear that either of these parameters must somehow define unique locations in Black Space, and may also to rank binder quality with respect to cracking, again with the caveat that the ranking may only hold when the binder modulus is near the failure region. Results from field tests showed that the correlation between Glover's parameter and ΔT_c was not quite as good for the field samples. Again, the very different slopes of the G^* vs phase angle mastercurves from the field samples, particular Conchas Lake, appear to be the cause. The Glover parameter is calculated at an asphalt modulus that is significantly softer than BBR test conditions, so ΔT_c is currently believed to be the better choice. However, both parameters should be considered in future field validations.

Observation 8: Oxidation rates decrease with pavement depth, causing a gradient in both G^* and δ .

Most chemical reactions are controlled by rules of kinetics, including the Arrhenius equation that defines how temperature will influence the rate of reaction. Although not exact, a useful rule-of-thumb is that any chemical reaction rate will double for each 10°C increase in temperature. Hence, oxidation always occurs faster at the highest pavement temperatures. Pavement temperature algorithms suggest that temperatures vary with depth. On the hottest afternoons, the highest temperature is at the surface, and the temperature will decrease by about 2°C with each additional inch in depth from the surface. Furthermore, chemical kinetic rates include concentrations of the needed reactants. Oxidation can only occur when molecular oxygen is present. Studies by Kemp^{iv} and others show that mixes with low air voids age-harden more slowly, almost certainly because the source of oxygen is limited when air voids are not interconnected.

Because temperatures and oxygen availability vary with pavement depth, aging creates a gradient in rheological properties. In the upper half-inch of the pavement, where temperatures are high and oxygen is abundant, the binder ages rapidly. In the Arizona desert, the G^* at high pavement temperatures may increase by an order of magnitude (10 times) in four years. But G^* is 50% lower in the second half-inch, and 75% lower in the third half-inch. The aged binder is certainly harder, but the loss in phase angle is potentially even more damaging. Even though wintertime temperatures are not very cold in that Arizona desert, the rapidly aging surface is constantly subjected to changing temperatures that build stresses. Now held together by a brittle binder unable to flow, the pavement surface literally expands and contracts until it breaks. The cracks then work their way downward into the pavement, stopping when binder properties have no longer reached their failure limits.

Observation 9: Binders do not all fail at the same thermal stress

Bouldin-Rowe noted that binders fail in tension at different strengths. This observation is particularly important to the tensile failure of networked polymer modified asphalts. Therefore, Direct Tension tests were introduced to identify temperatures where the thermal stress equals the DTT tensile strength at failure. However, DTT has a relatively short loading time, perhaps too short to differentiate the failure strengths for two materials with significantly different phase angles.

4.0 SUMMARY – BUILDING A FOUNDATION FOR A UNIVERSAL CRACKING MODEL

As previously noted, any model for predicting thermally induced cracking must begin by analyzing the thermal stresses as they build in the binder as aggregate volume changes with temperature.

As in equation 2 described earlier, a common approach is to treat stress development as an elastic problem, and then subtract out the stresses relieved through relaxation. Bouldin & Rowe provide a commonly referenced approach which appears to provide reasonable thermal stress curves at different cooling rates. However, the failure temperatures derived by their analysis have been questioned. Shenoy used the Bouldin-Rowe cooling curves to predict cracking temperatures that were higher. Applying

Shenoy's analysis to aged asphalts in this study showed his approach to consistently rank highly aged asphalts as poor performers in a manner consistent with the observations noted above. Unfortunately, Shenoy's method requires a fairly lengthy data extrapolation. The BBR mixture bending data from field cores exhibited very high variability in the thermal stress curves, so the Shenoy predictions were of little value.

The first function (f_1) in equation 2 defines the maximum stress if no relaxation occurs. The only binder parameter is modulus, and the major unknown remains the state of confinement. Bouldin-Rowe assumptions were built on transverse cracking assumptions that logically require total confinement in the horizontal direction. Shenoy used these same thermal stress curves, so his approach to crack prediction may likewise be limited to confined materials. An algorithm for calculating thermal stresses contributing to micro cracks in the unconfined BBR specimen is less obvious. Accurate predictions of block cracking temperatures will have to address this issue.

The second function in equation 2 is dominated by properties that reflect the quality of the binder itself. The function (f_2) can be evaluated most directly by extending Black Diagrams to three dimensional plots of G^* vs δ vs cooling time. In this space, the hypothesis would suggest there is a three dimensional failure surface which defines cracking. If the BBR limits of $S = 300$ MPa and m -value = 0.30 represents a specification which provides a sufficient safety margin so binders will not crack, then this point in black space needs to be expanded, first to a two dimensional failure curve in Black Space, and then to a three dimensional surface in the plot of G^* vs δ vs t_{cool} . The failure surface might be modeled, but significant laboratory and field data will be needed to validate its predictive capabilities. Since f_2 is only part of the thermal stress equation, these failure criteria will only apply to binders with equal stiffness placed in the same paving environment. It will provide a fairly accurate ranking of binder quality in cracking scenarios, but models which predict cracking temperatures will need to correctly interpret function 1 as well.

REFERENCES

-
- ⁱ Distress Identification Manual, FHWA-RD-03-031, 2003
- ⁱⁱ Reference final report from this project – AAPT 6-1
- ⁱⁱⁱ Marasteanu, M. and Anderson, D., “Time-Temperature Dependency of Asphalt Binders: An Improved Model,” AAPT, 1996, pp. 408-448
- ^{iv} Kemp, G.R. and Predoehl, N.H., “A Comparison of Field and Laboratory Environments on Asphalt Durability”, AAPT, 1981, pp. 492-560

APPENDIX B

LABORATORY TEST METHODS AND PROCEDURES USED TO SIMULATE AND
EVALUATE NON-LOAD ASSOCIATED DISTRESS IN HMA PAVEMENTS

APPENDIX B

LABORATORY TEST METHODS AND PROCEDURES USED TO SIMULATE AND EVALUATE NON-LOAD ASSOCIATED DISTRESS IN HMA PAVEMENTS

There have been a number of procedures developed to simulate the long term aging of asphalt binders and HMA mixtures. The goal of these procedures has been to simulate the effect of aging on asphalt binders.

In a comprehensive SHRP review of laboratory aging protocols for asphalt binder binders and mixes, Bell¹ described a broad range of simulation tests that have been proposed throughout the years. Chemical and rheological changes occurring during HMA construction at elevated temperatures have been relatively easy to replicate for conventional asphalt binders, using tests such as the Thin-Film Oven Test (TFOT), the Rolling Thin-Film Oven Test (RTFO), the Stirred Air-Flow Test (SAFT), and the German Rolling-Flask Test (GRF), to name a few. It has proven difficult to develop tests which accurately replicate the rheological changes that occur in an asphalt binder in the pavement over time. Attempts to accelerate the process for laboratory convenience by increasing temperatures, and/or exposing the binder to elevated pressure in air or pure oxygen have been problematic.

1.0 AGING OF ASPHALT BINDERS

There have been a number of test procedures developed that have been or are being used to evaluate the aging characteristics of asphalt binders. Testing of binder properties is performed to try to correlate these binder aging procedures to the actual aging that occurs in asphalt binders utilized in hot-mix asphalt (HMA), when in service on airfields. Developing correlations between lab binder aging procedures and actual field aging has been limited for a number of reasons.

First, the binder must be extracted from aged pavement cores. The extraction procedure may alter binder properties.

Second, the binder ages at different depths in the asphalt pavement cross section. Most aging will occur in the top of the pavement where the materials are most exposed to climatic changes and the sun. To illustrate this, typical results from the Witczak and Mirza global aging prediction model, that was calibrated using field data, are shown in Figure B-1.

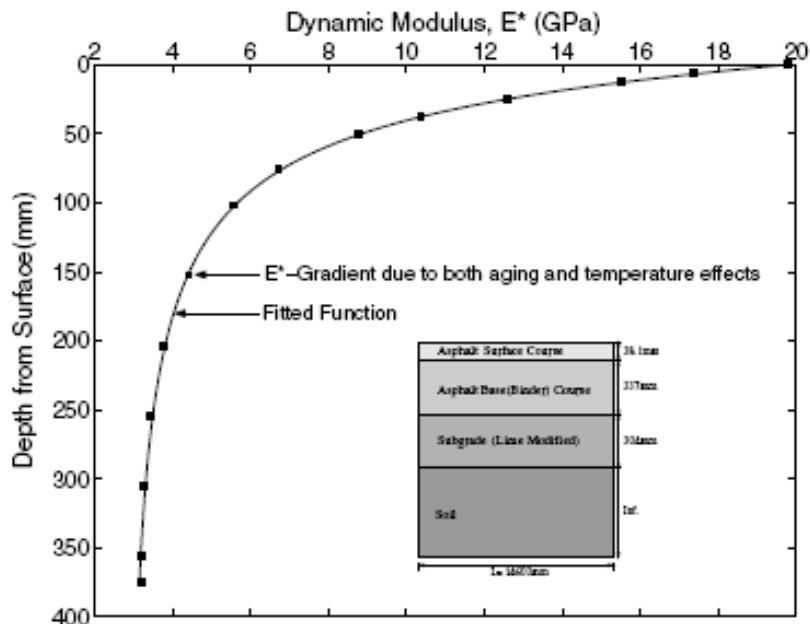


Figure B.1 Illustration of Severe Aging Gradients in Asphalt Pavements

The aging gradient presents a dilemma, with respect to both the development and calibration of mechanical laboratory tests to simulate field aging, which involve the testing of discrete thickness specimens. Usually, a minimum thickness of 50 mm or possibly 25 mm for mixtures with finer aggregates is required depending on the test method. Removing the top portion of the mixture can make the specimen more uniform for testing. But, by removing the top of the specimen, we may have greatly reduced our ability to properly measure a mixture's surface brittleness where environmental aging occurs.

Third, binder aging is dependent on mix properties. In particular, density or compaction level, which is not consistent across or within an asphalt pavement system, affects binder aging. Fourth, binder film thickness (asphalt coating on an aggregate particle) in a mixture is variable within a given mix and has not been simulated through a lab binder aging procedure. There are other reasons as well.

In spite of these limitations to developing laboratory to field correlations to model aging asphalt technologists have developed test procedures.

1.1 California Tilt-Oven Durability Test (TDOT)

As part of the comprehensive Caltrans asphalt binder durability study,² Predoehl and Kemp³ evaluated available accelerated aging tests, including extended time in the RTFO at 163° C and weathering under UV light, and found none of them could satisfactorily predict results of their field study. They then modified the AASHTO T-240 RTFO test by reducing the temperature to 113° C, increasing the aging time to 168 hours, and putting the oven on a 1° angle so the asphalt binder remained within the open tubes. The

authors reported that the lower temperature more accurately ranked binders according to their respective aging in the field, and added TODT to Caltrans binder specifications.

1.2 Thin-Film Accelerated Aging Test (TFAAT)

Peterson⁴ coated RTFO bottles with very thin asphalt binder films and then aged them in heated air for three days at 113° C (the same temperature specified by Caltrans). He recorded evolving asphalt binder viscosity and reported results which compared favorably to samples taken from the Zaca-Wigmore test road.

1.3 Rotating Cylinder Aging Test (RCAT)

A promising accelerated aging test has been developed at the Belgium Road Research Centre by Verhasselt⁵ and Choquet⁶. The authors compared evolving rheology as they varied a number of test conditions, including temperature (70-100° C), aging time (up to 576 hours), air/oxygen pressure, and cylinder rotation rate. Test conditions of 85° C and 1 rv/min with oxygen flow for 240 hours provided similar chemical properties to a binder aged for 15-20 years in a Belgian pavement. A field aging study is ongoing with the goal of optimizing lab conditions to simulate changing physical and chemical (carbonyl, Asphaltenes) properties during aging.

1.4 Thin-Film Oven (TFOT)

The TFOT procedure is performed by pouring a 50 ml (approximately 50 grams) sample of heated asphalt binder into a flat-bottomed, circular sample pan. The sample pans are placed on a rotating shelf in a ventilated oven operating at 163° C (325° F). The rotating shelf turns at a rate of approximately 5 to 6 revolutions per minute for a total testing time of 5 hours. After 5 hours, any sample pans being used for determining mass change are allowed to cool to room temperature before the final weight is determined. The remaining pans are then poured and scraped into a single sample container for testing.

1.5 Rolling Thin-Film Oven (RTFO)

The rolling thin film oven test (ASTM 1995) measures the effect of heat and air on a moving film of asphalt binder. Thirty-five grams of asphalt binder is poured in a glass bottle that has a narrow top opening. The glass bottle is placed in a carriage such that the bottle is horizontal. A jet of air is blown into the bottle. The sample is tested at 163° C and the carriage is rotated at the rate of 15 revolutions per minute for 85 minutes. As the bottle rotates in the carriage, the asphalt coats the inside of the bottle. After aging, the glass bottles are removed and weighed to measure any mass loss.

1.6 Pressure Aging Vessel (PAV)

As reviewed by Anderson⁷, numerous studies have used pressurized air or oxygen to accelerate aging in the laboratory. One notable precursor to Superpave's two step aging process was the Iowa durability test as developed by Lee and co-workers⁵, which combined TFOT with a low-temperature (150° F) binder aging test under air pressure and a mixture aging test to predict pavement aging. After finding that asphalt binders aged longer at RTFO temperatures did not satisfactorily fit the shape of rheological master curves from field specimens, SHRP researchers also elected to simulate

pavement aging by further aging the RTFO conditioned asphalt. The PAV used pressurized air to accelerate the process, while keeping temperatures between 60° C and 100° C. Although 60°C was preferred, aging under 300 psi air pressure at 100° C produced acceptable results within the 24 hour time limit needed by suppliers in order to satisfy QA/QC product certification protocols. The current practice is to use a pressure of 300 psi but vary the temperature from 90° C (for 52 grades and lower), to 100° C (for most “normal” grades PG 58-infinity), to 110° C (only used in desert/super-hot climates.) PAV is the long-term aging test now included in Superpave binder specifications. It is believed that the PAV aging simulates about seven to ten years of aging.

2.0 AGING OF HMA MIXTURES

As with the aging of asphalt binders, there are a number of test procedures developed that have been or are being used to evaluate the aging characteristics of an HMA mixture. The test results from these procedures have been correlated to the field aging of HMA pavements. The problem associated with these procedures is their limited ability to predict the aging characteristics within an HMA pavement at a particular airfield due to variable climatic conditions and HMA density levels.

2.1 Short-Term Oven Aging

Short-term oven aging of the loose mix was originally used to simulate haul times from the hot mix plant to the jobsite. The aging times vary from 30 minutes to about 2 hours. This procedure was standardized by the SHRP and consists of aging a loose HMA mixture for a period of time in a forced draft oven at 275° F. It was found that two important processes happen during the oven aging of the mixture. First, the asphalt absorbs into the aggregate changing the potential mixture maximum gravity (Gmm). Second, the asphalt aging causes the mixture to stiffen. SHRP chose four hours aging at 275°C, a common compaction temperature, as the new standard to simulate the absorption and aging that a mixture encounters through the construction process.

Once in use, it was determined that four hour aging was not needed in everyday production because only the absorption simulation was needed for use in the volumetric analysis procedures being used for quality control of HMA pavements. The procedure is now in two parts in AASHTO R30, Mixture Conditioning of Hot-Mix Asphalt: Short-Term Oven Aging for Volumetric Mixture Design (2 hours) and Short-Term Oven Aging for Mechanical Property Testing (4 hours). The aging temperature is set at the recommended compaction temperature of the hot mix asphalt.

2.2 Long-Term Oven Aging (Conditioning) of Prepared Specimens

To further age the mixture for mechanical property testing, SHRP introduced long-term oven aging of the compacted HMA sample.⁸ This aging further conditions the already short-term aged mixture to simulate the aging that occurs over the service life of a pavement (maybe seven to 15 years). This is similar to the PAV aging results above and is typically performed on surface mixtures that are more exposed to environmental aging. The advantage of aging the compacted sample is to better understand the effect of air voids and permeability on the mixture aging process. This can only be

accomplished when the mixture is in a compacted form. AASHTO R30, Section 7.3 requires that the sample be aged in a forced draft oven at 85C for 120 hours (5 days).

2.3 Weatherometer

HMA specimens could be manufactured and then placed in a weatherometer to expose the surface to ultraviolet lighting. This type of testing is routinely done on materials used for roofing. But, as discussed in the section on asphalt chemistry it is the thinking of the AMEC team that the aging of asphalt binders in an HMA mixture is primarily due to oxidation and the aggregate in the HMA mixture negates the influence of ultraviolet rays on the aging of the asphalt binder. Therefore, this technique is not recommended.

3.0 LABORATORY TESTS THAT COULD BE USED TO EVALUATE LONG-TERM AGING

Laboratory testing on thin field cores is limited. Most current mixture property testing is limited to 2 inch (50mm) thick specimens. This is thicker than the average construction lift thickness or overlay thickness on some airfield pavements. We recognize that the asphalt surface design may be 3 to 4 inches or more in total thickness, however, the construction lifts to place the surface is less. These layers are then bonded with asphalt tack. Mechanical mixture testing can only be performed on an overlay or single construction lift since layers will debond during mechanical testing.

Due to the overlay thickness being relatively thin, many surface property evaluations in the past have been limited to extraction and recovery of the asphalt binder and resilient modulus testing. In recent years, more mixture tests have been introduced to evaluate cores from surface layers. The following test procedures are being used to evaluate the effect of aging on asphalt binder binders.

3.1 Static Bending Test Using the Bending Beam Rheometer (BBR)

This procedure was developed by Dr. Marasteanu⁹ at the University of Minnesota. It uses thin mix specimens cut to the standard BBR test geometry and then applies a 500 gram load in a BBR device. The test is run at -6°C to 18°C and requires an upgrade to the standard BBR. The stiffness and the m-value of the mix are determined. It may provide a method to measure the change in the properties of the HMA mixture as the mixture is aged. This test can have high variability due to the small sample size.

3.2 G* from the Dynamic Shear Rheometer

This procedure evaluates the properties of the binder as it aged by aging the compacted HMA specimens or existing cores. The binder is chemically extracted from the mixture sample. The shear modulus of the binder is measured by the DSR. The disadvantage with the use of this procedure is that it requires chemical extraction of the binder, which if not done very carefully, can change the properties of the binder.

3.3 DSR Creep Testing

This test was developed by Gerald Reinke¹⁰ and consists of testing mixture specimens that are approximately 50 mm by 12 mm by 10 mm. The test is conducted using a

modified DSR. The test is a repeated creep test that consists of using a typical creep time of 1 second followed by a recovery time of 9 seconds. The repeated creep and recovery process is continued for 2000 cycles or until the specimen fails from fatigue. This test is very useful for determining the aging of an HMA sample by examining the effect of aging gradients of the pavement. Like the BBR mixture test, this test can have high variability due to the small sample size.

3.4 Dynamic Modulus

The dynamic modulus, sometimes called complex modulus, is determined by applying sinusoidal (haversine) vertical loads to the specimen at different frequencies and measuring the recoverable vertical strain. The test procedure for determining the dynamic modulus is provided in ASTM D-3497. The axial stress and strain are used to calculate the dynamic modulus. The dynamic modulus is calculated by dividing the repeated stress by the repeated strain. The difference between this test and the shear modulus test is the type of loading (axial versus shear loading) and that the dynamic modulus test is stress-controlled while the shear modulus test is strain-controlled. This test is used to describe the viscoelastic behavior of asphalt binder materials under axial loading. The results of this test are used to evaluate the rutting resistance of an HMA mixture. The advantage of using this test in this study is that samples can be manufactured and then monitored during the aging process.

3.5 Superpave Indirect Tensile (IDT) Strength

This test is used to determine the creep compliance and the indirect tensile strength of HMA mixes at low and intermediate pavement temperatures. It is possible that the IDT result may be related to the age oxidation of the asphalt binder and thus could be related to the onset of non-load associated cracking in an HMA pavement.

3.6 Viscosity of Extracted Binders

This test would consist of testing samples that have aged in the laboratory. A sample of the asphalt binder cement would be obtained through extraction and the asphalt binder would be tested using a standard capillary tube viscometer. The global aging system developed by Mirza and Witczak¹¹ uses viscosity as the basis for its predictive models.

3.7 M-value of Extracted Binders

Recent research has indicated that monitoring the m-value obtained using the Bending Beam Rheometer may provide a method for evaluating the aging characteristics of an asphalt binder.

3.8 Disk-Shaped Compact Tension Test (DC(T)) – ASTM D 7313

The DC(T) test was created by the University of Illinois at Champaign-Urbana (UIUC) to evaluate field cores and laboratory compacted HMA samples.¹² The University of Illinois

researchers have successfully used the results of this test procedure to rank HMA surfacing layers to rank the extent of pavement cracking.

The DC(T) test¹² is used to determine the fracture energy (G_f) of an HMA mixture using the disk shaped compact tension geometry. The disk-shaped compact tension geometry is a circular specimen with a single-edge notch loaded in tension. The fracture energy can be utilized as a parameter to describe the fracture resistance of asphalt binder concrete. The test is generally valid at temperatures of 10° C (50° F) and below, or for material and temperature combinations which produce valid material fracture.

The fracture energy is particularly useful in the evaluation of field cores. The DC(T) test has also been used on polymer-modified mixtures and categorizes the varying levels of performance well. In particular, the test has been shown to discriminate between the polymer mixtures more broadly than the IDT strength parameter.

Recently, the DC(T) was used to evaluate lab mixture aging with promising results in a similar unpublished study by Andrew F. Braham, Dr. William Buttlar, Timothy R. Clyne. In this recent unpublished study at UIUC, they examined the effect of laboratory and field aging on the mechanical properties of asphalt mixtures. Braham et al. attempted to develop a laboratory aging protocol to simulate field aging, based upon mechanical tests on asphalt mixtures such as creep, modulus, and fracture energy. Laboratory aging in a forced draft oven at 135 C produced a trend of fracture energy versus oven aging time as expected. Interestingly, fracture energy actually increased up to about 6 to 8 hours before decreasing, which was hypothesized to be related to additional mixture curing, where effects of mixture strengthening outweighed effects of mixture embrittlement on fracture energy at early stages of aging. Also, the fracture energy measured on field cores after field aging for eight years (using specimens with the top 12.5mm removed) was found to be only marginally lower than the unaged material.

4.0 LABORATORY STUDY

The research team reviewed laboratory procedures for aging asphalt binders and mixtures to select the most promising evaluation techniques. In the case where an HMA pavement is in the aging process (see Figure B.2) the DC(T) test was selected based on the following:

- This test is one of the few mixture tests that have successfully ranked field surface cores with pavement cracking.
- The DC(T) was successfully utilized in a recent Low Temperature Pool Fund study by northern states to better understand cracking in HMA pavements.
- This test has an ASTM standard procedure.

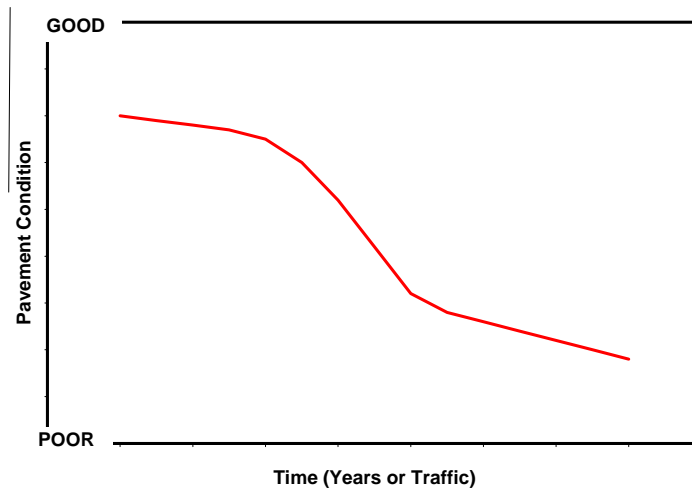


Figure B.2 HMA Pavement Deterioration Curve

The objective was to identify mixture and binder test(s) to measure non-load or environmental aging effects on asphalt surface mixtures taken from airfield pavements. Since surface layers are usually limited to 1 inch (25 mm) up to a typical maximum of 1 ½ inches (38 mm) in thickness, many current mixtures tests are eliminated. Current asphalt mixture tests are mostly designed to measure materials properties on laboratory compacted samples where the thickness can be specified. Since surface lifts on airfields can be less than 2 inches, applicable lab mixture testing procedures are limited because these current test procedures require more than 2 inch thick samples. In the past, testing has been limited to extraction and recovery of cores to evaluate the binder properties of the thinner surface layers. The binder properties are an indication of the age and performance of the in-place mixture, but are limited to the binder only. Also, extraction and recovery of the binder from the mixture is not as widely available today due to the handling of hazardous chemicals that is required. It is important to measure the complete mixture when possible to understand potential performance as it relates to the interaction of the binder and aggregate.

4.1 Test Matrix and Materials Preparation

The experimental matrix in Table B.1 was developed to determine if the DC(T) was able to measure the aging effect on a laboratory-produced mixture with two asphalt types and three aging levels. The test is run at three different temperatures and with 3 replicates for each cell, so a total of 54 test specimens were required.

Table B.1 Experimental Matrix

Aging Time	4-hours			4-hours + 1 day			4-hours + 5 days		
PG 64-22	0°C	-12°C	-24°C	0°C	-12°C	-24°C	0°C	-12°C	-24°C
PG 64-16	0°C	-12°C	-24°C	0°C	-12°C	-24°C	0°C	-12°C	-24°C

A standard Kentucky job mix formula (JMF), shown in Table B.2, was blended with 5.4 percent asphalt binder. The composition of the aggregates was 25 per cent limestone #8's, 26% limestone sand (unwashed), 14 percent limestone sand (washed), and 15 per cent natural sand (rounded). Two asphalt binders, PG 64-22 and PG 64-16, with different aging characteristics were used in this evaluation. The PG 64-22 was from a local terminal and used widely in KY. The PG 64-16 is made from a blend of West Texas sour crude. The PG 64-16 was selected since it has a tendency to age more than the average U.S. asphalt and was identified as such during the Strategic Highway Research Program asphalt evaluations. The binder properties are listed in Table B-3.

All materials were mixed at 149°C with a bucket mixer. The loose mixtures were aged 4 hours at the 135°C compaction temperature in accordance with AASHTO R30, *Mixture Conditioning of Hot-Mix Asphalt, Section 7.2 - Short-Term Conditioning for Mixture Mechanical Property Testing*. All samples had to be conditioned first with the 4-hour aging to simulate aging and absorption during the construction process. The mixtures were then compacted with a Superpave gyratory compactor set at an internal angle of 1.16°. The 6 inch (150 mm) diameter samples were cut into 2 inch (50 mm) tall samples and the mixture bulk specific gravities were measured. While the laboratory-produced samples were made 50mm thick, the DC(T) is not limited to this thickness. All samples had to meet a 7.0 ± 0.5 percent air voids tolerance. This measurement was important to reduce and control aging and testing variability.

Table B.2 Gradation of Laboratory Standard Mixture for Aging Evaluation

Sieve Size	Percent Passing
3/8 inch	95
#4	73
#8	49
#16	32
#30	19
#50	10
#100	7
#200	6.0

Table B.3 Asphalt Binder Properties of Laboratory Standard Sources

	PG 64-22 (Marathon)	PG 64-16 (West Texas Sour)
Original Binder		
DSR Test Temperature, °C	64	64
DSR G*, kPa	1.39	1.17
DSR Phase Angle, °	89.1	89.6
DSR G*/sin delta, kPa	1.39	1.17
RTFO Aged		
RTFO Mass Loss, %	0.106	0.002
DSR Test Temperature, °C	64	64
DSR G*, kPa	2.69	2.68
DSR Phase Angle, °	87.4	88.2
DSR G*/sin delta, kPa	2.69	2.68
PAV Aged @ 100°C		
DSR Test Temperature, °C	25	28
DSR G*, kPa	5430	6120
DSR Phase Angle, °	51.7	50.6
G*sin delta, kPa	4260	4730
BBR Test Temperature, °C	-12	-6
BBR Stiffness, (MPa)	210	144
BBR m-value	0.315	0.338
Nearest PG, °C	67-24	67-20

Next, the 54 samples were divided into three groups for the following aging levels:

- 4-hour short-term aging (on loose mix). No further aging of compacted sample – simulates construction aging (Year 0)
- 4-hour short-term aging (on loose mix) plus 1 day at 85°C on compacted sample, – to simulate some long-term aging
- 4-hour short-term aging (on loose mix) plus 5 days at 85°C on compacted sample – to simulate more long-term aging.

The 1 and 5 day aging was achieved with the same procedure as Section - 7.3, *Long-Term Conditioning for Mixture Mechanical Property Testing*, but on compacted samples.

Normally, the taller cylinder (70mm or 120mm) is aged before cutting. To tightly control the air voids and remove the portion of the sample with high density variability, it was important to trim the specimens first to 50mm and then age. Trimming the specimen ends removes the lower density material from the lab compaction process. Since it is difficult to age 50mm trimmed samples at 85°C without damage occurring from specimen creep in the oven, a modification to the standard was made. First, the specimens were placed on gyratory paper disks to keep them from sticking to the sheet of aluminum. The samples were spaced equally across the sheet of aluminum.

Second, support rings were fabricated by cutting stainless steel pipe in half. These support rings were placed around the specimens. Third, long springs were positioned around the steel support rings to lightly compress the steel around the sample. Fourth, the trays of samples were inserted in a forced draft oven at 85°C, Figure B.3. After 1 day, a group of samples were allowed to cool and then removed. The AASHTO R30 procedure was followed to allow the specimens to cool in the oven before removing. All samples were allowed to cool to room temperature (approximately 16 hours) with the oven doors open to prevent any damage to the sample while warm. The remaining samples were removed after 5 days of oven aging.

The advantage of aging the compacted mixtures under a long-term procedure allows the specimen to age similarly to an in-place pavement. Since pavement aging is a function of sample density (air voids and/or permeability), it was important to age the mixture in a compacted form.



Figure B.3 Long-term oven aging of laboratory compacted samples

The samples were then sent to UIUC by the Asphalt Institute for further preparation and testing. The description, test reporting, and analysis of these mixtures was provided by Alex Apeageyi, Ph.D and Dr. William Buttlar¹³. Many excerpts from this internal report are used in the following discussion. The samples were further prepared for the DC(T) testing fixture by blunting the end with a saw, cutting a notch for pre-cracking, and drilling two holes for mounting (Figure B.4).

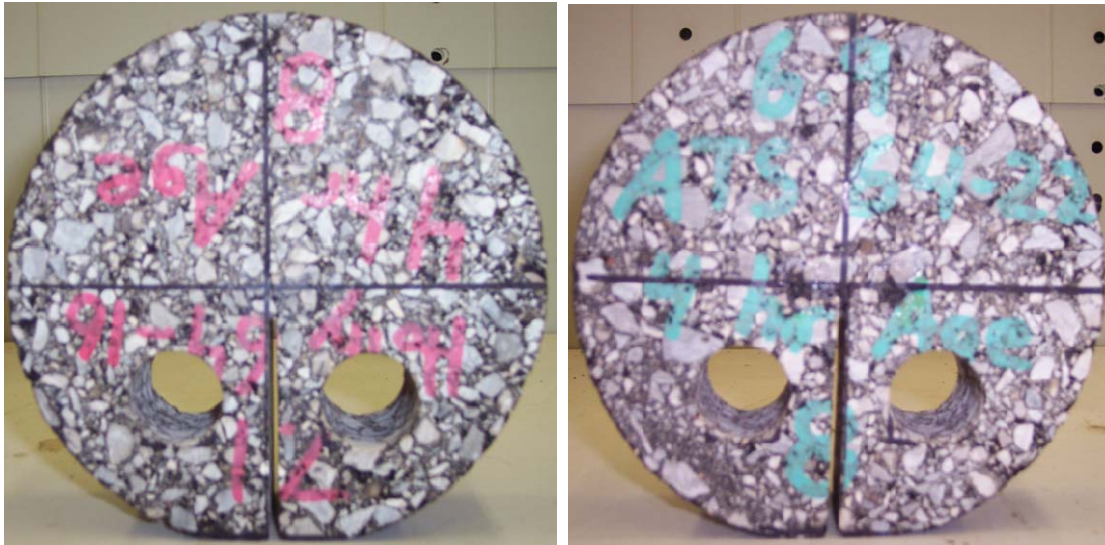


Figure B.4 DC(T) samples prepared for testing.

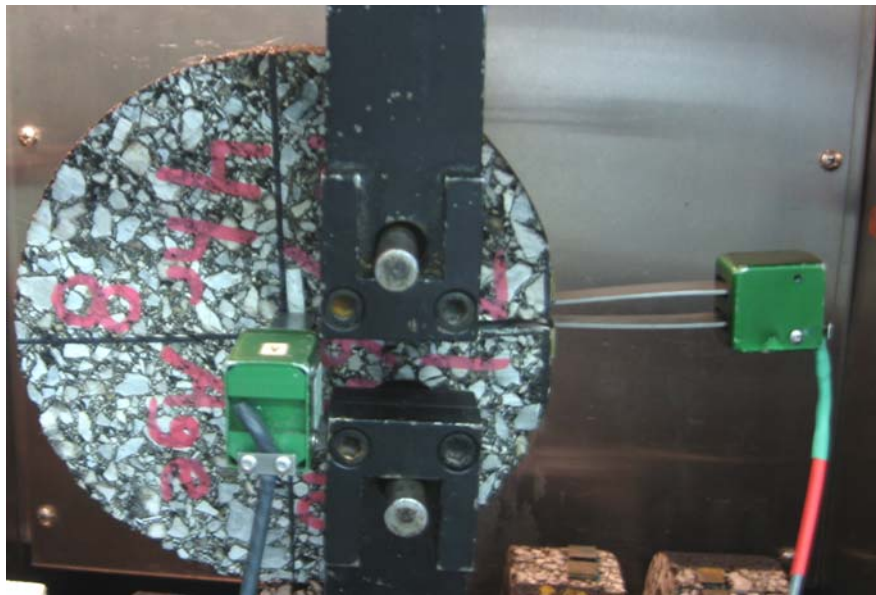


Figure B.5 DC(T) Fracture test showing crack-mouth opening displacement (CMOD) gage and δ_{25} clip-gage.

4.2 Testing

Three test temperatures are common for this test to evaluate the sample response over a range. The temperatures chosen were -24°C , -12°C and 0°C . Samples were conditioned at the test temperature for at least three hours. A strain-controlled loading rate of 1 mm/min was used for all the mixtures. Two clip gages, one attached to the crack mouth opening (CMOD) and other located close to the notch tip (δ_{25}) of the specimens were used to measure deformations needed to estimate fracture energy (see Figure B.5).

The use of CMOD and δ_{25} measurements provide two reference points for energy measurements. While one is not better than the other, they simply provide the technologist with measurement options. Some technologists prefer one over the other. CMOD allows for displacement (used in the energy calculation) measurements at the crack mouth opening where the movement is the largest. Using δ_{25} allows one to measure the displacement at the crack tip (end of saw cut on interior of specimen) process zone. The δ_{25} strain measurement targets are placed over a 25mm width at 12.5mm on each side of the crack tip. These two measurements allow for the calculation fracture energy at two separate locations. (For production use, this can be reduced to one measurement for simplicity.) The load is measured from a load cell on the test frame. The specimen is strained until fracture or weakening occurs.

4.3 Results

Fracture energy is calculated by measuring the area under the load-displacement curve and reported in units of J/m^2 for each sample. The area (m^2) represents the fracture area of the sample (thickness x ligament length). All results are displayed in Table B.4 for both CMOD and δ_{25} measured fracture energies. A summary of the data is shown in Figure B.6. It is normal to see a larger variation in results when using a fracture test versus a non-destructive test like modulus. Also, the researchers chose to use triplicate samples at three different test temperatures to provide future options. To simplify this data for production use, the measurements could be reduced to one (CMOD for example) and the test temperature to one based on climate location. Variability can be reduced by increasing the number of test replicates since this is a fracture test.

The results indicate that PG 64-22 (specifically 67-24) mixtures exhibited significantly higher fracture resistance at the temperatures tested compared to the PG 64-16 (specifically 67-20) mixtures. This is to be expected based on the Superpave grading system. It is worth noting that the DC(T) was able to see these differences even though the low temperature was within 4°C of each other.

The effect of aging was most significant for the DC(T) fracture test conducted at 0°C. For most of the mixtures tested, no significant differences in fracture energy were observed at the lowest test temperature of -24°C.

A closer look at this data reveals that little, if any, additional aging occurred with the 5-day 85°C oven aging for most of the mixtures. AASHTO R30 refers to this 5-day aging process as long-term conditioning for mechanical property testing. The lack of aging at 5-days was not expected. In their recent study, Braham et al. also found this same lack of aging under the 5-day long-term aging condition. This raises awareness that the 5-day aging on compacted samples may not be long enough to simulate long-term aging. This also raises question like: "When the 5-day aging was utilized in SHRP, what was it supposed to simulate and was it test specific?"

It is also possible that the specimens could have been damaged due to creep over the 5-day condition time. This does not seem logical since the specimens would have been weaker (less energy) if they had been damaged in the conditioning process.

Table B.4 Summary of DC(T) Fracture Energy Test Results

Binder Type	Temp. (°C)	Age	Fracture energy G_f (J/m ²)			
			CMOD		δ_{25}	
			Mean	COV (%)	Mean	COV (%)
PG 64-22	-24	4-hr	313	11.8	159	11.6
		4-hr + 1 day @ 85°C	312	9.2	141	10.7
		4-hr + 5 days @ 85°C	309	19.6	138	19.8
	-12	4-hr	538	20.9	242	20.0
		4-hr + 1 day @ 85°C	396	9.2	180	11.5
		4-hr + 5 days @ 85°C	452	6.5	218	14.5
	0	4-hr	781	8.0	337	24.0
		4-hr + 1 day @ 85°C	639	12.3	273	12.6
		4-hr + 5 days @ 85°C	648	9.3	255	12.9
PG 64-16	-24	4-hr	232	12.8	116	12.3
		4-hr + 1 day @ 85°C	208	5.6	93	21.7
		4-hr + 5 days @ 85°C	373	18.0	167	19.3
	-12	4-hr	366	12.2	183	13.8
		4-hr + 1 day @ 85°C	404	21.2	176	20.4
		4-hr + 5 days @ 85°C	348	12.8	153	15.4
	0	4-hr	612	4.4	272	22.0
		4-hr + 1 day @ 85°C	453	10.7	207	15.5
		4-hr + 5 days @ 85°C	653	12.8	275	16.8

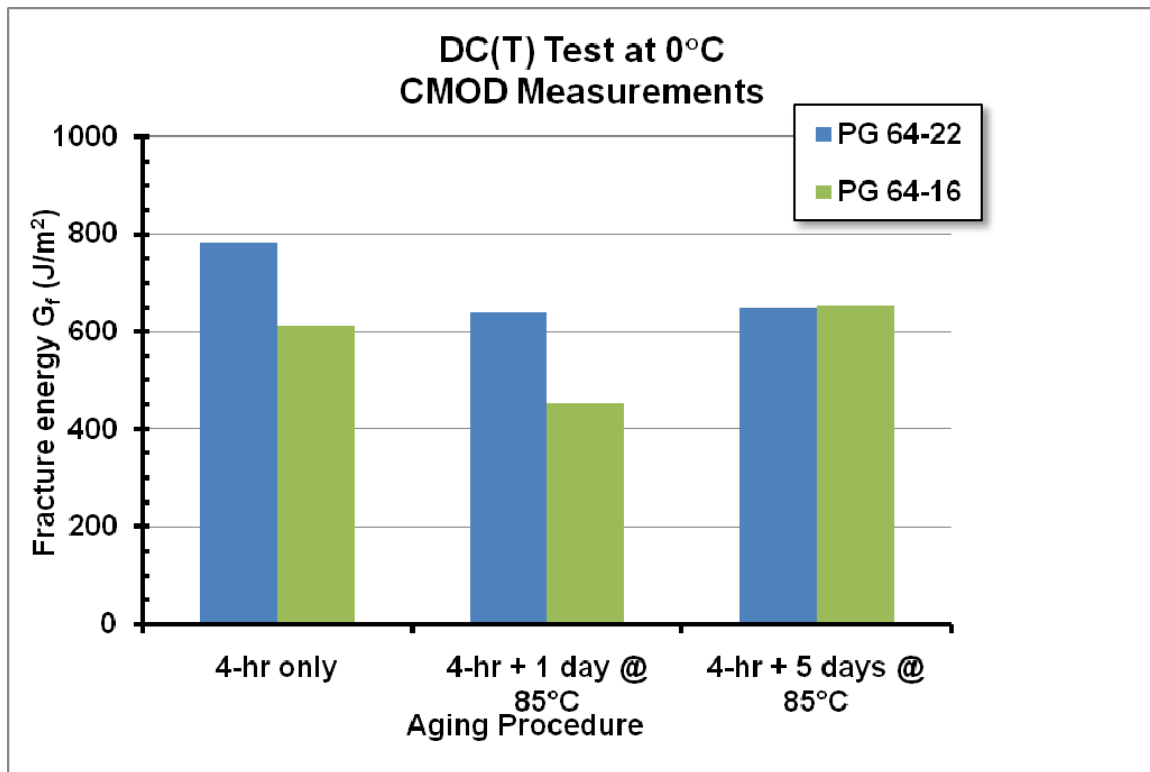


Figure B.6 Comparison of CMOD fracture energy for asphalt mixture types subjected to various aging levels.

4.4 Conclusions

A total of 54 specimens were tested in the DC(T) device using one gradation, two asphalt binders, and three aging levels. The goal was to see if the newer DC(T) test could differentiate between the various binders and aging levels.

The following can be concluded from this abbreviated laboratory aging study:

- From review of current testing options for thin (less than 2 inches) lifts/layers and latest testing technology, the DC(T) shows much promise based on the literature search. Based on previously reported results by the University of Illinois, the DC(t) can differentiate between brittle, non-brittle, and highly polymerized pavement cores.
- In this limited laboratory study, the DC(T) differentiated between the two asphalt binders representing two crudes that age differently. The PG 64-22 (specifically 67-24) mixtures exhibited significantly higher fracture resistance at the temperatures tested compared to the PG 64-16 (specifically 67-20) mixtures. This was important since the binders were only subtly different by -4°C on the low temperature grading.
- The current AASHTO long-term aging method (R30, Section 7.3) for mechanical property testing may not be severe enough to simulate long-term aging. It does not seem possible or logical to globally use one aging time or process for all test devices or process to represent any pavement depth. Much work seems needed

in this area to better simulate sample aging/conditioning for various test protocols to represent a pavement near the end of its service life.

4.5 Recommendations

While limited, the initial data suggests that the DC(T) should be able to differentiate the effect of aging of various airfield asphalt surfaces. To further validate this test, measurements on field cores from a sampling of airfield pavements should be made in Phase 2. For example, if a taxiway or runway has been sealed and the shoulder has not been sealed, a comparison could be made from cores of these locations to measure the effectiveness of the sealant to reduce aging, assuming the shoulder surface is made of similar materials. Cores can also be taken from new construction as a baseline for a new pavement that should exhibit no cracking. Cores should be sampled from varying locations of non-load distresses in wet-freeze, dry-freeze, wet -no freeze, and dry-no freeze climatic zones.

To provide other testing options to the research review panel for Phase 2, other tests can be evaluated in addition to the DC(T) test recommendation. Extra samples (4 each) conditioned at the three aging levels were stored and can be used for further testing. More samples can be easily duplicated since this mixture is from a local KY standard aggregate source and similar binders can be obtained.

Some binder tests that could be used to further evaluate the aging of the mixture are, but not limited to: classification using the dynamic shear rheometer (DSR) and bending beam rheometer (BBR), capillary tube viscosity, and the newer Multiple Stress Creep Recovery (MSCR) test. The binder tests are useful when sample size is limited, but require chemical extraction of the asphalt binder.

A strong potential mixture test is the BBR mixture test by Dr. Marasteanu. This test has shown much initial promise using a small sample. In this test, mixtures can be compacted and cut into small beams similar in size to asphalt binder BBR beams. The beams are then tested in a BBR that has been retrofitted to handle the stiffer mixture sample. The small sample size lends itself to higher variability.

Since the most severe environmental aging occurs closer to the surface, it seems logical that a test must be able to evaluate this material. Any test that is chosen should meet constraints of being able to take measurements from relatively thin (~25mm) airfield pavement surfaces obtained from coring with as little trimming as possible.

REFERENCES

1. Bell, Chris A. "Aging of Asphalt Aggregate Systems," Prepared for the Strategic Highway Research Program, National Research Council, *SR-OSU-A-003A-89*-September 1989.
2. Kemp, G.R. and Predoehl, N.H., "A Comparison of Field and Laboratory Environments on Asphalt binder Durability," AAPT, 1981, pp. 492-560
3. Predoehl, N.H. and Kemp, G.R., "An Investigation of the Effectiveness of Asphalt binder Durability Tests – Initial Phase," Caltrans Laboratory Research Report FHWA-CA-78-26, 1978
4. Petersen, J.C., "A Thin-Rim Accelerated Aging Test for Evaluating Asphalt binder Oxidative Aging," AAPT, V. 58, 1989, pp. 220-237
5. Verhasselt, A, "Long-term Aging of Bituminous Binders," Symposium – Aging of Pavement Asphalt binders, Laramie, 2003
6. Choquet, F, and Verhasselt, A, "Long-term Aging of Bituminous Binders," Rome International Asphalt binder Chemistry Symposium, 1991
7. Anderson, D.A, Christensen, D.W., Bahia, H.U., Dongre, R, Sharma, M.G, and Antle, C.E., "Binder Characterization and Evaluation: Volume 3 – Physical Characterization," SHRP report 369, reference Ch. 5 "Oxidative Aging Studies," 1993, pp. 303-401
8. R.B. McGennis, R.M. Anderson, R.M., Kennedy, T.W., Solaimanian M. "Background of SUPERPAVE Asphalt Mixture Design & Analysis" FHWA SA-95-03, 1994
9. Zofka, A., Marasteanu, M.O., Li, Xinjun, Clyne, T.R., McGraw, J. 2005. Simple method to obtain asphalt binders low temperature properties from asphalt mixtures properties. AAPT. Volume 74, 2005, pp 255-282.
10. Reinke, Gerald, "Report to NCAT-Rejuvenator Study - Study of Rejuvenator Type of Mixture Stiffness" Mathy Technology and Engineering Services, Inc, May 2002
11. Mirza, M.W. and Witczak, M.W., "Development of a Global Aging System for Short- and Long-Term Aging of Asphalt Cements", AAPT, Vol. 64, 1995, pp. 393–424
12. Wagoner, M.P., W.G., Buttlar, G.H., Paulino, and P. Blankenship. Investigation of the Fracture Resistance of Hot-Mix Asphalt Concrete Using a Disk-Shaped Compact Tension Test. Transportation Research Record No. 1929, Transportation Research Board, Washington, D.C., pp 183-192, 2005.
13. Apeageyi ,A.K. and W.G. Buttlar. Characterization of Asphalt Institute Mixture Specimens using the ASTM D7313-06 Fracture Energy Test: AAPT Aging Study. Internal report, June 24, 2008.